

Understanding dilated cardiomyopathy using cardiomyocytes made from patient-derived induced pluripotent stem cells

Cara Hawey

Degree of Master of Science  
Department of Pharmacology and Therapeutics  
McGill University, Montreal

July 2022

*A thesis submitted to McGill University in partial fulfillment of the requirements of the degree of Master of Science*

© Cara Hawey, 2022

## ACKNOWLEDGEMENTS

I would first like to thank my supervisor Dr. Terry Hébert for accepting me in his lab and for his guidance over the duration of my degree. Terry has helped to shape the kind of scientist I want to become with his passion for science as well as his kindness and understanding. Terry has always believed in me and supported my path, which is something I will always be grateful for.

Thank you to my advisor Dr. Anne McKinney and the rest of my committee, Dr. Stéphane Laporte and Dr. Alvin Shrier for their encouragement and valuable insights into improvements for my project. I'd also like to thank Dr. Nicolas Audet from the IMBP and members of the ABIF, Dr. Joel Ryan and Dr. Michiel Krols for their help with teaching me microscopy and troubleshooting my experiments. Thank you to Ronald Knox for all his help with the CardioExcyte96. Thank you to McGill Faculty of Medicine and the Courtois Foundation for funding my project.

I'd like to give a huge thank you to the members of the HID team, Kyla Bourque, Alyson Jiang, Karima Alim, Grace Mazarura, and Hooman Sadighian for all their help with troubleshooting, media changes, and overall support. I couldn't have asked for a better team! Thank you to the remaining members of Terry's lab (Darlaine Pétrin, Dr. Dominic Devost, Phan Trieu, Dr. Jace Jones-Tabah, Dr. Étienne Billard, Dr. Juliana Dallagnol, Deanna Sosnowski, Hanan Mohammad, Kim Martins-Cannavino, Jacob Blaney, and Emma Paulus) for your help and making the lab a welcoming and fun place to be. Thank you to my students, Said Ashkar and Tina Aghdam for helping me to become better at teaching and for all their help with my work and for Tina's translation of my abstract. I would also like to thank our collaborators, Dr. Nadia Gianetti, Dr. Renzo Cecere, Natalie Gendron, and their teams, especially Ida Derish, Jeremy Zwaig, and Kashif Khan for driving the HID project.

Finally, thank you to my friends and family for all of their support over the last 2 years.

## TABLE OF CONTENTS

Acknowledgements.....	1
Abstract.....	4
Résumé.....	5
Contribution of Authors.....	7
List of Abbreviations .....	8
List of Tables and Figures.....	10
1. Introduction.....	12
1.1 Dilated cardiomyopathy .....	12
1.2 Cardiomyocyte physiology and DCM.....	14
1.3 Adrenergic signalling in DCM.....	18
1.4 Disease modeling using iPSC-CMs .....	22
1.5 Methods to evaluate calcium handling in iPSC-CMs .....	26
1.6 Thesis objectives and rationale .....	28
2. Materials and Methods.....	31
2.1 Cell lines.....	31
2.2 Reagents .....	31
2.3 Cell maintenance and differentiation .....	32
2.4 Calcium handling .....	34
2.5 Sarcomere organization.....	34
2.6 Contractility and Electrophysiology.....	36
2.7 Treatments.....	37
2.8 Data analysis .....	37
3. Results.....	40
3.1 Calcium handling and sarcomere organization .....	40
3.1.1 Calcium handling differs between healthy controls and DCM patients.....	40
3.1.2 Sarcomere organization of iPSC-CMs from healthy controls and DCM patients.....	42
3.1.3 Calcium handling differs in response to treatment in a healthy control cell line .....	45
3.1.4 Calcium handling differs in response to treatment in a DCM patient cell line .....	47

3.1.5 Calcium handling and sarcomere organization in response to chronic treatment .....	48
3.3 Contractility and electrophysiology .....	52
3.3.1 Evaluating contractility in control iPSC-CMs.....	53
3.3.2 Evaluating contractility and electrophysiology in DCM patient derived iPSC-CMs...	54
4. Discussion .....	61
4.1 Calcium handling .....	61
4.2 Sarcomere organization.....	66
4.3 Contractility and Electrophysiology.....	68
4.4 Limitations .....	73
4.5 Future directions.....	77
5. Conclusion .....	82
6. References.....	84

## **ABSTRACT**

Dilated cardiomyopathy (DCM) is one of the most common types of disease that affects cardiac muscle. DCM is characterized by ventricular dilation and contractile dysfunction, resulting in insufficient supply of oxygenated blood to the rest of the body. This leads to severe consequences such as heart failure and ultimately the need for transplantation. Treatments such as  $\beta$ -blockers are used to modulate dysregulated signalling pathways to improve patient outcomes and quality of life; however, morbidity and mortality rates remain unacceptably high. There is a need to better understand the mechanisms underlying DCM to develop improved therapeutic strategies. Induced pluripotent stem cells (iPSCs) are tools used to model human diseases in a dish and can be used in a bedside-to-bench-to-beside approach to personalize treatment. Using iPSC-derived cardiomyocytes originating from patients and healthy control subjects, the goal of this research is to develop tools to phenotype features underlying DCM and to investigate the role of  $\beta$ -adrenergic signalling in disease pathogenesis and therapeutic responses. To this end, four main features of iPSC-cardiomyocytes were investigated: sarcomere organization, calcium handling, contractility, and electrophysiology. Sarcomere organization and calcium handling were evaluated using a genetically-encoded biosensor, RGECO-TnT, which is fused to proteins localizing to the myofilament. Contractility and electrophysiology were measured using impedance- and extracellular field potential-based methods. These parameters were assessed in response to both acute and chronic  $\beta$ -adrenergic stimulation in the presence and absence of clinically relevant  $\beta$ -blockers. DCM is a complex disease with many etiologies therefore phenotypes are expected to differ on a patient-to-patient basis. This research contributes to the development of tools needed to characterize DCM using patient-derived iPSC-cardiomyocytes in order to stratify patients based on similar phenotypes and responses to drugs, to generate better treatment options.

## RÉSUMÉ

La cardiomyopathie dilatée (CMD) est une des maladies les plus communes qui affecte le muscle cardiaque. La CMD se caractérise par une dilatation ventriculaire et des problèmes de contractilité, entraînant un apport insuffisant de sang oxygéné à travers le reste du corps. Cela mène à des conséquences sévères, dont l'arrêt cardiaque, nécessitant ultimement une transplantation. Des traitements comme les  $\beta$ -bloquants sont utilisés de manière à moduler les voies de signalisation dérégulées afin d'améliorer les performances et la qualité de vie des patients. Cependant, les taux de morbidité et de mortalité demeurent à un niveau inacceptable. Il est nécessaire de mieux comprendre les mécanismes liés à la CMD pour développer de meilleures stratégies thérapeutiques. Les cellules souches pluripotentes induites (CSPi) sont des outils qui servent à modéliser des maladies humaines en culture et qui peuvent être utilisés dans une approche allant du patient au laboratoire et retournant vers le patient afin de personnaliser les traitements. En utilisant des cardiomyocytes dérivés de CSPi provenant de patients et de sujets témoins sains, le but de cette recherche est de développer des outils pour déterminer les caractéristiques liées à la CMD et d'évaluer l'implication de la signalisation  $\beta$ -adrénergique dans sa pathogenèse et ses réponses thérapeutiques. À cette fin, quatre composantes principales des cardiomyocytes CSPi ont été étudiées: l'organisation des sarcomères, la manipulation du calcium, la contractilité et l'électrophysiologie. L'organisation des sarcomères a été évaluée en utilisant un biosenseur encodé génétiquement, le RGEKO-TnT, qui est fusionné à des protéines localisées dans le myofilament. La contractilité et l'électrophysiologie ont été mesurés à l'aide de méthodes basées sur l'impédance et le potentiel de champ extracellulaire. Ces paramètres ont été évalués en réponse à une stimulation aiguë et/ou chronique du système  $\beta$ -adrénergique en présence et absence de  $\beta$ -bloquants utilisés en clinique. La CMD est une maladie complexe relevant de multiples étiologies,

faisant en sorte que les phénotypes attendus puissent différer d'un patient à l'autre. Cette recherche contribuera au développement d'outils nécessaires à caractériser la CMD par l'usage de cardiomyocytes CSPi afin de classer par similarité les patients selon leur phénotypes et réponses à des drogues pour ainsi générer de meilleures options de traitement.

## **CONTRIBUTION OF AUTHORS**

Kyla Bourque provided help with the experimental design of section 3.1.3. The experiment done in section 3.3.1 was completed by both Cara Hawey and Kyla Bourque. Tina Aghdam assisted with data analysis in section 3.1.2 and section 3.1.5. Tina Aghdam and Dr. Étienne Billard translated the abstract into French. Ida Derish, Jeremy Zwaig, Kashif Khan, David Derish, Janice To, and Patrick Young generated the HID project iPSC lines from patient and control subject blood samples.

Unless specified above, all work in this thesis was completed by Cara Hawey. This thesis was written by Cara Hawey and edited by Dr. Terry Hébert.

## LIST OF ABBREVIATIONS

ACE inhibitors	Angiotensin-converting enzyme
AM	Acetomethoxy
CACNA1C	Calcium voltage-gated channel subunit alpha 1 C
CAMK2D	Calcium/calmodulin dependent protein kinase II delta
cAMP	Cyclic adenosine monophosphate
CM	Cardiomyocyte
cpEGFP	Circularly permuted enhanced green fluorescent protein
DCM	Dilated cardiomyopathy
DMSO	Dimethyl sulfoxide
EFP	Extracellular field potential
EHT	Engineered heart tissue
FPD	Field potential duration
GECI	Genetically-encoded calcium indicators
GPCR	G protein- coupled receptor
iPSC	Induced pluripotent stem cell
ISO	Isoproterenol
KOSR	Knockout serum replacement
LMNA	Lamin A
LTCC	L-type calcium channel
NCX	Sodium-calcium exchanger
NIF	Nifedipine
NOR	Norepinephrine

PKA	Protein kinase A
PKC	Protein kinase C
PLN	Phospholamban
PBMC	Peripheral blood mononuclear cells
RBM20	RNA-binding motif 20
ROCK inhibitor	Rho kinase inhibitor
RyR	Ryanodine receptor
RYR2	Ryanodine receptor (gene)
SERCA2a	Sarco-endoplasmic reticulum Ca <sup>2+</sup> -ATPase
SR	Sarcoplasmic reticulum
TnC	Troponin C
TnI	Troponin I
TnT	Troponin T
TTN	Titin
VEH	Vehicle
$\alpha$ 1AR	$\alpha$ <sub>1</sub> - adrenergic receptor
$\beta$ <sub>1</sub> AR	$\beta$ <sub>1</sub> - adrenergic receptor
$\beta$ <sub>2</sub> AR	$\beta$ <sub>2</sub> - adrenergic receptor
$\beta$ -MHC	$\beta$ - myosin heavy chain

## LIST OF TABLES AND FIGURES

Figure 1. Mechanism of excitation-contraction coupling in cardiomyocytes.....	15
Figure 2. Cardiac responses to stressors. ....	17
Figure 3. Bedside-to-bench-to-bedside pipeline using patient-derived iPSC-CMs.....	23
Figure 4. Methods to assess calcium transients using fluorescence microscopy.....	27
Figure 5. Guidelines to classify sarcomere organization of iPSC-CMs. ....	36
Figure 6. Features of calcium transients that can be analyzed using the Transient Analysis app in OriginPro2022.....	39
Figure 7. Features of calcium transients in iPSC-CMs derived from healthy controls and DCM patients. ....	41
Figure 8. Sarcomere organization evaluated using RGECCO-TnT to visualize troponin T in the myofilament. ....	43
Figure 9. Calcium transients in iPSC-CMs derived from control HID041004 in response to acute treatment. ....	46
Figure 10. Calcium transients in iPSC-CMs derived from DCM patient HID041019 in response to acute treatment.....	47
Figure 11. Features of calcium transients in iPSC-CMs from DCM patient HID041020 in response to 7 days of treatment.....	49
Figure 12. Comparison of features of calcium transients in DCM patient HID041020 before treatment and after 7 days of treatment.....	50
Figure 13. Sarcomere organization of iPSC-CMs from DCM patient HID041020 after 7 days of treatment. ....	52
Figure 14. Pilot assay of healthy control AIW002-2 iPSC-CMs using the CardioExcyte96 to evaluate contractility.....	54
Figure 15. Contractility and electrophysiology of DCM patient HID041020 in response to treatment with norepinephrine. ....	56
Figure 16. Contractility and electrophysiology of DCM patient HID041020 in response to treatment with isoproterenol. ....	59

## Supplemental Figures

Figure S1. Intensiometric calcium biosensor RGECO-TnT expressed in iPSC-CMs.

Figure S2. Single cell calcium transients for iPSC-CMs derived from healthy controls and DCM patients.

Figure S3. Features of calcium transients in iPSC-CMs from DCM patient HID041020 in response to 7 days of treatment.

Figure S4. Optimizing the seeding density of DCM patient line HID041020 iPSC-CMs.

Figure S5. Single cell calcium transients for iPSC-CMs derived from DCM patient HID041020 in response to 7 days of treatment.

## 1. INTRODUCTION

### *1.1 Dilated cardiomyopathy*

Cardiomyopathies are a family of diseases that affect the muscle of the heart. This heterogenous family of diseases can be brought on by genetic or acquired causes and is associated with poor patient outcomes, often progressing to heart failure and sudden cardiac death. The main types of cardiomyopathies include hypertrophic, restrictive, arrhythmogenic, and dilated [1]. Hypertrophic cardiomyopathy often occurs as the result autosomal dominant mutations in the contractile machinery of heart muscle cells, or cardiomyocytes, and is characterized by the thickening of the myocardial wall which leads to a smaller chamber volume thus a lower cardiac output [2]. Restrictive cardiomyopathy is also commonly caused by mutations in genes encoding contractile proteins and occurs when the myocardium becomes rigid, impairing the ability of the heart to effectively pump blood to the rest of the body [3]. Arrhythmogenic cardiomyopathy is characterized by myocardial dysfunction and life-threatening arrhythmias and can lead to sudden cardiac death [4]. Dilated cardiomyopathy is the most common form of cardiomyopathy and will be the topic of this thesis [1].

Dilated cardiomyopathy (DCM) is a condition that is characterized by dilation of walls of the heart chambers, starting with the left ventricle, which can lead to contractile dysfunction [5]. Dilation of the ventricle results in inefficient pumping of blood to the rest of the body and can lead to pulmonary and peripheral edema and heart rhythm abnormalities [5]. Patients with DCM also commonly present with fatigue, shortness of breath during exertion and at rest, chest pain or discomfort, a cough, and lightheadedness or fainting. However, symptoms may not present until later in the disease progression when substantial dilation has already occurred, and the disease has begun to progress toward heart failure. DCM is a leading cause of heart failure, with a 50%

mortality rate within 5 years of diagnosis. Treatments remain incompletely effective and do not generally modify the course of the disease, contributing to the reason why DCM is a common indication for heart transplant [6]. DCM primarily affects those between the ages of 20-60 years old and has many etiologies; however, about 25-50% of patients with DCM have no identified cause [7, 8]. Among known causes of DCM are genetic mutations, viral infection, toxic exposures (drugs, chemotherapeutic agents, alcohol), and immune- or inflammation- mediated events. Pre-existing cardiac conditions such as coronary artery disease, hypertension, and valvular disease can progress to DCM [5]. Current treatment strategies include angiotensin-converting enzyme (ACE) inhibitors, angiotensin receptor antagonists, combined angiotensin receptor blocker/neprolysin inhibitors,  $\beta$ -blockers, aldosterone receptor antagonists, and sodium/glucose cotransporter-2 inhibitors [9]. These drugs can be used to manage disease and improve patient outcomes[10-12]; however, morbidity and mortality rates remain unacceptably high. DCM is often underdiagnosed because patients may be asymptomatic in the early stages of disease [13]. There is a clear need to better understand mechanisms underlying DCM progression so that we can diagnose the disease earlier, improve therapeutic strategies, and personalize treatments to improve patient outcomes. Toward this end, research is required to study characteristics of disease on a cellular and genetic level to gain a better understanding of the mechanisms underlying disease and develop cellular profiles associated with each patient. These profiles can be compared to clinical data in order to draw associations between *in vitro* investigations and patient symptoms, outcomes, and response to treatments. This data can be compared on a patient-to-patient level in order to identify clusters of patients with similar characteristics and response to drugs to ultimately develop more personalized treatment strategies for these clusters [14, 15].

## *1.2 Cardiomyocyte physiology and DCM*

Many DCM-causing mutations are found in genes encoding sarcomeric proteins such as those found in the cardiac troponin complex (TNT/I/C),  $\beta$ -myosin heavy chain ( $\beta$ -MHC), titin and cardiac actin [8, 16, 17]. The sarcomere is the contractile unit of heart muscle cells, or cardiomyocytes. It is composed of an interlacing pattern of thin (actin) and thick (myosin) filaments that interact in response to calcium binding, resulting in a contraction. In the process that initiates contraction, known as excitation-contraction coupling, calcium is essential in the conversion of electric stimulation into muscle contraction. The plasma membrane of cardiomyocytes is depolarized by an action potential, which triggers the opening of L-type calcium channels (LTCCs), allowing extracellular calcium into the cell (step 1 **Figure 1**) [18]. This initiates calcium-induced calcium release, a large-scale release of calcium into the cytosol from the intracellular calcium stores in the sarcoplasmic reticulum (SR) through ryanodine receptors (RyRs) (step 2 **Figure 1**) [18]. Calcium then binds the troponin complex in the myofilament which induces a conformational change in tropomyosin, allowing actin to bind myosin thus resulting in contraction (step 3 **Figure 1**) [19]. Troponin T acts to anchor the troponin complex to tropomyosin while troponin I binds actin and blocks myosin binding sites until a conformational change occurs in response to calcium binding troponin C [20]. The contraction ceases when calcium is released from the troponin complex and is returned to the SR via the sarco-endoplasmic reticulum  $\text{Ca}^{2+}$ -ATPase (SERCA2a) or exits the cell via the sodium-calcium exchanger (NCX) (step 4 **Figure 1**) [21]. As a result, calcium handling is an important and tightly regulated process in cardiomyocytes that when dysregulated, can lead to disease.

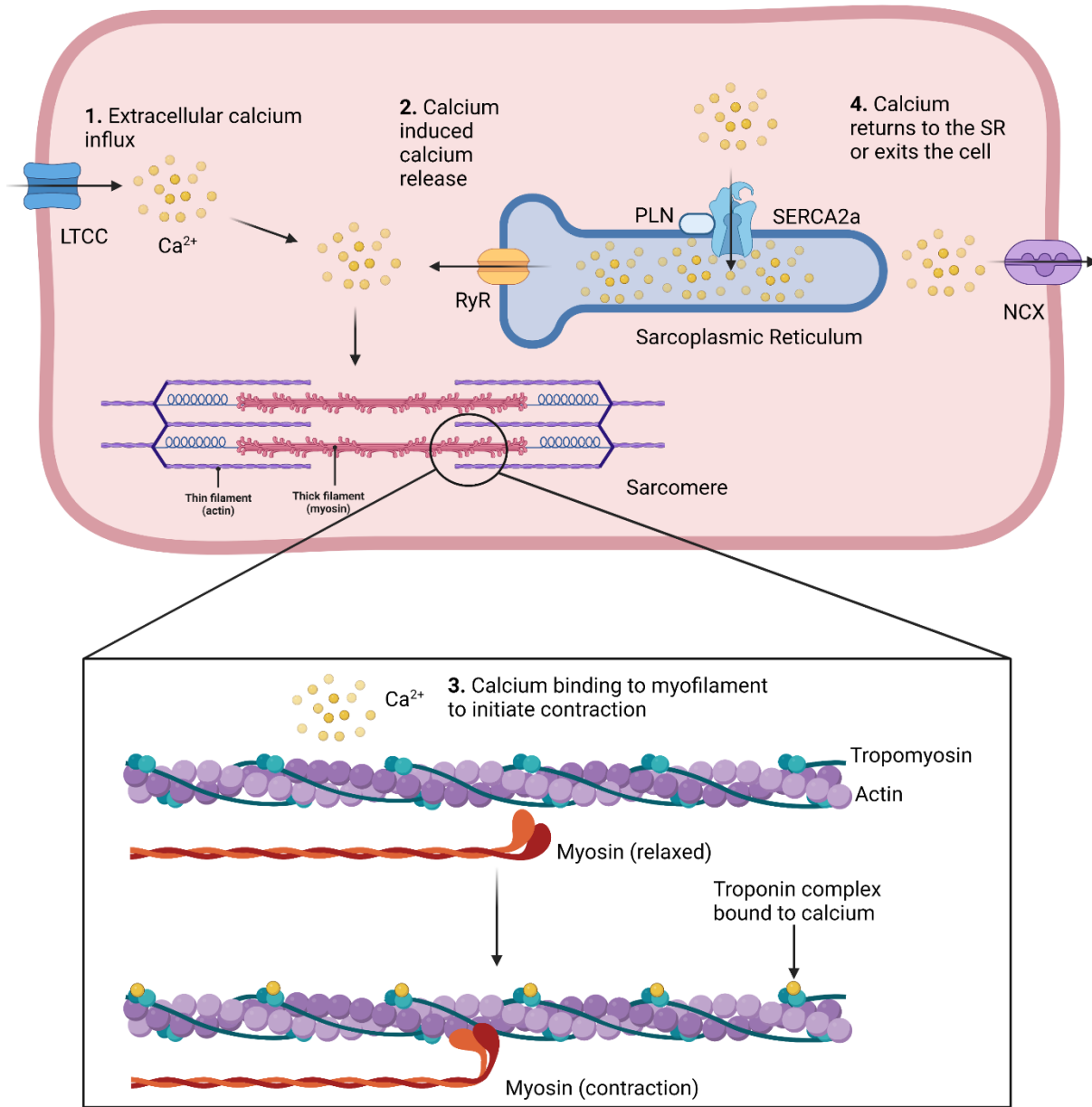


**Figure 1. Mechanism of excitation-contraction coupling in cardiomyocytes.**

1. Following membrane depolarization by an action potential, calcium is allowed into the cell by L-type calcium channels (LTCCs). 2. The influx of calcium triggers large-scale calcium release through ryanodine receptors (RyRs) from intracellular stores in the sarcoplasmic reticulum (SR). 3. Calcium binds troponin C of the troponin complex on the myofilament, which results in a conformational change in tropomyosin that frees the myosin-binding sites on actin that were previously blocked by troponin I. This allows actin to bind to myosin, resulting in the contraction of the cardiomyocyte. 4. The contraction cycle ends when calcium is released from the troponin complex and returns to the SR via the sarco-endoplasmic reticulum  $\text{Ca}^{2+}$ -ATPase (SERCA2a) or exits the cell via the sodium-calcium exchanger (NCX). Figure made using BioRender.

It has been reported that calcium handling is compromised in DCM, with alterations in sensitivity to calcium at the myofilaments, abnormal expression and function of calcium handling proteins, decreased peak height of calcium transients during systole, decreased calcium reuptake during diastole, and reduced contractile function [22]. Furthermore, defective calcium handling proteins have been noted in other cardiac diseases such as heart failure, congenital long QT syndrome, and catecholaminergic polymorphic ventricular tachycardia and has been shown to contribute to the pathogenesis of arrhythmias [23, 24]. However, the mechanisms underlying these changes are complex and still not fully understood, thus requiring further study.

Cardiomyocytes undergo several compensatory mechanisms when faced with genetic mutations or injuries that impair contractility or cardiac function. These mechanisms include cellular remodeling, neurohormonal stimulation, an upregulated fibrotic response, and cell death (**Figure 2**). In response to impaired contractility and insufficient oxygen supply, stroke volume and/or stroke rate increase to preserve cardiac output. For example, when contractility is impaired, cardiomyocytes undergo a hypertrophic response by adding more sarcomeres to preserve contractile force [25]. Sarcomeres can be added in parallel or in series, resulting in an increase in width or length of the cardiomyocyte, respectively. Adding sarcomeres in parallel increases wall thickness and can lead to hypertrophic cardiomyopathy while adding sarcomeres in series leads to the dilation of the heart chambers [26, 27]. In any case, while this mechanism initially serves to increase cardiac output, it can become a maladaptive response that further impairs cardiac function. Alternatively, endogenous catecholamines such as norepinephrine and epinephrine are released to increase the rate and force of contraction.

Increased demand due to volume or pressure overload and damage to the myocardium can ultimately lead to cell death, resulting in thinning of the walls which reduces contractility and

promotes DCM [25]. In response to injury and cell death, cardiac fibroblasts become activated to increase production of extracellular matrix, which acts to provide structural support and secrete factors that regulate myocyte survival signalling [28]. Persistent increased production of extracellular matrix components eventually leads to maladaptive scarring known as fibrosis. Fibrosis can worsen cardiac function by stiffening the myocardium, effectively reducing the filling capacity of the heart and leading to the characteristic cardiac remodeling associated with DCM [29].

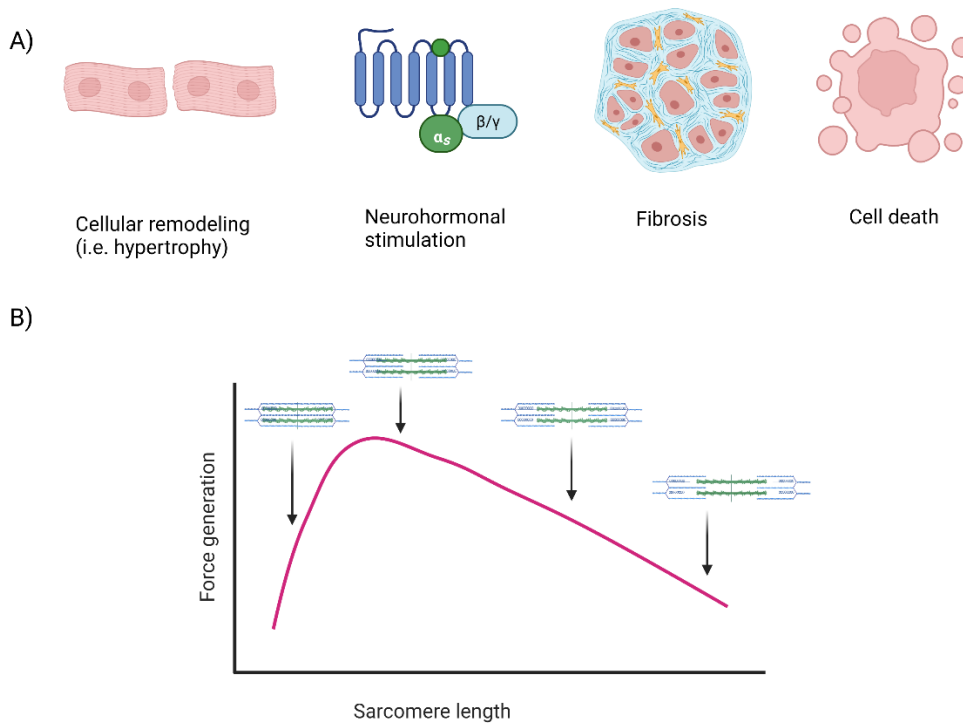


**Figure 2. Cardiac responses to stressors.**

(A) When the myocardium undergoes stress or insult, it can react by compensatory mechanisms such as undergoing hypertrophy, responding to neurohormonal stimulation, undergoing fibrosis, or by undergoing cell death. (B) The Frank-Starling mechanism outlines the compensatory response of cardiomyocytes to reduced cardiac output. Sarcomeres increase in length to generate a larger force of contraction; however, with too much stretching sarcomeres cannot contract effectively thereby reducing force generation. Figure made using BioRender.

Stretching the ventricular wall in the heart results in greater force of contraction, according to the Frank-Starling mechanism (**Figure 2**) [30]. Increasing the volume of blood in the left ventricle in turn increases the amount of stretch posed to the wall of the ventricle. By stretching the ventricular wall, the sarcomeres of cardiomyocytes become stretched and elongated. Increased sarcomere length results in increased force of contraction as well as increased calcium sensitivity at the troponin complex [20, 30, 31]. However, these benefits last only up to a certain point. With chronic stressors, this compensatory mechanism continues to stretch sarcomeres to excess until the overlap between actin and myosin is too small for effective binding and therefore effective contractions, leading to serious cardiovascular consequences such as DCM and heart failure [30, 31]. Decreased cardiac output is also compensated by the release of catecholamines such as epinephrine and norepinephrine to activate adrenergic signalling and increase rate and force of contraction [25].  $\beta$ -adrenergic signalling and how it relates to DCM is described in more detail below.

### *1.3 Adrenergic signalling in DCM*

Adrenergic receptors are members of the G protein-coupled receptor (GPCR) family and consist of the  $\alpha$  and  $\beta$  adrenergic receptor subfamilies.  $\beta_1$ -adrenergic receptors ( $\beta_1$ ARs) are the predominately expressed subfamily in human hearts; however,  $\alpha_1$  and  $\beta_2$ -adrenergic receptors ( $\alpha_1$ ARs and  $\beta_2$ ARs) are also present [32]. Adrenergic receptors are bound by endogenous catecholamines such as epinephrine and norepinephrine as well as clinically relevant drugs such as isoproterenol and phenylephrine to initiate signalling cascades that result in inotropic and chronotropic response as well as adaptive responses to myocardium damage or decreased cardiac function [32]. For instance,  $\beta$ -adrenergic receptor activation results in the phosphorylation of important proteins involved in excitation-contraction coupling such as L-type calcium channels

(LTCCs), sarco-endoplasmic reticulum  $\text{Ca}^{2+}$  ATPase (SERCA2a), ryanodine receptors (RyRs), troponin I (TnI), and phospholamban (PLN) by protein kinase A (PKA) [33]. Phosphorylation of these proteins plays a role in the various phases of cardiomyocyte contraction. In response to contractile and functional deficits, catecholamines are released to bind adrenergic receptors to initiate a signalling cascade that increases rate and force of contraction [25].

$\alpha_1$ AR signalling is thought to play a role in cardio-protection against stress through activating pathways that result in cardiomyocyte hypertrophy, cell survival, and increased contractility [32]. In contrast to maladaptive response,  $\alpha_1$ AR signalling is thought to mediate adaptive hypertrophy, which occurs without cell death and fibrosis to maintain cardiac function [32]. The  $\alpha_1$ AR acts through the  $G_{q/11}$  signalling pathway which results in the activation of protein kinase C (PKC) that goes on to mediate inhibition of apoptotic pathways and enhancement of heart rate and contractility [34]. Upon the activation of  $\beta_1$ ARs and  $\beta_2$ ARs by catecholamines,  $G_{\alpha s}$  and  $G_{\alpha i}$  proteins modulate PKA activity by stimulating or inhibiting the activity of adenylyl cyclase and the production of cyclic AMP (cAMP), respectively [34]. Adenylyl cyclase acts to raise intracellular concentrations of cyclic AMP (cAMP), thereby increasing activity of PKA [35]. PKA then goes on to directly phosphorylate or mediate the phosphorylation of targets listed above to regulate the contraction of cardiomyocytes. Phosphodiesterases break down cAMP which results in termination of downstream activity [36]. During events that impair cardiomyocyte contractility, endogenous catecholamines are released to increase beat rate and force of contraction in attempt to compensate for the loss of function. However,  $\beta_1$ ARs and  $\beta_2$ ARs mediate different downstream signalling pathways that result in differential cardiac outcomes. Generally,  $\beta_1$ AR signalling pathways are said to mediate maladaptive responses while  $\beta_2$ ARs mediate adaptive or cardioprotective responses [37].

Ca<sup>2+</sup>/calmodulin-dependent protein kinase II (CaMKII) can be activated by PKA to phosphorylate key proteins involved in cardiomyocyte contractility [34]. CaMKII can also be activated directly by G $\alpha$ s following  $\beta_1$ AR activation. This PKA-independent activation of CaMKII then goes on to mediate cardiomyocyte apoptosis and maladaptive hypertrophy [34, 37]. As a result, persistent activation of CaMKII by  $\beta_1$ ARs can lead to cardiomyopathy. On the other hand, activation of  $\beta_2$ ARs has been shown to be associated with improved cardiac performance and protection against apoptosis [37].  $\beta_2$ ARs are coupled to both G $\alpha$ s and G $\alpha$ i and can regulate the inotropic response of cardiomyocytes both positively and negatively [38]. Persistent activation of  $\beta_2$ ARs leads to cardioprotective effects through G $\alpha$ i-mediated activation of cell survival pathways and countering the effects of G $\alpha$ s signalling [38, 39]. Chronic activation of  $\beta_1$ ARs can lead to the desensitization of these receptors and decreased receptor expression [40, 41]. The decreased receptor expression results in a destructive cycle in which more catecholamines are released in attempt to bind  $\beta_1$ ARs and  $\beta_2$ ARs to increase force and frequency of contractions of the defective cardiomyocytes that become increasingly impaired by catecholamine stimulation. To counter this,  $\beta$ -blockers are used to modulate  $\beta$ AR-mediated signalling pathways. Clinically it has been shown that long-term use of  $\beta$ -blockers improves cardiac function and reverses maladaptive remodeling [38]. While the exact mechanism has yet to be fully elucidated, there are several theories on how  $\beta$ -blockers act to preserve heart function. It has been suggested that  $\beta$ -blockers act by disrupting the destructive cycle of catecholamine release and long-term  $\beta$ AR activation [39].  $\beta$ -blockers may also act by preventing the downregulation of receptors in order to maintain physiological receptor number or act as biased signalling ligands to promote cardioprotective pathways [39].

Patients with DCM have been found to have dysregulated  $\beta$ -adrenergic signalling. For example, heart tissue from a DCM patient showed upregulation of various phosphodiesterases

compared to a healthy control, indicating increased breakdown of cAMP and therefore reduced downstream PKA activity, which may be a factor in the development of impaired contractility and DCM [36]. Furthermore, various studies have showed that cardiomyocytes from patients with DCM were more sensitive to stimulation by  $\beta$ -adrenergic agonists such as norepinephrine or isoproterenol as indicated by deficits in contractility, increased sarcomere disorganization, decreased cell viability, and dysregulated calcium handling [36, 42-44]. These effects were shown to be mitigated by treatment with  $\beta$  blockers such as propranolol, carvedilol, or metoprolol [36, 42-44].

Signalling pathways may also be disrupted by mutations in key proteins involved in contractility. For instance, PLN is a regulatory protein that inhibits SERCA2a and is modulated by  $\beta$ -adrenergic signalling pathways. PLN releases SERCA2a when phosphorylated by PKA, allowing for calcium reuptake into the sarcoplasmic reticulum. Cardiomyocyte contractility and rate of relaxation have been shown to be increased by increased SERCA2a activity [45]. A mutation has been recorded in the PLN binding site for PKA that prevents PLN dissociation from SERCA2a, resulting in constitutive inhibition and delayed calcium transient decay [46]. Family members affected by this autosomal dominant mutation developed DCM by the age of 30 years old, as indicated by increased chamber dimensions and decreased contractile function [46]. These individuals progressed to heart failure within 5 to 10 years of symptom onset with some requiring heart transplant [46]. Personalized disease modeling is a strategy to offer patients such as these access to precision medicine and more favorable disease outcomes. In recent years, induced pluripotent stem cells (iPSCs) have been used to model diseases such as DCM to determine features underlying the disease and to improve treatment strategies for these patients.

#### *1.4 Disease modeling using iPSC-CMs*

The advent of induced pluripotent stem cells (iPSCs) has revolutionized disease modelling as well as drug discovery and development. Somatic cells such as peripheral blood mononuclear cells (PBMCs) can be taken from any patient and reprogrammed into iPSCs, which then have the capacity to be differentiated into virtually any cell type [47]. These patient-derived iPSCs have been shown to recapitulate features underlying disease and can be used to study altered cellular phenotypes, making them a very useful *in vitro* model to study “diseases-in-a-dish” and potentially develop personalized therapeutic strategies. Since Lian et al (2013) developed a protocol to differentiate iPSCs into functionally beating cardiomyocytes (CMs), iPSC-CMs have been used to study various heart diseases including long QT syndrome [48], myocardial infarction [49], cardiovascular consequences of Duchenne muscular dystrophy [50], and DCM [36, 42, 43, 51-56]. iPSC-CMs may also have use in predicting patient response to treatment with cardiotoxic drugs such as doxorubicin [57, 58]. In a study that compared iPSC-CMs from cancer patients who received doxorubicin treatment, iPSCs from the group who developed cardiotoxicity recapitulated this response as indicated by their increased sensitivity to doxorubicin, decreased cell viability, calcium handling, and altered production of reactive oxygen species compared to the doxorubicin tolerant group [57, 58]. iPSC-CMs can also be derived from patients with genetic variants of DCM in order to phenotype underlying features of disease to determine mechanistic pathways and improve personalized treatment options (**Figure 3**). The upcoming section discusses various examples of using patient-derived iPSCs used to model genetic DCM.

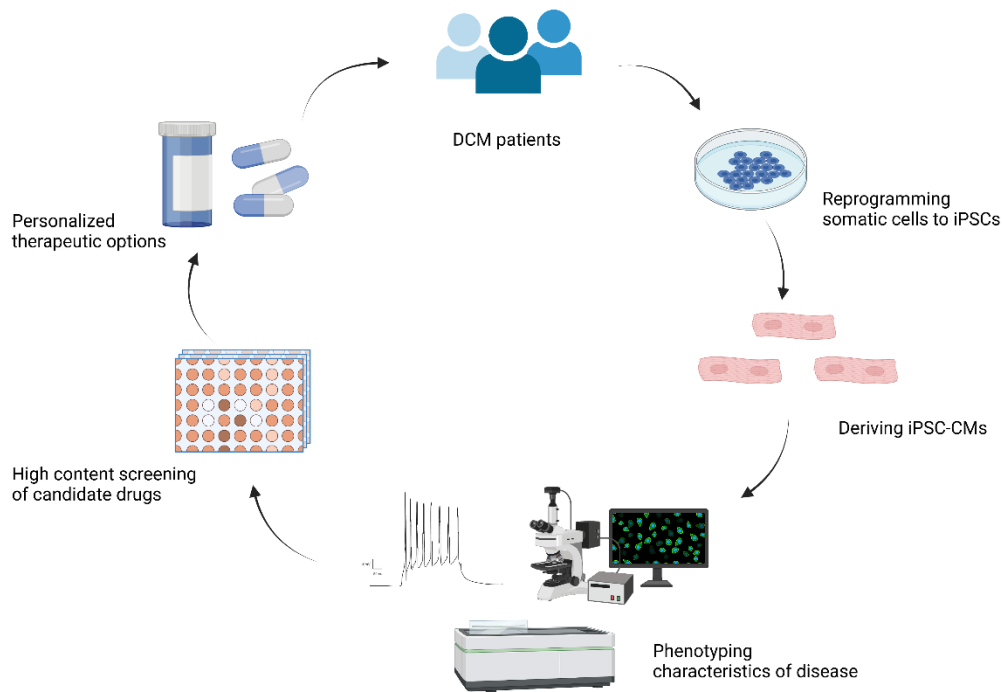


**Figure 3. Bedside-to-bench-to-bedside pipeline using patient-derived iPSC-CMs.**

Bedside-to-bench-to-bedside pipeline using patient-derived iPSC-CMs. Somatic cells from patients with DCM are reprogrammed into iPSCs. iPSCs are differentiated into cardiomyocytes using defined protocols and have been shown to recapitulate features of disease. Various features of disease can be investigated including calcium handling, contractility, sarcomere organization, and cell viability. Once characterized, high content screening can be used to determine the optimal therapeutic strategy for each patient, completing the bedside-to-bench-to-bedside pipeline in personalized medicine. Figure made using BioRender.

The first report of iPSCs being used to model DCM was with a case of familial DCM caused by the R173W mutation in troponin T (TnT-R173W) [36, 51, 52]. Patients with this mutation frequently develop heart failure at an early age and experience sudden cardiac death [51]. Initial investigations comparing iPSC-CMs derived from several individuals with this mutation with healthy controls from the same family revealed disorganized sarcomeres and abnormal calcium handling [51]. In response to  $\beta$ -adrenergic stimulation by norepinephrine, iPSC-CMs displayed severely disorganized sarcomeres and impaired contractility [51]. Treatment with  $\beta$ -blocker metoprolol was shown to improve sarcomere organization, in the presence or absence of norepinephrine [51]. Studies were then performed to further probe dysregulated  $\beta$ -adrenergic

signalling and mechanisms behind sarcomere disorganization and impaired contractility [36, 52]. iPSC-CMs from patients with the TnT-R173W mutation showed an epigenetic upregulation in phosphodiesterases, which act to break down cAMP and can thus result in impaired  $\beta$ -adrenergic signalling, as demonstrated by impaired contractility [36]. Evidence also showed increased mutant TnT localization to the nucleus, which may have gone on to interact with epigenetic enzymes that upregulate phosphodiesterase gene expression, ultimately resulting in impaired contractility [36]. The mechanism behind contractile deficits resulting from TnT-R173W was further investigated and revealed impaired interactions between the troponin complex and tropomyosin [52]. The mutation in TnT impaired its interactions with PKA, which in turn reduced the phosphorylation of TnI. As a result of this impaired interaction, tropomyosin was not able to achieve the correct conformation to allow for myosin to bind actin, which in turn limited the initiation of the contraction. AMP-activated protein kinase (AMPK), a protein involved in the regulation of metabolic pathways, also plays a role in sarcomere-cytoskeleton filament interactions by acting as a cytoskeleton remodeling protein [59, 60]. Activation of AMPK improved sarcomere organization as well as contractility by restoring the destabilized interactions with the troponin complex [52]. These findings help to understand the mechanisms underlying DCM caused by TnT-R173W and may help guide the development of therapeutic strategies to improve patient outcomes.

iPSCs have also been used to model DCM caused by a mutation in RNA-binding motif protein 20 (RBM20) [42, 43, 53, 61-63]. RBM20 is a splicing regulator for sarcomeric genes (titin and  $\beta$ -MHC) and genes involved in calcium handling (CAMK2D, RYR2 and CACNA1C) [42, 53]. Mutations in RBM20 lead to severe DCM, with younger age at diagnosis and a high degree of morbidity and mortality [42]. iPSC-CMs from patients with RBM20 DCM showed sarcomere disorganization, calcium dysregulation, impaired contractile function and increased cell death

which worsened with norepinephrine treatment; however, iPSC-CMs from patients with more advanced DCM showed a more pronounced phenotype compared to healthy controls [42, 43, 53]. Treatment with the  $\beta$ -blocker carvedilol or the L-type calcium channel blocker verapamil improved calcium dysregulation under basal conditions and verapamil protected iPSC-CMs from norepinephrine-induced calcium abnormalities and cell death [43]. Interestingly, iPSC-CMs from patients with RBM20 mutations were more susceptible to  $\beta$ -adrenergic stress than iPSC-CMs from patients with the TnT-R173W mutation, showing severe sarcomeric disarray after only 2 days with norepinephrine treatment as opposed to one week [43, 51]. Upregulation of endogenous RBM20 has been identified as a potential treatment strategy to improve contractile function in iPSC-CMs from patients with mutations in RBM20 [62].

The arginine 14 deletion (R14del) mutation in phospholamban (PLN) has also been reported in cases of DCM [54-56]. PLN acts to regulate calcium cycling in cardiomyocytes by inhibiting SERCA2a which effectively inhibits calcium reuptake into the sarcoplasmic reticulum. Patients with this mutation suffer from ventricular dilation, contractile deficits, and arrhythmias, with a high risk of progressing to heart failure by middle age [54]. Using iPSC-CMs derived from a patient with the PLN R14del mutation, researchers noted abnormal calcium handling, irregular electrical activity, and an increase in the expression of hypertrophic markers [54]. Gene editing and gene therapy approaches were used to correct the mutation in iPSC-CMs, resulting in a normal phenotype [54]. Further research using this PLN R14del patient line investigated the contractility of iPSC-CMs grown as 3D engineered cardiac tissue [55]. Amplitude, rates of contraction and relaxation, and force of contraction were found to be impaired in 3D engineered cardiac tissue; however, gene editing rescued contractile deficits, resulting in contractility comparable to healthy controls [55]. 3D engineered cardiac tissue derived from another patient with the PLN R14del

mutation showed impaired calcium handling and contractility compared to an isogenic control, as indicated by prolonged calcium transient decay time as well irregular beat patterns and lower contraction force [56]. Expression of calcium-binding proteins improved the phenotype by decreasing the amount of available cytoplasmic calcium, suggesting cytosolic calcium scavenging as a promising therapeutic approach to treat patients with the PLN R14del mutation.

The use of iPSC-CMs in personalized disease modeling of patients with DCM is now well-supported in the literature. iPSC-CMs recapitulate features of disease in a dish, allowing us to study underlying mechanisms and identify targets for new therapeutics. Novel personalized treatment strategies have already been suggested with the help of iPSC-CM models. By using iPSC-CMs, DCM patients can be phenotyped on a molecular and cellular level as well as clinically. This information can be used to cluster patients into groups in order to determine optimal therapeutic strategies for patients sharing similar phenotypes.

### *1.5 Methods to evaluate calcium handling in iPSC-CMs*

This thesis largely focuses on developing methods to evaluate calcium handling, given the important role it plays in cardiomyocyte physiology and dysregulation in DCM as described above. This section will outline methods available to measure calcium handling and provide rationale for the selected method I used in my thesis work.

Intracellular calcium can be measured in iPSC-CMs using a variety of methods, the most widely used being intracellular calcium-sensitive whole-cell dyes such as Fluo-4 or Fura-2 and genetically-encoded calcium indicators (**Figure 4**). Fluo-4 is a single wavelength calcium indicator while Fura-2 is a double wavelength indicator that has a shift in its excitation wavelength in response to calcium binding [64, 65]. Single wavelength indicators tend to have higher fluorescence intensities compared to double wavelength indicators; however, double wavelength

indicators give ratiometric measurements that allow for quantitative measurements [64]. Fluo-4 and Fura-2 are esterified with an acetomethoxy (AM) group that allows the compounds to cross cell membranes. AM gets cleaved by intracellular esterases, trapping Fluo-4 and Fura-2 inside the cell to fluoresce in the presence of calcium.

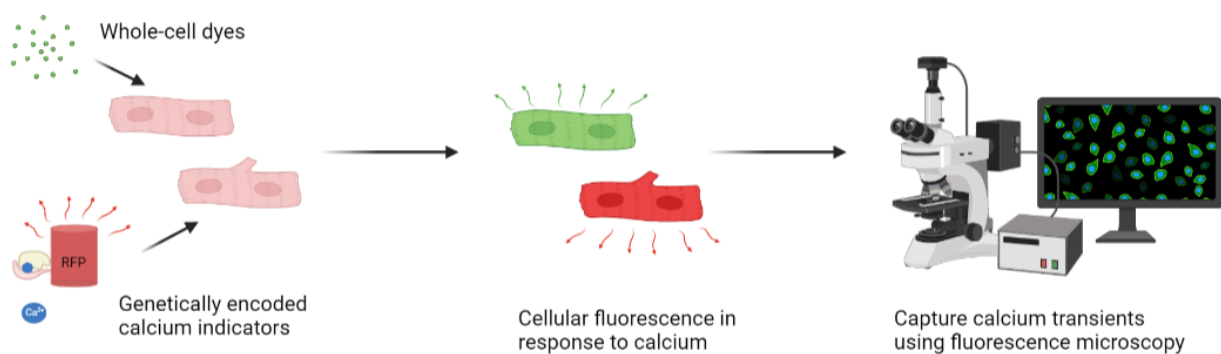


**Figure 4. Methods to assess calcium transients using fluorescence microscopy.**

Whole-cell dyes and genetically-encoded calcium indicators are the most commonly used to measure intracellular calcium. Figure made using BioRender.

Genetically-encoded calcium indicators (GECIs) are composed of a calcium binding domain (e.g. calmodulin or troponin T) and one to two fluorescent proteins [66, 67]. GcaMP GECIs are a series of calcium sensors composed of circularly permuted enhanced GFP (cpEGFP), calmodulin, and M13, a target sequence of calmodulin [68]. Calcium binds calmodulin which induces a conformational change in cpEGFP that changes fluorescence intensity [68]. Since the development of GcaMP, newer versions have been developed to improve upon fluorescence intensity, sensitivity, and dynamic range of calcium detection [69-72]. Another class of GECIs are the GECO series of sensors. Similar to GcaMP, GECOs are a calcium binding protein fused to a fluorescent protein. In contrast to GcaMP, GECOs are offered in the red spectrum (RGECO), which helps to lower phototoxicity and provide greater tissue penetration because of the longer wavelength, making them useful in organoids or in tissue [73].

RGECO was successfully conjugated to troponin T (TnT) without interfering with contractility to form the GECI RGECO-TnT. RGECO-TnT is the first reported myofilament-localized calcium indicator and was able to reveal findings not seen using whole-cell methods [74]. For example, RGECO-TnT showed that myosin ATPase inhibitor MYK-461 altered calcium binding, release, and signal amplitude when the same result had not been observed using whole-cell dyes [74]. Additionally, a larger effect size was seen at the myofilament versus at the whole-cell level in response to calcium sensitizer levosimendan. RGECO-TnT is a useful tool to investigate calcium handling in the myofilament microdomain in order to better understand dysregulated calcium signalling and the role it may play in DCM phenotypes such as impaired contractility [74]. For these reasons, RGECO-TnT was selected to assess calcium transients in iPSC-CMs to gain a better understanding of myofilament calcium handling in DCM.

### *1.6 Thesis objectives and rationale*

DCM is a complex disease with many etiologies and underlying mechanisms of pathogenesis. Despite available treatments, morbidity and mortality remain unacceptably high and many patients progress to heart failure, resulting in the need for transplantation. There is a great need to better understand the mechanisms underlying DCM on a patient-to-patient basis so that personalized treatment options can be developed in order to improve patient outcomes. iPSC-CMs are useful tools in personalized disease modeling, as they recapitulate features of disease from the patient they were derived. iPSC-CMs are widely used to study diseases in a dish and have been demonstrated in their ability to model DCM to gain a better understanding of the disease and suggest novel personalized therapies. Methods to evaluate DCM using iPSCs have been published; however, have not yet been validated in our hands.

The objective of this thesis is to develop methods to characterize phenotypic features of DCM using patient-derived iPSCs. We hypothesize that iPSC-CMs can be used to evaluate phenotypes underlying DCM on a patient-to-patient level. A hallmark of DCM is impaired contractility, therefore features to be evaluated include sarcomere organization, calcium handling, contractility, and electrophysiology. Many known mutations target genes that encode proteins involved in excitation-contraction coupling, for example members of the troponin complex, RNA binding motif 20, phospholamban, titin, and myosin heavy chain [8, 16, 17]. Furthermore, patients present clinically with deficits in contractility, which has been recapitulated by various *in vitro* studies [42, 51, 54]. This thesis provides the groundwork for developing assays using iPSC-CMs from DCM patients to gain better insight to mechanisms of DCM and the associated functional consequences.

This project focuses primarily on the implementation of a phenotyping pipeline in the Hébert lab pipeline, and on the troubleshooting and development of these methods, many of which were new to the laboratory. A genetically-encoded calcium indicator was used to measure calcium transients in iPSC-CMs and a custom-made application was developed with OriginLab for calcium transient analysis. First, calcium transients of iPSC-CMs from healthy controls as well as DCM patients were evaluated and compared to demonstrate that differences can indeed be observed on a patient-to-patient level. Once this was confirmed, the response of iPSC-CMs derived from a healthy control were recorded in response to acute calcium treatment to demonstrate the functionality of the assay. The experiment was then done in iPSC-CMs derived from a DCM patient to confirm that response to treatment can be measured in iPSC-CMs derived from both DCM patients and healthy controls. Finally, DCM patient iPSC-CMs were evaluated in response

to chronic treatment with compounds previously demonstrated to stress iPSC-CMs from DCM patients but not healthy controls.

Using the same cells from the evaluation of calcium handling on a patient-to-patient basis and from the chronic treatment experiment, sarcomere organization was evaluated using microscopy-based methods. The goal of this experiment was to develop a method to multiplex assays in order to gain as much information as possible from a single plate.

Finally, additional optimizing experiments were completed to bring a specialized instrument, the CardioExcyte96 (Nanon Technologies) to our lab. The CardioExcyte96 is designed to measure contractility and electrophysiology in cardiomyocytes. Various troubleshooting and optimizing steps were performed to validate the use of this machine, and recommendations for future use will be outlined in detail.

## 2. MATERIALS AND METHODS

### 2.1 Cell lines

iPSC lines were generated by the Cecere lab (McGill University) from samples derived from patients participating in the “Heart-in-a-Dish” project run by Dr. Nadia Gianetti, Dr. Renzo Cecere, and Dr. Terry Hébert, funded by the Courtois Foundation. Briefly, peripheral blood mononuclear cells (PBMCs) were reprogrammed to iPSCs using the the Epi5™ Episomal iPSC Reprogramming Kit (Invitrogen, A15960) and the Neon Transfection System (Invitrogen, MPK5000) [75]. iPSC lines were validated using immunofluorescent staining for pluripotency markers, RT-PCR and the trilineage differentiation assay (**I. Derish, data not shown**) [76]. The following cell lines were used in the research completed in this thesis: HID041004 (healthy control), HID041019 (DCM patient), HID041020 (DCM patient), HID041100 (DCM patient), HID041101 (healthy control), and HID041110 (DCM patient). One iPSC line from a healthy volunteer, AIW002-2, was generously obtained from the Montreal Neurological Institute through the Open Biorepository, C-BIGR, and has been previously described and validated [77]. The researchers were blinded with respect to clinical information associated with each patient cell line, including sex and age.

### 2.2 Reagents

Media used in cell culture included DMEM/F12 (Wisent, 319-085-CL), mTesRPlus kit (STEMCELL Technologies, 100-0276), RPMI1640 (Wisent, 350-007-CL), RPMI1640 without D-glucose (Wisent, 350-060-CL), and RPMI1640 without phenol red (Wisent, 350-046-CL). Cells were cultured on 100mm tissue culture dishes (VWR, 10062-880), 24-well plates (Corning, 3526), 6-well plates (Thermo Scientific, 140675), or black-walled 96-well plates (Thermo Scientific Nunc, 165305). Cell culture plates were coated with Matrigel® (Corning, 355277) diluted in

DMEM/F12 or with human plasma fibronectin (Sigma Aldrich, FC010-10MG) diluted in phosphate buffered saline without  $\text{Ca}^{2+}$ , without  $\text{Mg}^{2+}$  (Corning, 21-040-CM). Cells were dissociated from plates using Accutase (Sigma Aldrich, A6964-500ML) or gentle cell dissociation reagent (STEMCELL Technologies, 100-0485). Media was supplemented with rho kinase (ROCK) inhibitor Y27632 (Selleck Chemicals, S1049) and/or knockout serum replacement (KOSR; Gibco, 10828028) following dissociation to mitigate cell death. Directed differentiation of iPSCs to cardiomyocytes was completed using CHIR99021 (Cayman Chemicals, 13122), IWP2 (Selleck Chemicals, 3533), B27 without insulin (50x) supplement (Life Technologies, 0050129SA), and B27 (50x) supplement (Life Technologies, 15504-044). Purification of iPSC-CMs was done using sodium-L-lactate (Sigma Aldrich, L7022-10G) prepared in HEPES (Fisher Scientific, BP410-500). Cells were treated with norepinephrine (Sigma Aldrich, A9512-250MG) and isoproterenol (Sigma Aldrich, I6504-1G) prepared at 100 mM in water. Cells were also treated with the following drugs prepared in dimethyl sulfoxide (DMSO; Sigma Aldrich, D2650): 10 mM nifedipine (Sigma Aldrich, N7634-1G), 100 mM propranolol HCl (Sigma Aldrich, 222984), and 100mM carvedilol (Cayman Chemicals, 15418). For experiments, cells were transduced with AAV6-RGECO-TnT made by the Canadian Neurophotonics Platform Viral Vector Core Facility (RRID:SCR\_016477). The plasmid pShuttle CMV RGECO-TnT was a gift from Matthew Daniels & Paul Robinson & Hugh Watkins (Addgene plasmid #124643 ; <http://n2t.net/addgene:124643> ; RRID:Addgene\_126463).

### *2.3 Cell maintenance and differentiation*

Plates were coated with a 1:100 dilution of Matrigel matrix in cold DMEM/F12 or 1:100 dilution of fibronectin in cold PBS. Matrigel- and fibronectin-coated plates were left to polymerize at 37°C for at least one hour. iPSCs were plated on 100mm dishes coated with Matrigel and

maintained in mTeSR Plus media with media changes every other day. At 80% confluency cells were passaged or plated for differentiation. All cells are kept in a humidified cell culture incubator set to 37°C and 5% CO<sub>2</sub>.

**Passaging:** Cells were rinsed once with DMEM/F12 before the addition of 4 mL Gentle Cell Dissociation Reagent. Cells are incubated at room temperature for 5 minutes before aspirating Gentle Cell Dissociation Reagent, rinsing cells once with DMEM/F12, and replacing with 10 mL of DMEM/F12. Cells were gently scraped and gathered for centrifugation (3 minutes at 1,200 rpm) using a glass pipette to prevent spontaneous differentiation. DMEM/F12 was aspirated, and the pellet was resuspended in mTeSR Plus by gently pipetting up and down no more than 3 times. Cells were split and transferred to a Matrigel-coated plate with a final volume of 8 mL mTeSR Plus media.

**Differentiation:** Cells were rinsed once with DMEM/F12 before the addition of 4 mL Accutase. The plate was incubated for 5 minutes at 37°C before the addition of 4 mL DMEM/F12. Cells were collected using a glass pipette and centrifuged (3 minutes at 1,200 rpm). Cells were plated in a Matrigel-coated 24 well plate at 500,000 cells per well in mTeSR Plus supplemented with rock inhibitor. The following day, media was changed to mTeSR Plus. The differentiation protocol begins on day 0 with a 5 µM CHIR99021 treatment prepared in RPMI1647 supplemented with B27 without insulin. On day 1 media was replaced with RPMI/B27 without insulin. On day 3 cells were treated with 10 µM IWP2 prepared in B27 without insulin for 2 days before replacement with RPMI/B27 without insulin on day 5. On day 7 media was changed to RPMI supplemented with complete B27 and cells began to spontaneously beat, indicating successful differentiation to cardiomyocytes. Cells were maintained in RPMI/B27 by changing media every 2-4 days. On day 12/13 RPMI1640 (no glucose) supplemented with B27 and 4 mM lactate was

used to select for cardiomyocytes. On day 16-18 cells were replated to a fibronectin-coated 6 well dish at a density of 1-1.5 million cells per well in replating media (RPMI supplemented with B27, 5% KOSR, and rock inhibitor). Media was changed every 2-3 days with RPMI/B27. Cells were replated to fibronectin-coated assay plates between days 21-23. Cells were seeded at densities between 10,000 to 60,000 cells per well in 96 well plates. iPSC-CMs were maintained in RPMI/B27 with media changes every 2-4 days and matured past day 28 before performing experiments.

#### *2.4 Calcium handling*

Calcium handling was monitored using the genetically-encoded intensiometric RGECO-TnT biosensor that localizes to troponin T in the myofilament of cardiomyocytes [74]. Cells were plated at 20,000 cells per well in 96 well plates at least 3 days before transduction. 5 days before the experiment, cells were transduced with AAV6-RGECO-TnT at a MOI of 5000 and media was changed 3 days before the experiment. On the day of the experiment, media was changed to RPMI (no phenol red) supplemented with complete B27 to minimize background caused by fluorescent phenol red. Spontaneous calcium transients in iPSC-CMs were captured at 10.4 frames per second for 15 seconds using a Zeiss Axio Observer fully automated inverted microscope with a Zeiss 20x PLAN APOCHROMAT (NA 0.8), X-Cyte 120 LED light source, and FS-14 RFP filter set (560/26 nm excitation, 620/60 nm emission, 565 dichroic mirror). For the duration of recording, cells were kept in a gas and temperature-controlled chamber (5% CO<sub>2</sub>, 37°C).

#### *2.5 Sarcomere organization*

Since RGECO-TnT localizes to the myofilament, it can be used to visualize sarcomeres. Following transduction with AAV6-RGECO-TnT, iPSC-CMs were fixed in 2% paraformaldehyde for 10 minutes and the nuclei were stained with Hoescht at a 1:1000 dilution in PBS for 10 minutes.

Images were captured using the Opera Phenix high content microscope at 20x (Perkin Elmer). Analysis was performed using Columbus (Perkin Elmer) or by blinded manual counting. For Columbus analysis, Haralick's texture features were used to evaluate sarcomere organization. The Columbus software was trained to recognize 4 levels of organization from highly organized and well-aligned sarcomeres to punctate, or severely disorganized (**Figure 5**) [77]. To train the program, at least 100 cells from each category were selected. Results are presented as percent of cells in each level of organization. Blinded manual counting used the same organization criteria on 100 cells from each cell line or treatment group.

(A)

Level	Description
1	Severely disorganized, punctate sarcomeres
2	Disorganized, little parallel arrangement of sarcomeres
3	Fairly organized, mixture of parallel and irregular arrangement of sarcomeres
4	Highly organized, all sarcomeres are parallel

(B)

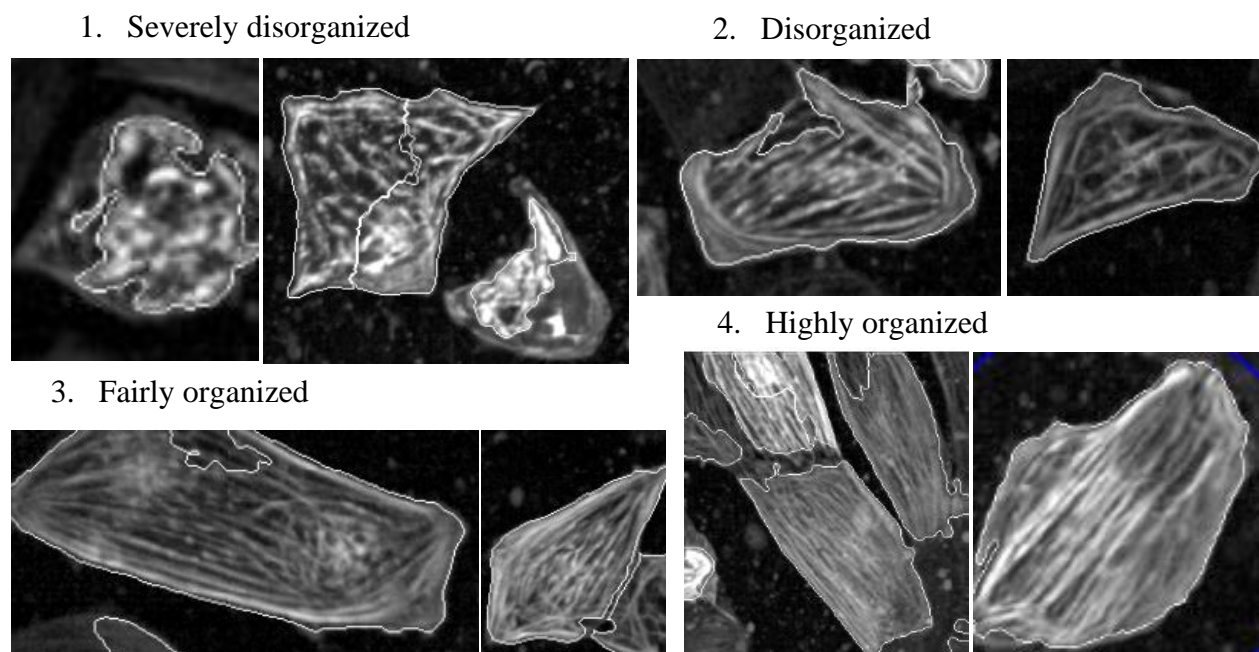


## **Figure 5. Guidelines to classify sarcomere organization of iPSC-CMs.**

**(A)** Table summarizing levels of sarcomere organization and corresponding description.

**(B)** Examples of cells that fall within each level of organization.

### *2.6 Contractility and Electrophysiology*

Contractility and electrophysiology were evaluated using the CardioExcyte96 (Nanon Technologies). The CardioExcyte96 uses electrodes to measure impedance and extracellular field potential to determine contractility- and electrophysiology-like features. This instrument was new to the lab, thus experiments focused on determining which plate types to use and how to best prepare and treat cells. Two plate types were tested: NSP-96-type standard 2mm and NSP-96 type standard stim (Nanon Technologies). Both plate types contain a reference and sensing electrode on the bottom of the well; however, the standard stim plate also includes a stimulating electrode to pace iPSC-CMs. The CardioExcyte96 can be used to measure impedance and extracellular field potential. Impedance is a measure of the resistance posed by the cells to the alternating current between the reference and sensing electrodes. As cardiomyocytes contract, their shape changes. This changes the resistance detected between the reference and sensing electrodes, giving a surrogate for contractility in the form of impedance measurements. Extracellular field potential (EFP) is a measurement of electric activity outside of the cell during a contraction cycle and serves as a surrogate measure for action potential. Formation of a monolayer is extremely important for the accurate measurement of impedance and EFP.

Plating densities were optimized using clear-bottom 96-well plates and optimal densities were found to be 50,000 to 60,000 cells per well for various iPSC-CM lines. Cells were plated 5 days in advance of an experiment to allow the monolayer to form. Media was changed on days 1 and 5 after plating.

## 2.7 Treatments

Given the role adrenergic signalling plays in cardiac physiology and disease progression, iPSC-CMs were evaluated in response to adrenergic stimulation by norepinephrine and isoproterenol. Clinically relevant  $\beta$ -blockers were used to evaluate their effects on iPSC-CMs in response to adrenergic agonists.

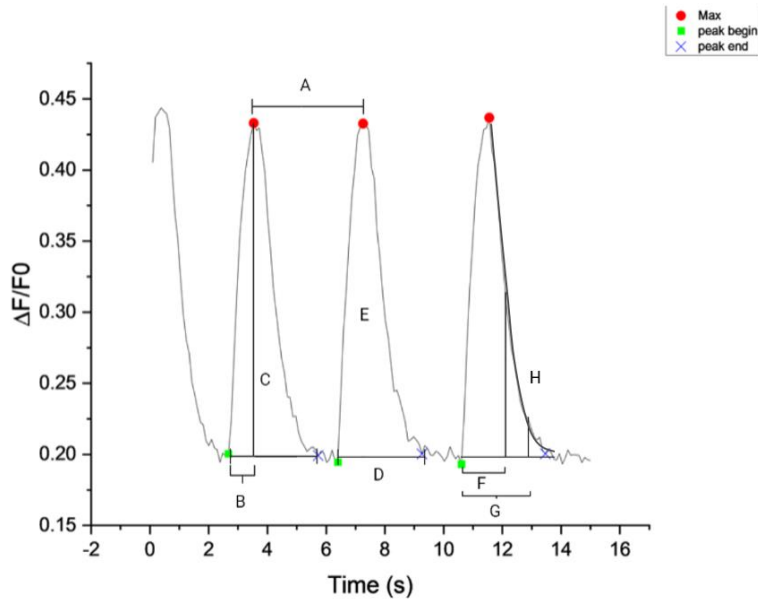
For acute experiments, cells were treated with 10  $\mu$ M norepinephrine, 10  $\mu$ M isoproterenol, 1  $\mu$ M nifedipine (L-type calcium channel blocker), or a DMSO vehicle control. To study calcium transients, 15 second videos were recorded 5 minutes after the addition of these compounds. To study contractility and electrophysiology, readings were recorded after compound addition every 4 minutes for 20 minutes then every 10 minutes for one hour and finally every 20 minutes for another 2 hours.

For chronic experiments, cells were treated with 10  $\mu$ M norepinephrine, with or without 0.25  $\mu$ M carvedilol. A DMSO vehicle control was prepared following the same dilutions during preparation of carvedilol. Media with ligand was refreshed every day for 7 days and calcium transients were recorded on Day 0 before treatment and every 24 hours for 7 days.

## 2.8 Data analysis

Sarcomere organization was determined manually and using Columbus software v2.7.1 (Perkin Elmer) as described above. Single cell calcium transients were extracted from image stacks using ImageJ and were analyzed using the custom Transient Analysis app in OriginPro 2021b v9.8.5 (OriginLab). Transients were assessed for time to peak, peak amplitude, time between peaks, transient duration, area under the curve, time to reach 50% baseline, and time to reach 90% baseline (**Figure 6**). Other values calculated but not shown in **Figure 6** are transient frequency and

upstroke velocity. Values were averaged for all transients that occurred in each video to give one value per cell. Graphing and statistical analysis was done using the Paired Comparison Plot app in OriginPro 2021b with a Tukey correction or by using GraphPad Prism v9.3.1 with a one-way ANOVA and Tukey's multiple comparisons test. Sarcomere organization was graphed using GraphPad Prism.



Identifier	Feature	Definition
-	Baseline	Fluorescence between spontaneous beats
A	Time between peaks (s)	Time between successive peaks
B	Time to reach peak maximum (s)	Time taken to reach maximum peak height from baseline
C	Transient amplitude (dF/F0)	Distance between baseline and maximum peak height
D	Transient duration (s)	Time taken to reach peak end from peak beginning
E	Area under the curve (dF/F0)	Integral of a transient
F	Time taken to reach 50% baseline (s)	Time taken from the peak to reach 50% between peak and baseline
G	Time taken to reach 90% baseline (s)	Time taken from the peak to reach 90% between peak and baseline
H	Decay tau (s)	Exponential time constant found by monoexponential curve fitting
-	Upstroke velocity (dF/(F0*s))	Speed at which the transient reaches peak maximum from minimum
-	Transient frequency	Number of transients that occur in one minute

**Figure 6. Features of calcium transients that can be analyzed using the Transient Analysis app in OriginPro2022.**

Analysis is conducted on a single-cell level to generate one transient graph per cell. The features of calcium transients that are analyzed are shown on the graph and defined in the table. Features are determined for each transient in a given video and averaged to give one value per cell.

Impedance and extracellular field potential measurements were analyzed using Nanion's DataControl96 software v1.8.0. For impedance, beat rate and amplitude were assessed and for extracellular field potential, amplitude and field potential duration were assessed. Graphs were taken directly from the DataControl96 software or made using GraphPad Prism.

### 3. RESULTS

The goal of this thesis was to develop assays to phenotype features underlying disease in iPSC-CMs derived from DCM patients. Given the prominent role dysregulated contractility plays in the pathology of DCM, assays were developed to interrogate features of cardiomyocyte contractility. These features include calcium handling, sarcomere organization, functional contractility, and electrophysiology. Since adrenergic signalling plays a role in cardiac physiology and pathophysiology, assays were developed to measure iPSC-CM response to adrenergic ligands.

#### *3.1 Calcium handling and sarcomere organization*

RGECO-TnT is an intensimetric-based biosensor that localizes to troponin T in the myofilament of cardiomyocytes. RGECO-TnT fluoresces to indicate calcium binding to the troponin complex, which initiates the contraction of myofilaments ([Figure S1](#)). Individual cells can be discerned in the captured image stacks, allowing the monitoring of single-cell calcium handling of iPSC-CMs. A method was developed to use RGECO-TnT to monitor single-cell calcium transients at the myofilament level in iPSC-CMs derived from DCM patients and healthy controls under basal conditions and in response to treatment. Since RGECO-TnT is expressed at the myofilament, it can also be used to visualize the sarcomeres of cardiomyocytes to evaluate their level of organization. To the best of our knowledge, this thesis marks the first comparison of iPSC-CMs from 2 control subjects and 4 DCM patients in terms of calcium handling and sarcomere organization, making it one of the largest comparisons to date.

##### *3.1.1 Calcium handling differs between healthy controls and DCM patients*

This method to detect myofilament-localized single-cell calcium transients using iPSC-CMs expressing RGECO-TnT was first validated by measuring calcium transients in iPSC-CMs from two healthy controls and four DCM patients (**Figure 7** and **Figure S2**).

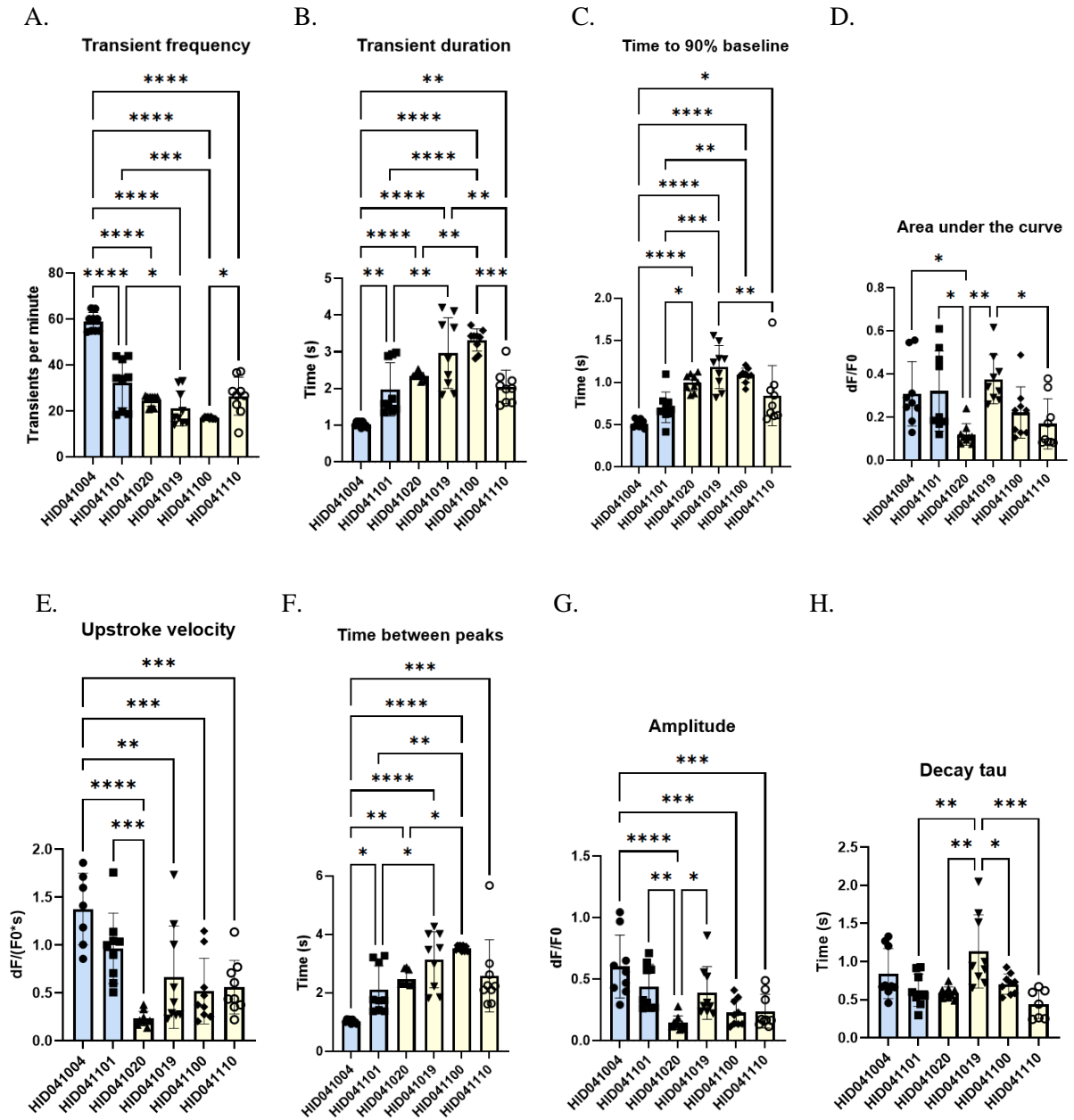


**Figure 7. Features of calcium transients in iPSC-CMs derived from healthy controls and DCM patients.**

Calcium handling was assessed in iPSC-CMs derived from healthy controls (blue: HID041004 and HID041101) and DCM patients (yellow: HID041020, HID041019, HID041100, HID041110). Features evaluated include: A. Transient frequency (transients per minute), B. Transient duration (seconds), C. Time to 90% baseline (seconds), D. Area under the curve (dF/F0), E. Upstroke velocity (dF/(F0\*s)), F. Time between peaks (seconds), G. Amplitude (dF/F0), and H. Decay  $\tau$  (seconds). n = 9 cells from 1-2 biological replicates. Single cell transients for each cell line are found in Figure S2. \* = p<0.05, \*\* = p<0.01, \*\*\* = p<0.001, \*\*\*\* = p<0.0001.

Initial proof-of-concept results indicate that differences in myofilament-localized calcium handling between DCM patients and healthy controls as well as between DCM patients can be detected using an iPSC-CM model. Features of calcium transients such as time between peaks, transient frequency, and upstroke velocity show a general trend of iPSC-CMs from DCM patients having slower spontaneous calcium transients than iPSC-CMs from healthy controls (**Figure 7**). Furthermore, calcium transients from DCM patients were shown to have lower amplitudes and longer transient durations than healthy controls. Features such as time to 90% baseline, transient duration, decay tau, and area under the curve exemplified that this model of RGECO-TnT expressed in iPSC-CMs can be used to detect differences in myofilament-localized calcium handling between DCM patients (**Figure 7**). Single cell calcium transients (**Figure S2**) show no variation in transient patterns between iPSC-CMs from healthy control HID041004 and little variation between cells from healthy control HID041101. DCM patient HID041020 showed a pattern of single cell calcium transients comparable to that of healthy control HID041101. DCM patients HID041019 and HID041110 showed a less uniform interval of time between calcium transients while HID041100 showed a uniform, but increased interval of time between transients compared to healthy controls. These interesting initial results indicate RGECO-TnT expressed in iPSC-CMs can be used to detect differences in myofilament-localized calcium handling on a patient-to-patient level.

### *3.1.2 Sarcomere organization of iPSC-CMs from healthy controls and DCM patients*

Sarcomere organization was evaluated using the same plates from the experiments evaluating calcium handling in iPSC-CMs derived from healthy controls and DCM patients. Two methods to evaluate sarcomere organization were compared: manual sorting and a machine-trained

algorithm (Figure 8). Both methods utilized the guidelines outlined in Figure 5 to assess sarcomere organization on a scale from severely disorganized to highly organized.

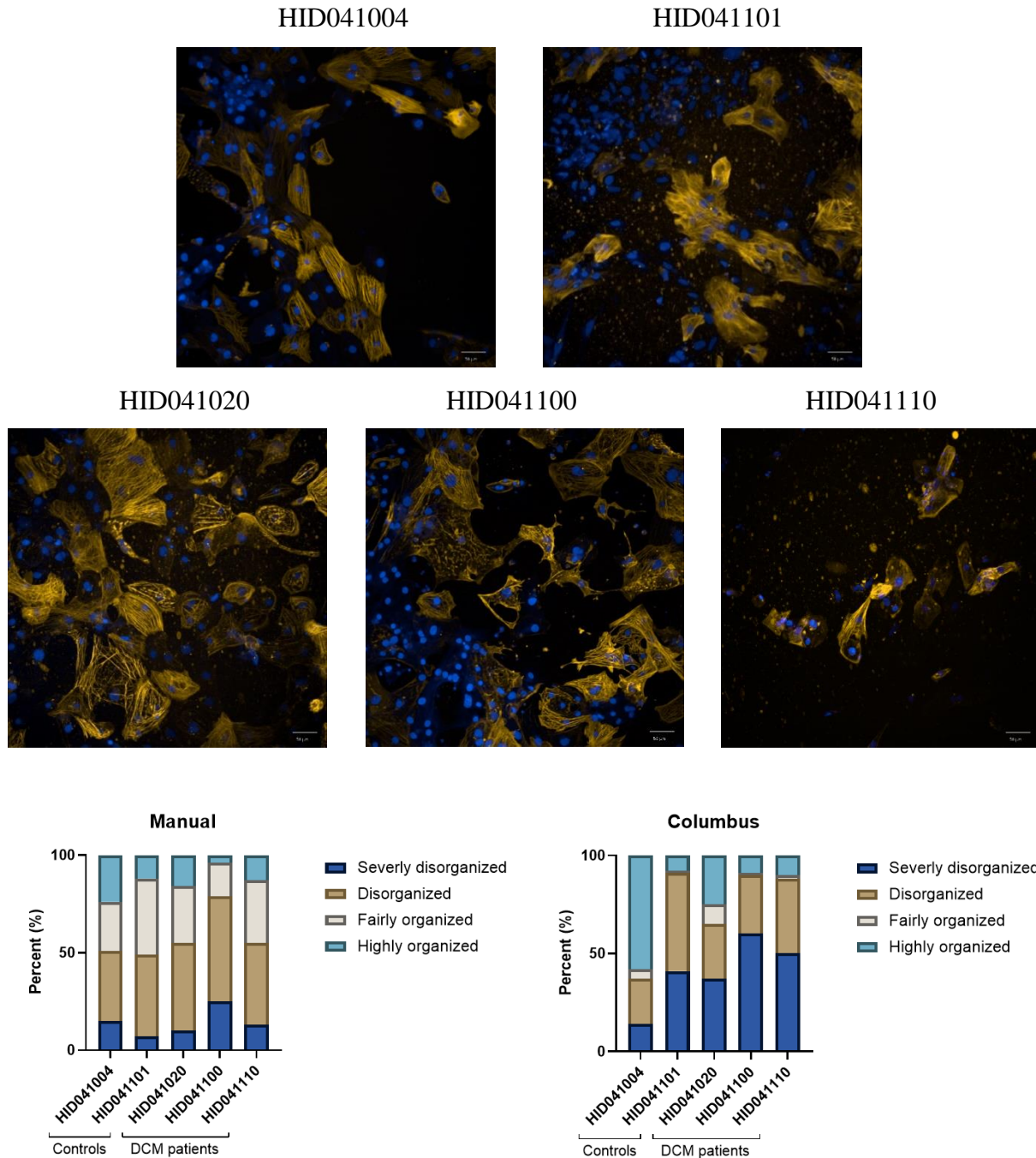


**Figure 8. Sarcomere organization evaluated using RGEKO-TnT to visualize troponin T in the myofilament.**

Top: Representative fluorescent pictures of 2 healthy control iPSC-CM lines (HID041004 and HID041101) and 3 DCM patient lines (HID041020, HID041100, HID041110) expressing

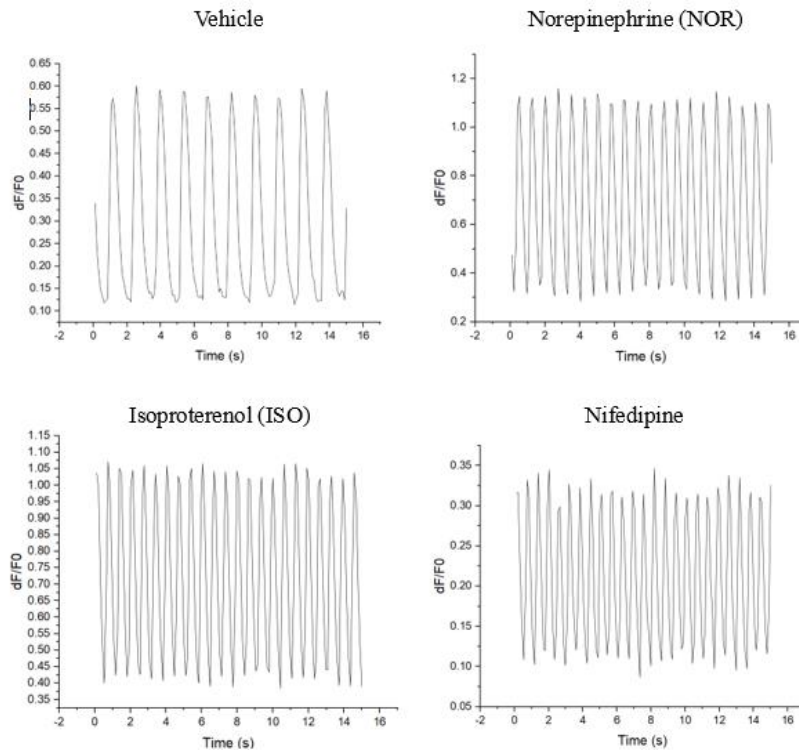
RGECO-TnT. Yellow: RGECO-TnT, Blue: Hoescht. The scale bar in the bottom right corner indicates 50  $\mu$ M **Bottom**: Comparison of methods to evaluate sarcomere organization. Manual sorting of 100 cells per cell line into the appropriate level of organization versus a trained program on Columbus that identified the organization of 500-3000 cells per line.

The two methods to classify sarcomere organization of iPSC-CMs yielded widely differing results with Columbus identifying more severely disorganized cells yet a higher proportion of highly organized cells compared to manual counting (**Figure 8**). The majority of cells counted manually fall within the disorganized or fairly organized categories. There are various factors that can play into this discrepancy such as number of cells counted and ability of Columbus to accurately recognize cells. While Columbus can be trained to sort thousands of cells into levels of varying organization, the program struggles with accurately identifying the border of cardiomyocytes when sarcomeres are being visualized. The linear nature of sarcomeres can disguise them as the border of the cell and may not be accurately distinguished, especially when cells grow densely packed as a group. Settings in the program can be adjusted to those that best and most accurately identify individual iPSC-CMs. Despite this limitation, the vastly larger number of cells used to evaluate sarcomere organization as well as reducing investigator bias by generating an algorithm to objectively sort cells into groups makes Columbus an attractive option to measure sarcomere organization.

When using Columbus to evaluate sarcomere organization, control line HID041004 shows a high proportion of nicely aligned sarcomeres, as expected. In the contrary, the other control line evaluated, HID041101, showed a highly disorganized pattern similar to that of the DCM patients. Out of the patient lines, HID0401020 showed the highest proportion of organized cells and the other lines showed similar distributions of sarcomere organization. Future studies will optimize membrane stains that can be used to assist Columbus in accurately recognizing individual cells.

### 3.1.3 Calcium handling differs in response to treatment in a healthy control cell line

To determine if RGECO-TnT can be used to detect changes in myofilament-localized calcium handling in response to treatment, iPSC-CMs from control line HID041004 were treated acutely with adrenergic agonists isoproterenol and norepinephrine as well as calcium channel blocker nifedipine. Isoproterenol and norepinephrine were selected due to chronotropic activity and nifedipine was selected to demonstrate a decrease in calcium signal in response to inhibition of calcium channels.



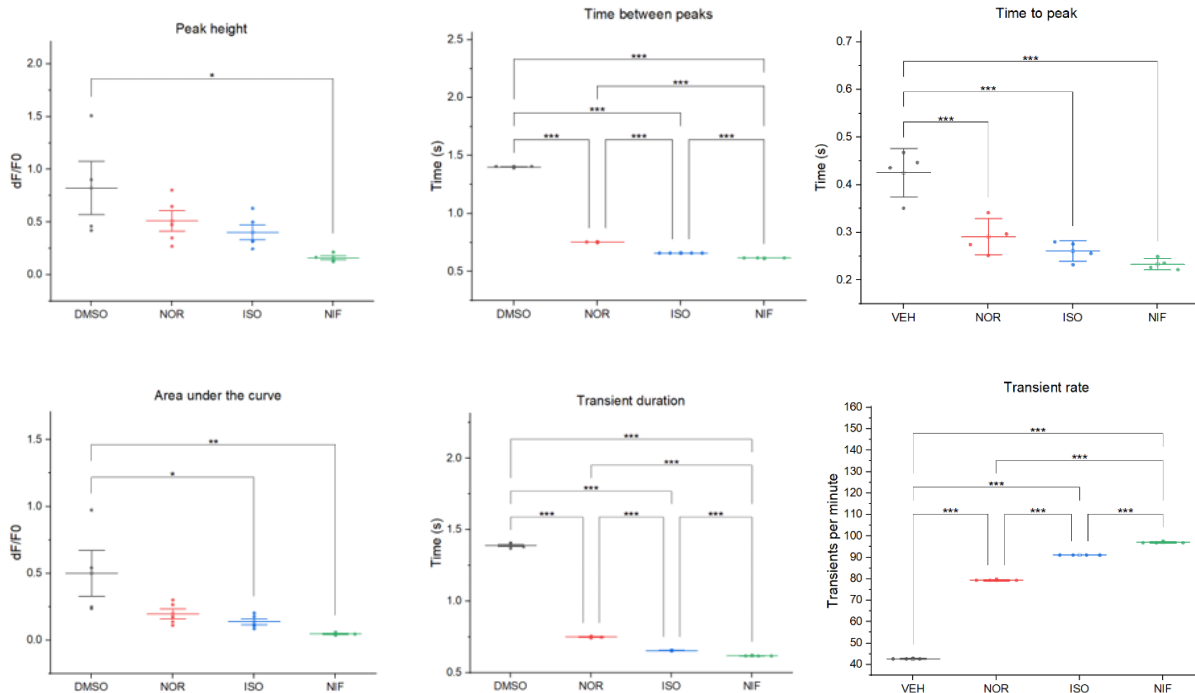


**Figure 9. Calcium transients in iPSC-CMs derived from control HID041004 in response to acute treatment.**

Top: Representative single-cell calcium transients in response to 5 minutes of treatment with vehicle, norepinephrine, isoproterenol, or nifedipine. Bottom: Features of calcium transients in response to treatment. n=1, 3-5 cells per treatment condition. \* = p<0.05, \*\* = p<0.01, \*\*\* = p<0.001.

As expected, the positive chronotropes isoproterenol and norepinephrine increased transient rate as indicated by a decrease in time between peaks and transient duration (**Figure 9**). Nifedipine decreased peak height and area under the curve after 5 minutes of treatment compared to the vehicle control, indicating decreased calcium handling activity (**Figure 9**). No other features of transients showed statistically significant differences.

### 3.1.4 Calcium handling differs in response to treatment in a DCM patient cell line

Following method validation for measuring single-cell calcium handling in a healthy patient line, response to chronotropic compounds isoproterenol and norepinephrine were evaluated in DCM patient line HID041019 to determine if changes can be detected in the patient population.

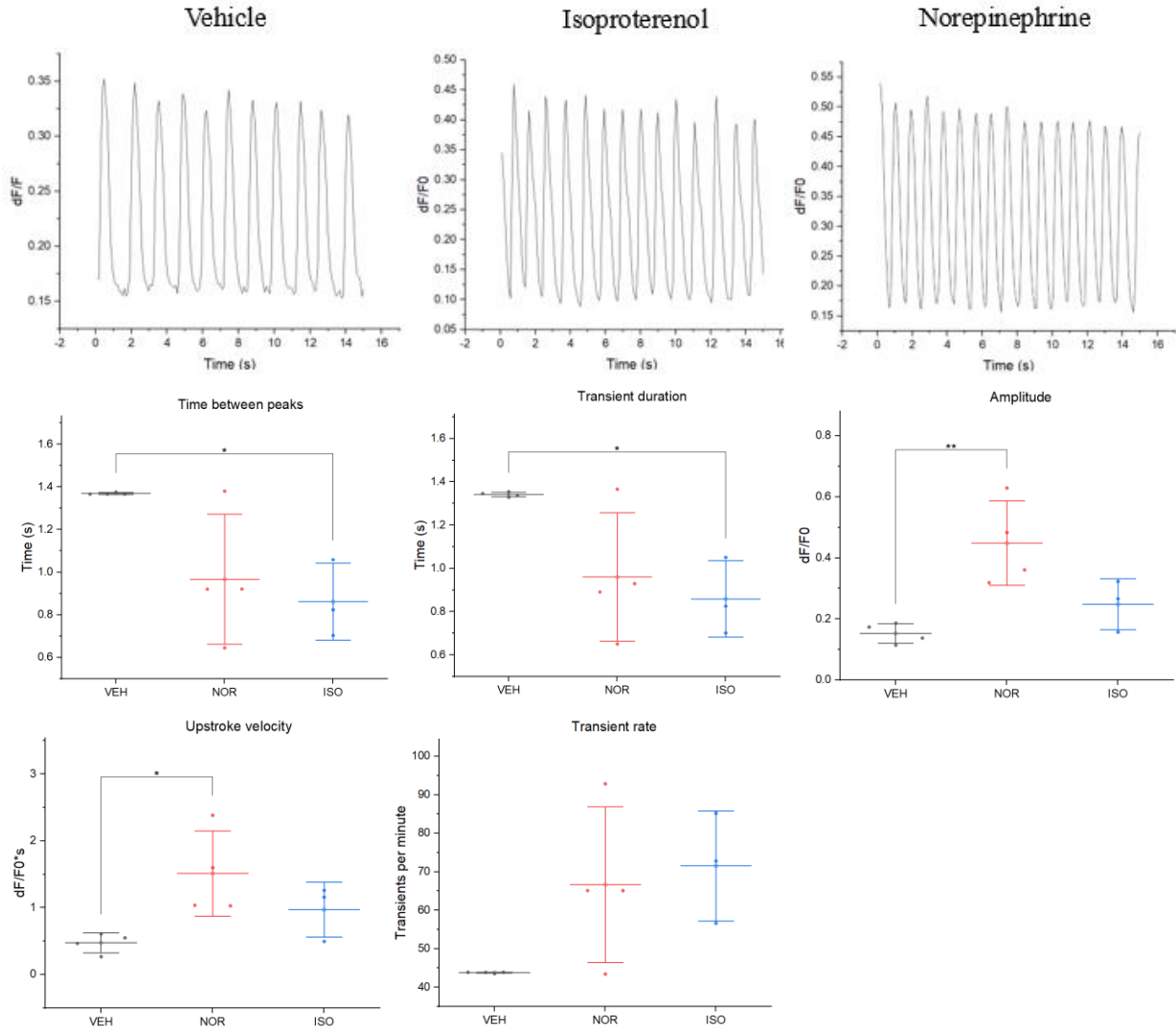


**Figure 10. Calcium transients in iPSC-CMs derived from DCM patient HID041019 in response to acute treatment.**

Top: Representative single-cell calcium transients in response to 5 minutes of treatment with vehicle, norepinephrine or isoproterenol. Bottom: Features of calcium transients in response to treatment. n=1, 3-5 cells per treatment condition. \* = p<0.05, \*\* = p<0.01.

As seen in the control cell line HID041004, the DCM patient line also demonstrated an increase of calcium transient frequency in response to isoproterenol as indicated by the decreased time between peaks and transient duration (**Figure 9** and **Figure 10**). However, no statistical change in these features were noted in response to norepinephrine. Norepinephrine treatment increased peak amplitude and upstroke velocity (**Figure 10**). No other features of transients showed statistically significant differences.

These experiments demonstrated that RGECO-TnT can be used to measure myofilament-localized calcium transients in response to acute treatment in iPSC-CMs derived from both healthy controls and DCM patients. The following experiment investigated using RGECO-TnT to measure calcium handling and sarcomere organization in response to a stressor in a DCM patient iPSC-CM line.

### *3.1.5 Calcium handling and sarcomere organization in response to chronic treatment*

DCM patients have been reported to have dysregulated adrenergic signalling pathways, which can lead to the destructive cycle of desensitization of adrenergic receptors and the overproduction of catecholamines such as norepinephrine and ultimately disease pathogenesis [36]. The norepinephrine stress test is used to recreate an environment that could lead to the development of contractile dysfunction and dysregulated calcium handling seen in DCM patients [43]. In previous studies iPSC-CMs from patients with DCM were exposed to 10  $\mu$ M norepinephrine every day for 2-7 days, after which calcium handling and sarcomere organization were recorded for the development of abnormalities [43, 51]. iPSC-CMs were treated with clinically used  $\beta$ -blocker carvedilol to determine its effect in cells stressed with norepinephrine. Treatments were assessed over the course of 7 days (**Figure 11**) and features of calcium transients before treatment (baseline) and after 7 days of treatment were compared (**Figure 12**). At the end

of the 7-day treatment, sarcomere organization was assessed to determine the effect of norepinephrine, in the presence and absence of carvedilol (**Figure 13**).

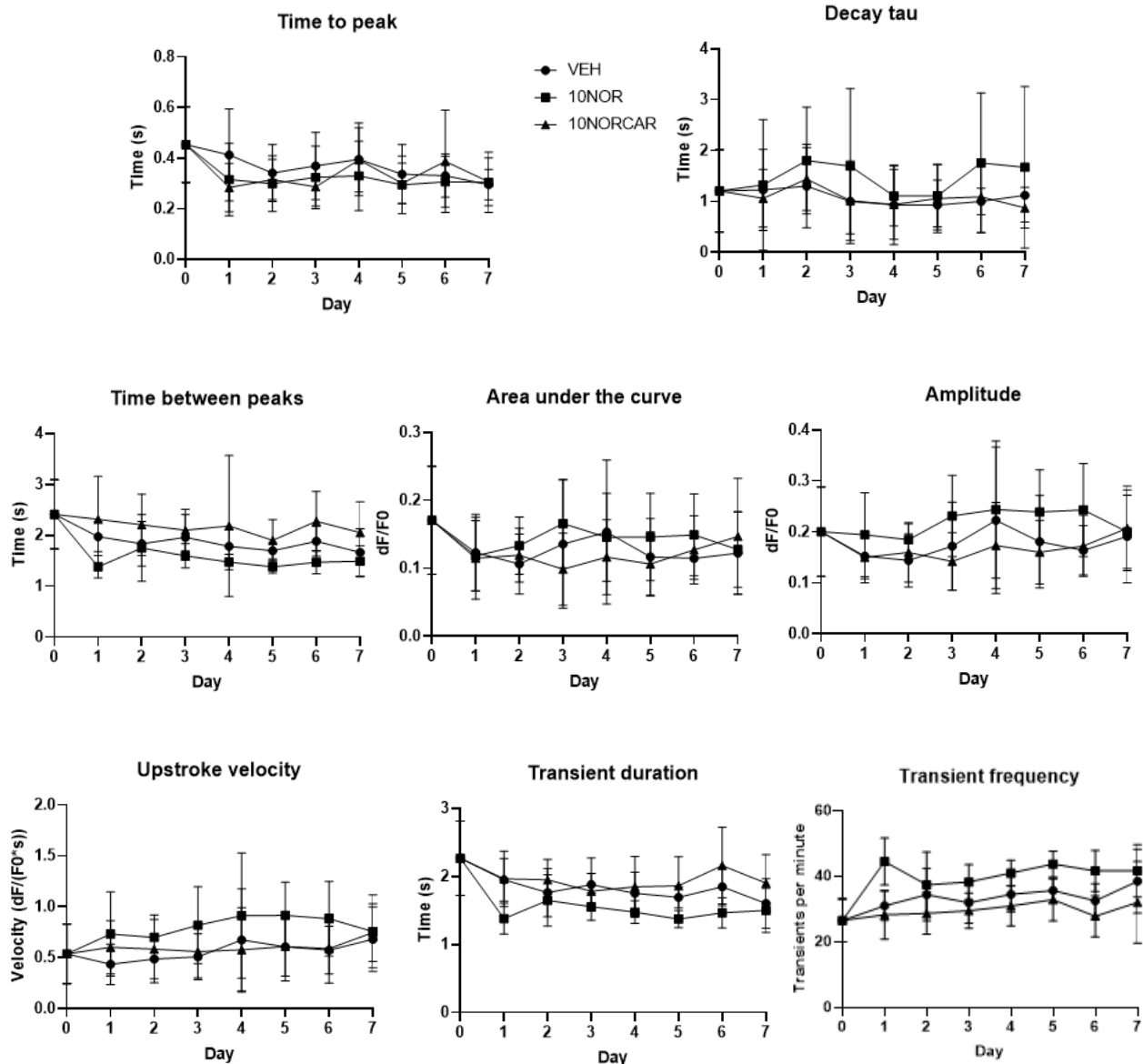


**Figure 11. Features of calcium transients in iPSC-CMs from DCM patient HID041020 in response to 7 days of treatment.**

Cells were treated with 10 μM norepinephrine, in the presence and absence of 0.25 μM carvedilol. Recordings were taken before treatment and every 24h after treatment for 7 days. Media containing DMSO (VEH), 10 μM norepinephrine (10NOR), and/or 0.25 μM carvedilol (10NORCAR) was refreshed every 24h. n = 4 biological replicates, 15-25 cells per condition.

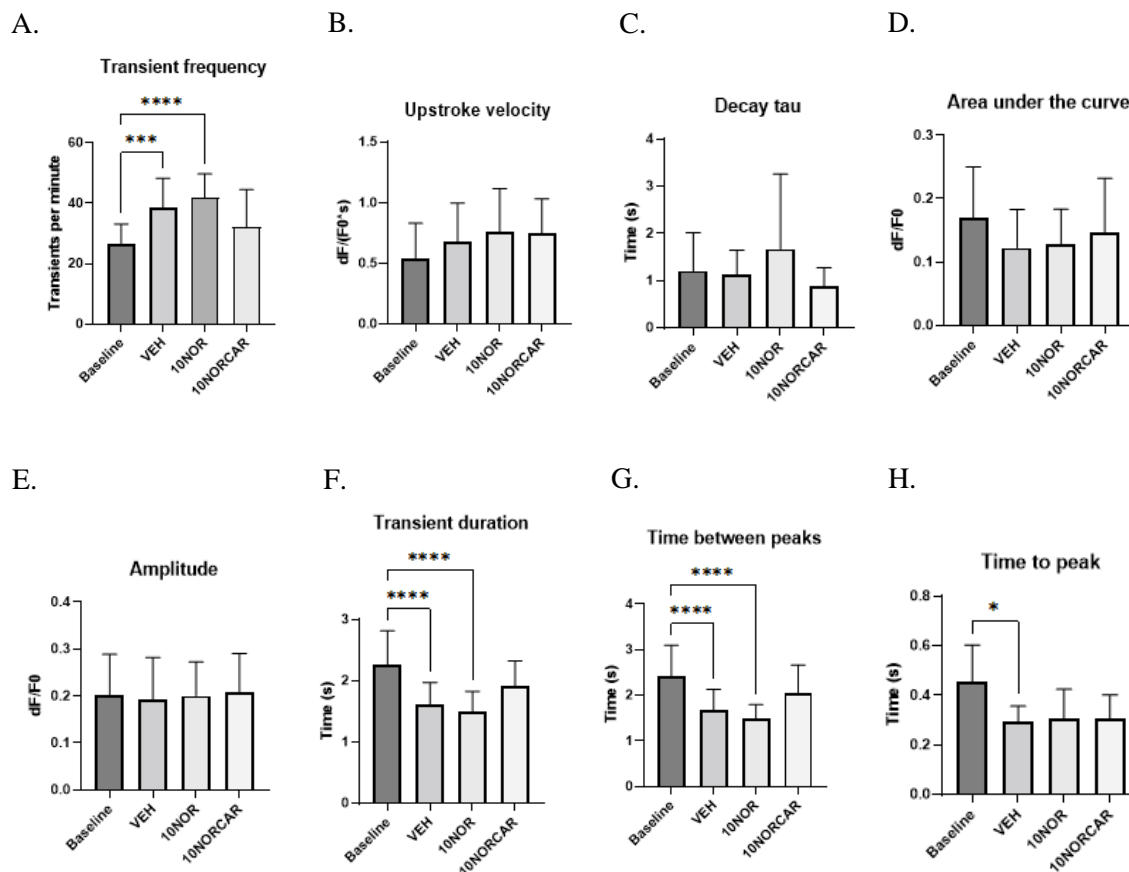


**Figure 12. Comparison of features of calcium transients in DCM patient HID041020 before treatment and after 7 days of treatment.**

iPSC-CMs were treated for 7 days with 10  $\mu$ M norepinephrine (10NOR), in the presence and absence of 0.25  $\mu$ M carvedilol (10NORCAR) or with DMSO (VEH). Comparison of iPSC-CMs from DCM patient HID041020 at baseline (before treatment) and after 7 days of treatment. Features evaluated include: A. Transient frequency (transients per minute), B. Upstroke velocity ( $dF/(F_0 \cdot s)$ ), C. Decay  $\tau$  (seconds), D. Area under the curve ( $dF/F_0$ ), E. Amplitude ( $dF/F_0$ ), F. Transient duration (seconds), G. Time between peaks (seconds), and H. Time to peak (seconds).  $n = 4$  biological replicates, 15-25 cells per condition \* =  $p < 0.05$ , \*\*\* =  $p < 0.001$ , \*\*\*\* =  $p < 0.0001$ .

Over the course of 7 days, an unexpected change in features related to frequency of calcium transients was noted in non-treated cells (**Figure 11**, **Figure 12**, and **Figure S3**). Transient frequency showed an increasing trend while transient duration, time between peaks, and time to peak showed a decreasing trend over the course of 7 days, indicating shorter and more frequent transients in response to vehicle (**Figure 11**). As expected, norepinephrine treatment showed an increasing trend in transient frequency and decrease in time between peaks and transient duration

(**Figure 11**). Carvedilol in addition to norepinephrine rendered results to become more similar to that of the vehicle control (**Figure 11**). However, these observations are simply based on trends. When comparing iPSC-CMs before treatment and after 7 days of treatment, few statistically significant changes were observed (**Figure 12**). As noted above, an unexpected change in features such as transient frequency, transient duration, time between peaks, and time to peak were observed in response to treatment with vehicle (**Figure 12** and **Figure S3**). This may be due to changes in iPSC-CM maturity over time. Previously we found that expression of key cardiac genes in iPSC-CMs does not change significantly after 28 days in culture therefore this was our chosen benchmark for iPSC-CM maturity (**H. Sadighian, data not shown**); however, change in basal calcium handling over time has not yet been evaluated. The issue of maturity in iPSC-CMs will be further elaborated in the discussion section. In response to 7 days of treatment with norepinephrine, transient frequency increased while transient duration and time between peaks decreased compared to before treatment (**Figure 12**). This indicates faster and shorter calcium transients in response to norepinephrine treatment. These changes in calcium transients were diminished by the presence of carvedilol, as indicated by results similar to the baseline (**Figure 12**). Following collection of calcium transient data, iPSC-CMs were prepared for sarcomere assessment (**Figure 13**). In response to 7 days of treatment with norepinephrine, there was no difference in sarcomere organization noted. The proportion of cells with highly organized, fairly organized, disorganized, and severely disorganized sarcomeres remained constant between vehicle, norepinephrine, and norepinephrine with carvedilol (**Figure 13**).

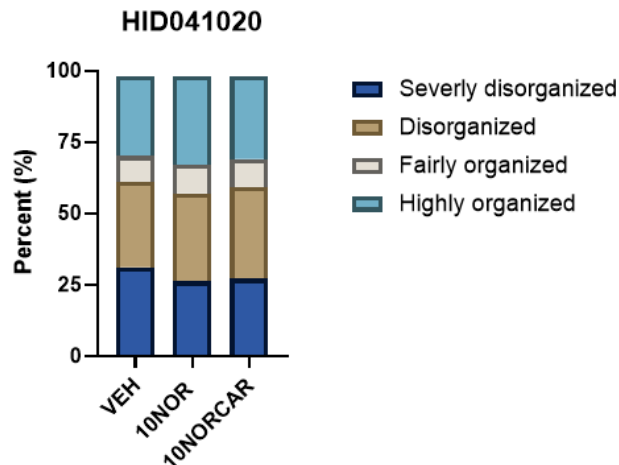


**Figure 13. Sarcomere organization of iPSC-CMs from DCM patient HID041020 after 7 days of treatment.**

iPSC-CMs were treated with DMSO (VEH), 10  $\mu$ M norepinephrine (10NOR), and 0.25  $\mu$ M carvedilol with norepinephrine (10NORCAR). Images were evaluated using a program trained using our data on Columbus, n=2500-3000 cells per condition.

In summary, RGECCO-TnT was shown to not only be able to measure myofilament-localized single cell calcium transients, but also measure sarcomere organization of iPSC-CMs from both healthy control and DCM patient populations. Differences in calcium handling and sarcomere organization was observed both on a patient-to-control and patient-to-patient basis. Furthermore, acute response to adrenergic agonists were able to be detected in both control- and patient- derived iPSC-CMs in terms of calcium handling. Finally, chronic treatment with norepinephrine was evaluated in a DCM patient cell line to evaluate the effect of stress on iPSC-CMs on calcium handling and sarcomere organization. While some changes were observed, this did not reflect the severe responses reported in literature [43, 51].

### 3.3 Contractility and electrophysiology

Contractility and electrophysiology were assessed using the CardioExcyte96 by Nanion Technologies. Nanion Technologies offers a variety of plates designed for this system. These 96-well plates have electrodes on the bottom of the wells to measure impedance- and extracellular

field potential- based measures to evaluate contractility and electrophysiology of iPSC-CMs. All CardioExcyte96 plates come with reference and sensing electrodes and some models come with a stimulating electrode that allows for pacing of cells and less noisy measurements. To optimize this experiment, plates with and without stimulating electrodes were used and iPSC-CMs were evaluated in response to adrenergic stimulation.

### *3.3.1 Evaluating contractility in control iPSC-CMs*

The first optimization experiment was done using a standard NSP 96-well plate without a stimulating electrode. AIW002-2 control iPSC-CMs were plated at various cell densities from 20,000 to 50,000 cells per well to determine the optimal density to achieve a monolayer. Cells were then treated with norepinephrine and vehicle control (DMSO). Beat rate and amplitude over time in response to treatment are shown in **Figure 14** for wells plated at 50,000 cells per well. Densities lower than 50,000 cells per well had very noisy or no measurements, indicating improper formation of the monolayer (results not shown). An increase in beat rate is noted in response to both vehicle control and norepinephrine, with norepinephrine evoking a higher response before falling back down about 30 minutes after treatment. An increase in peak amplitude is noted about 10 minutes after treatment with vehicle followed by a gradual decline in peak height to lower than the before-treatment baseline. This unexpected increase is likely due to interference by removing the plate for compound addition, resulting in aberrant and noisy results. A similar trend is noted in response to norepinephrine treatment; however, to a much lower degree. Norepinephrine has a lower baseline amplitude than vehicle control, which may be due to lower impedance. This could indicate poor formation of the monolayer, which is a critical factor in measuring impedance.

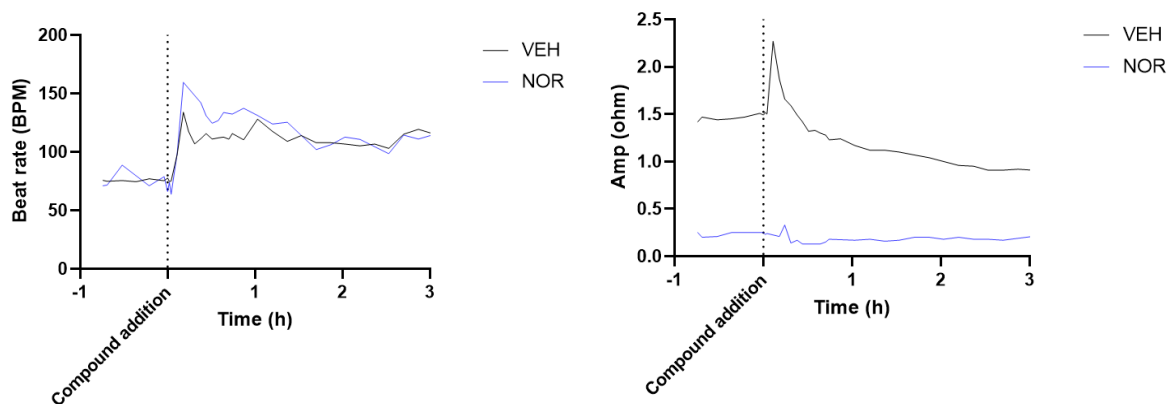


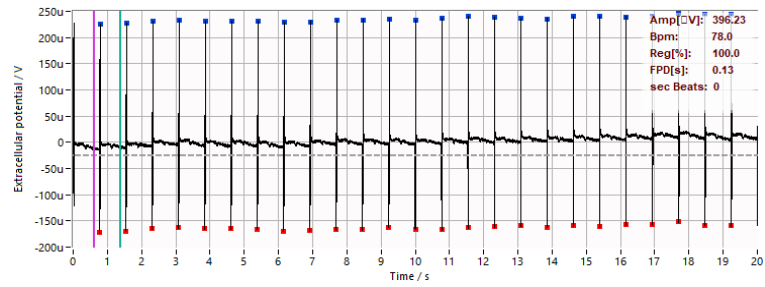
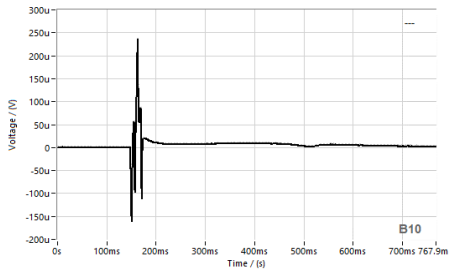
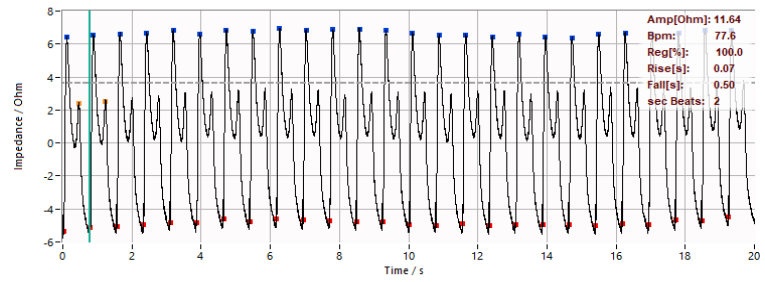
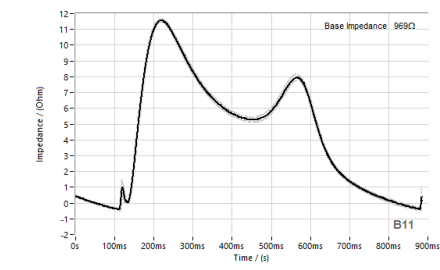
**Figure 14. Pilot assay of healthy control AIW002-2 iPSC-CMs using the CardioExcyte96 to evaluate contractility.**

Beat rate (left) and amplitude (right) of iPSC-CMs from a healthy control subject (AIW002-2) in response to treatment with 10  $\mu\text{M}$  norepinephrine (NOR) or a DMSO control (VEH)  $n=3$  wells.

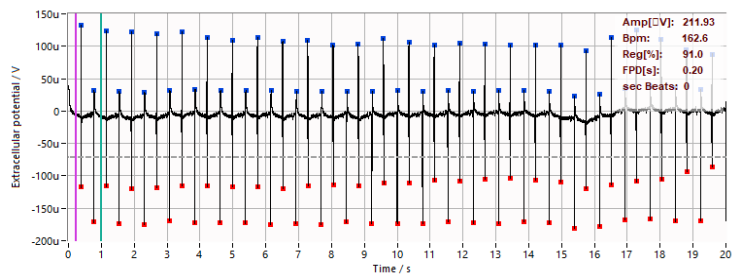
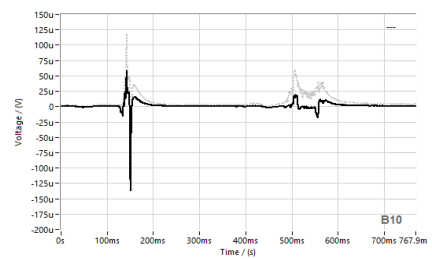
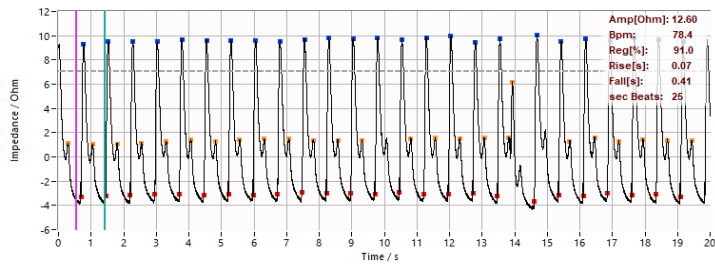
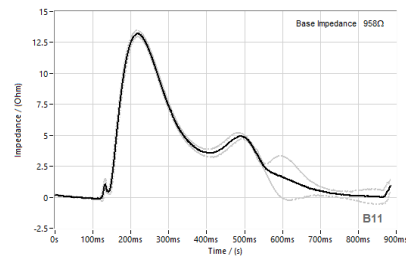
### 3.3.2 Evaluating contractility and electrophysiology in DCM patient derived iPSC-CMs

The next experiment evaluated iPSC-CMs derived from a DCM patient on a plate with stimulating electrodes. Since previous results indicated the importance of ensuring a properly formed monolayer, cell density was first optimized by plating iPSC-CMs at densities between 20,000 to 100,000 cells per well and staining with CellMask to image the plasma membrane (**Figure S4**). A seeding density of 50,000 to 60,000 cells per well was determined to form a monolayer 7 days after plating. HID041020 DCM patient iPSC-CMs were plated at 50,000 cells per well on a NSP96 plate with a stimulating electrode and allowed to grow for 7 days before the experiment. Cells were paced at 1 Hz and pre-treated with  $\beta$ -blocker propranolol (5  $\mu\text{M}$ ) for 30 minutes before treatment with norepinephrine (10  $\mu\text{M}$ ) or isoproterenol (10  $\mu\text{M}$ ). Changes in beat rate and amplitude (impedance-based) and between amplitude and field potential duration (EFP-based) over time were recorded (**Figure 15** and **Figure 16**).

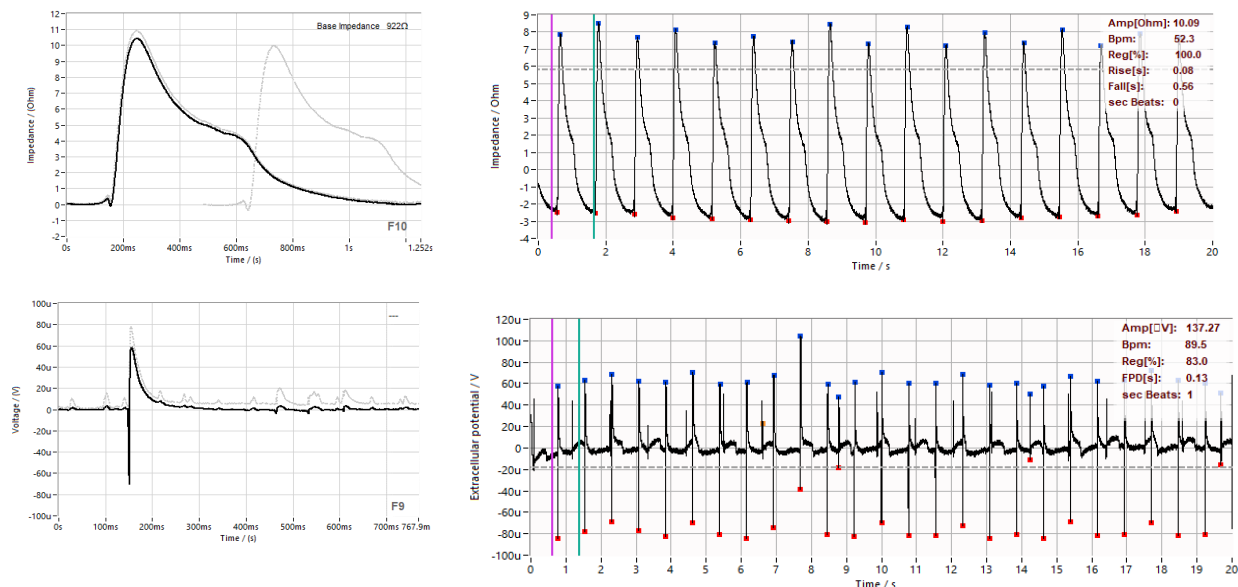
## A. Before norepinephrine treatment



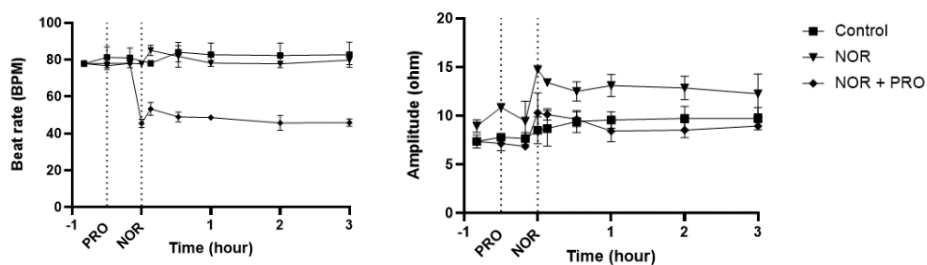
## 10 minutes after norepinephrine treatment



## 10 minutes after norepinephrine treatment with propranolol pre-treatment



### B. Impedance:



### Extracellular field potential:

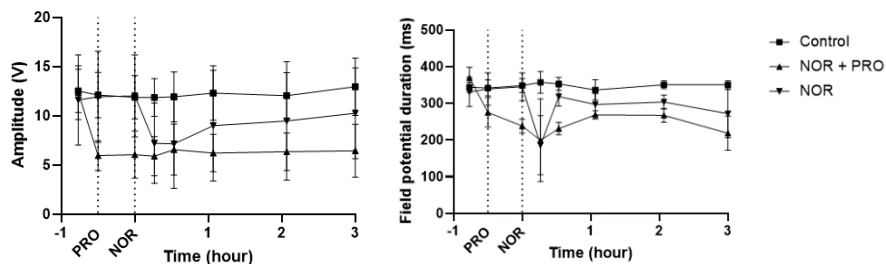


**Figure 15. Contractility and electrophysiology of DCM patient HID041020 in response to treatment with norepinephrine.**

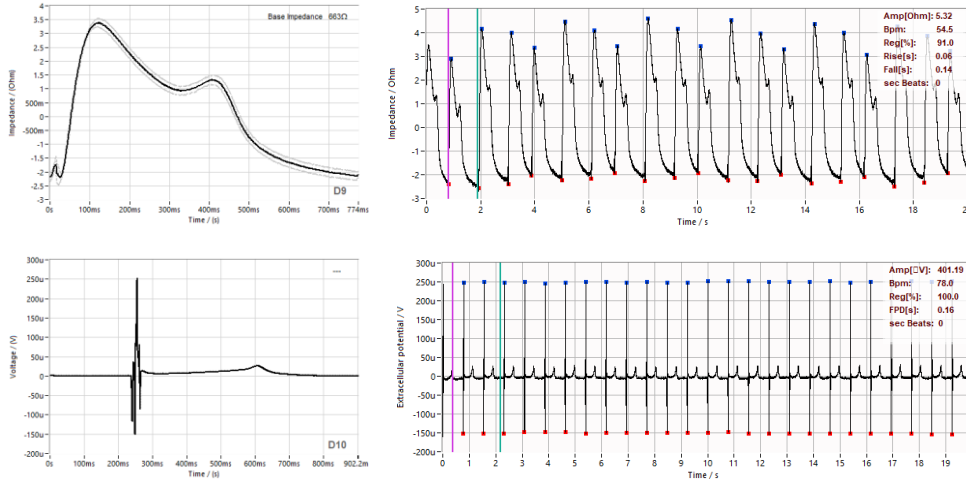
**A.** Representative example mean beats and sequence of contractions as well as mean EFP traces and sequence of traces of iPSC-CMs from a DCM patient (HID041020) in response to norepinephrine treatment. Cells were treated for 10 minutes with norepinephrine (NOR) treatment, with and without a 30 minute propranolol (PRO) pretreatment. **B.** Impedance- and extracellular field potential- based measurements over time in response to norepinephrine treatment, with and without propranolol pre-treatment, n=3.

Using DataControl96 software (Nanon Technologies), we are able to visualize the mean beat of a population of cells in a well in addition to all of the traces over the recording duration. At baseline before norepinephrine treatment, an irregular beat shape is observed as indicated by the second peak within the period of one beat (**Figure 15A**). EFP traces showed no abnormalities. In response to 10 minutes of treatment with norepinephrine, an abnormal EFP measure was developed and impedance results show an irregular beating pattern (**Figure 15A**). With the addition of propranolol, the irregular beating pattern was corrected; however, EFP worsened and became more irregular (**Figure 15A**). Change in impedance- and EFP- based measures can also be tracked over the course of several hours (**Figure 15B**). Surprisingly, no change in beat rate was noted in response to norepinephrine treatment; however, there was a decrease in response to propranolol pre-treatment that did not increase with norepinephrine and was sustained over the duration of the experiment. There was an increase in impedance amplitude and decrease in EFP amplitude within 10 minutes following norepinephrine treatment (**Figure 15B**). Impedance amplitude remained increased while EFP amplitude gradually began to return to pre-treatment status. Propranolol decreased EFP amplitude and remained unchanged with norepinephrine treatment and alone did not change impedance amplitude but muted the increase in amplitude following norepinephrine treatment (**Figure 15B**). Both propranolol pre-treatment and norepinephrine treatment decreased field potential duration (FPD) and norepinephrine further decreased FDP following propranolol pre-treatment (**Figure 15B**). FPD recovered approximately 30 minutes following norepinephrine treatment; however, pre-treatment with propranolol impaired this recovery.

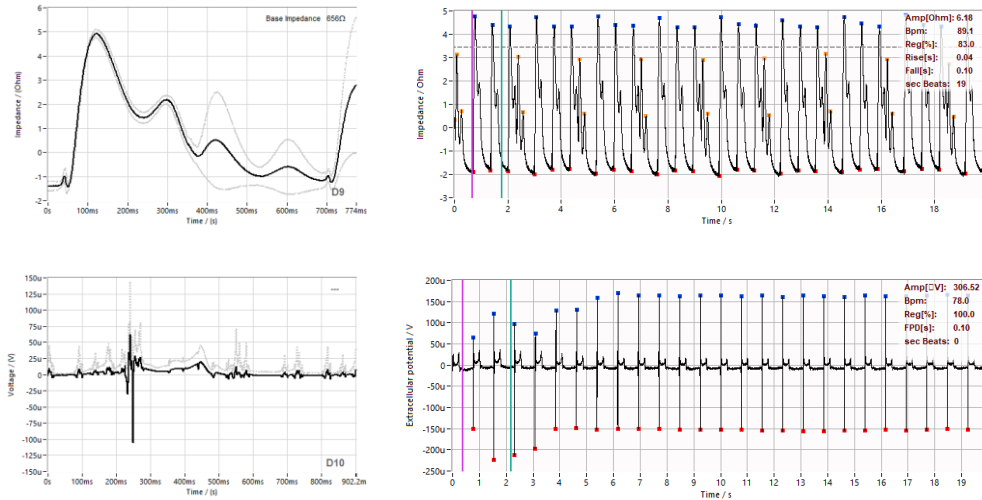
The response of DCM patient HID041020 iPSC-CMs to isoproterenol was also evaluated. Norepinephrine binds both  $\alpha$  and  $\beta$ -ARs while isoproterenol is more selective for  $\beta$ -ARs. As with

norepinephrine, results were reported to show short-term response as well as response over time to isoproterenol, with and without propranolol pre-treatment (**Figure 16 A and B**).

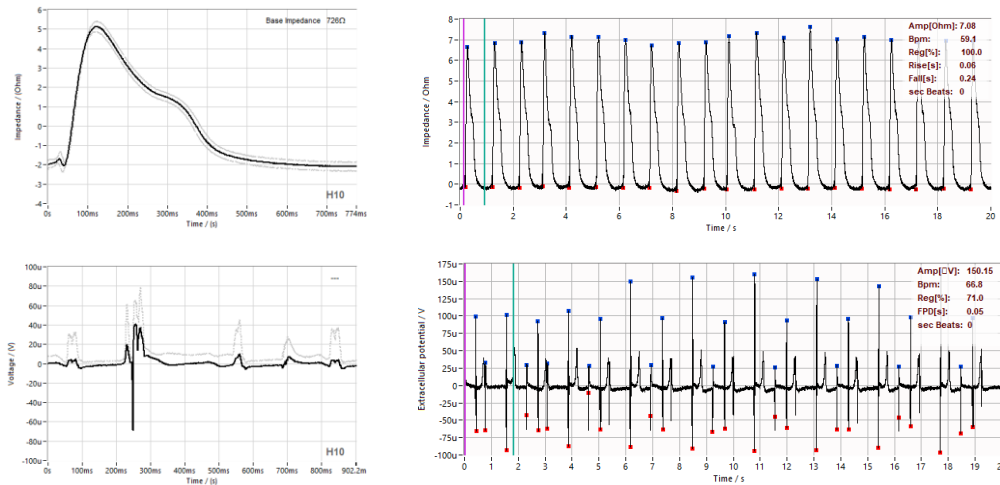
### A. Before isoproterenol treatment



### 10 minutes after isoproterenol treatment

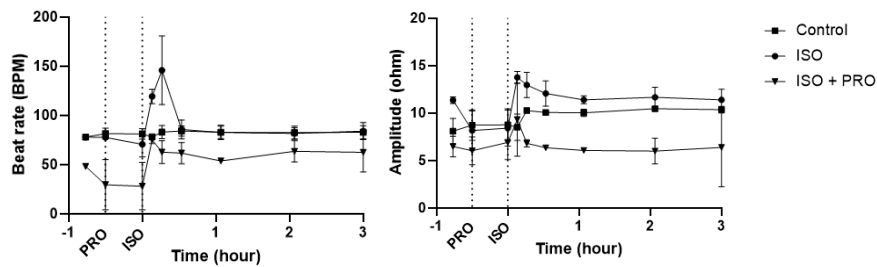


10 minutes after isoproterenol treatment with propranolol pre-treatment



**B.**

Impedance:



Extracellular field potential:

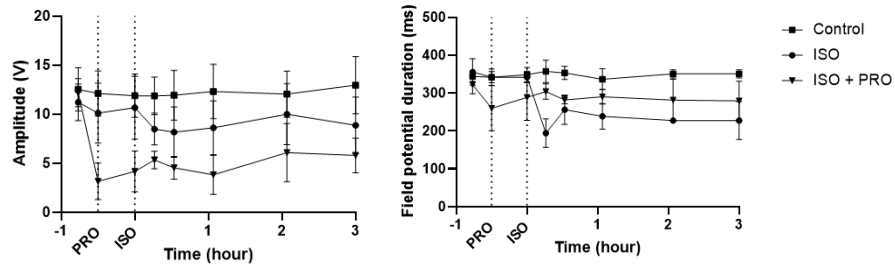


**Figure 16. Contractility and electrophysiology of DCM patient HID041020 in response to treatment with isoproterenol.**

**A.** Representative example mean beats and sequence of contractions as well as EFP traces and sequence of traces of iPSC-CMs from a DCM patient (HID041020) in response to isoproterenol treatment. Cells were treated for 10 minutes with isoproterenol (ISO) treatment, with and without 30 minutes of propranolol (PRO) pretreatment. **B.** Impedance- and extracellular field potential-

based measurements over time in response to isoproterenol treatment, with and without propranolol pre-treatment, n=3.

In response to 10 minutes of treatment with isoproterenol, both impedance and EFP measures became irregular compared to before treatment (**Figure 16A**). Impedance improved with propranolol pre-treatment whereas EFP did not. In contrast to norepinephrine treatment, isoproterenol increased both beat rate and impedance amplitude for about 30 minutes before returning to baseline (**Figure 16B**). Isoproterenol was also observed to briefly increase beat rate and amplitude before returning to baseline despite propranolol pre-treatment. Similar to norepinephrine, isoproterenol treatment had little effect on the EFP amplitude of iPSC-CMs pre-treated with propranolol. Isoproterenol alone slightly decreased EFP amplitude (**Figure 16B**). FPD was reduced approximately 15 minutes following treatment with isoproterenol and did not recover to before treatment levels for the duration of the experiment (**Figure 16B**). Propranolol pre-treatment slightly reduced FPD and blunted the response to isoproterenol.

In summary, pilot experiments using the CardioExcyte96 revealed important factors that must be considered when designing experiments. For instance, plating density must be optimized for each cell line to ensure accurate and reliable measurements. Treatments must be added carefully to avoid noisy results following addition. Finally, plates with the stimulating electrode allows for cell pacing. This is advantageous because the experiment will not depend on spontaneously beating cells, which may vary on a batch-to-batch basis. Since electrophysiology is closely related to the mechanical contraction, variability in beat rate can affect other outcomes such as FPD.

## 4. DISCUSSION

DCM is a serious disease that leads to high morbidity and mortality rates among adults. It is a heterogeneous disease with many potential etiologies such as familial/genetic roots, chemotherapy, pregnancy, and immune diseases, among other causes. Unfortunately, between 25-50% of DCM cases present in the clinic as idiopathic, which contributes to the difficulty in understanding mechanisms underlying disease pathogenesis, treatment modality, progression to heart failure and the need for transplant. Given the high prevalence and poor patient outcome, there is a great need to have a better understanding of DCM to provide better treatment options. iPSC-CMs provide an excellent platform for personalized disease modeling and have proven their ability to recapitulate features underlying DCM. Using iPSC-CMs derived from patients with DCM we can gain a better understanding of the mechanisms contributing to the pathogenesis of their disease and determine the best course of treatment for these patients in a bedside-to-bench-back to-bedside approach.

This thesis is among the first steps towards developing the bedside-to-bench-to-bedside approach. The “bedside-to-bench” phase of the pipeline has been established by our collaborators and we are now working to develop assays to deeply phenotype iPSC-CMs derived from patients with DCM in order to bring the pipeline back to the bedside in this personalized disease modeling approach. To this end, assays were developed to investigate key features of iPSC-CMs, including calcium handling, sarcomere organization, contractility and electrophysiology.

### *4.1 Calcium handling*

Calcium handling was measured using RGECO-TnT, a genetically encoded biosensor that localizes to troponin T in the myofilament of cardiomyocytes, allowing the visualization of calcium transients at the site of contraction initiation [74]. The developers of this biosensor found

that RGECO-TnT detected changes in calcium transients not observed using traditional whole cell dyes [74]. For instance, RGECO-TnT showed that myosin ATPase inhibitor MK-461 altered calcium binding, release, and signal amplitude when the same result had not been seen using whole cell dyes. Additionally, a larger effect size was seen in at the myofilament versus at the whole-cell level in response to calcium sensitizer levosimendan [74]. RGECO-TnT is a useful tool to investigate calcium handling in the myofilament microdomain in order to better understand dysregulated calcium signalling and the role it may play in DCM phenotypes such as impaired contractility. For these reasons, RGECO-TnT was selected instead of whole cell dyes traditionally used to assess calcium transients in cardiomyocytes.

To assess the functionality of this assay, RGECO-TnT was virally transduced into both healthy control and DCM patient iPSC-CMs, and spontaneous calcium transients were recorded. Differences between patients and controls as well as between patients were observed. Further experiments involved acute responses to norepinephrine, isoproterenol, and nifedipine to demonstrate the functionality of this assay. The goal of these proof-of-concept experiments was to determine if (1) differences can be detected between cell lines, and (2) differences in response to treatment could be detected using RGECO-TnT expressed in iPSC-CMs. Initial results indicate that indeed, differences between iPSC-CMs derived from both patients and controls can be detected using RGECO-TnT (**Figure 7**). These differences include time between peaks, transient frequency, upstroke velocity, transient duration, and amplitude. Results indicated a general trend of iPSC-CMs from DCM patients having slower spontaneous calcium transients as well as decreased amplitude when compared to healthy controls. This has been previously reported in iPSC-CMs when comparing a DCM patient with controls [36, 78]. One study showed that compared to the wild-type control, iPSC-CMs derived from a patient with DCM had a decreased

transient amplitude as well as increased transient duration [78]. Although not reported as significant, several studies showed a general trend of decreased transient amplitude in iPSC-CMs from DCM patients compared to controls [36, 51]. Given the complexity and heterogeneity of DCM, we expect varying results in terms of calcium handling on a patient-to-patient basis. In the patients investigated in this thesis, features such as time to 90% baseline, transient duration, decay tau, and area under the curve differed from patient-to-patient (**Figure 7**). Furthermore, differences in the pattern of calcium transients on a cell-to-cell level had been noted (**Figure S2**). This may be due, in part, to the heterogeneity of iPSC-CM cultures that consist of atrial, ventricular, and nodal CMs [79]. However, control line HID041004 showed no cell-to-cell variation and HID041101 show little variation between cells. It can be suggested that heterogenous response on a cellular level could be an indicator of disease, with higher variation being associated with disease phenotype. However, this has yet to be investigated in detail. To our knowledge, the comparison of calcium handling in as many as four DCM patient derived iPSC-CMs has not yet been done. Large-scale analysis of calcium transients in DCM patients is required in order to cluster patients into groups and gain better insight into how cellular phenotypes relate to clinical presentation.

Following confirmation that changes can be detected between cell lines derived from different individuals, experiments were done to demonstrate that response to treatment can be detected as well. Initial results indicate that changes in calcium transients can be detected in response to treatments in both control (HID041004) and DCM patient (HID041019) iPSC-CMs (**Figure 9** and **Figure 10**). iPSC-CMs were treated with norepinephrine, isoproterenol, and/or nifedipine. Norepinephrine is an endogenous ligand for  $\alpha_1$ -,  $\alpha_2$ -,  $\beta_1$ -, and  $\beta_2$ -adrenergic receptors while isoproterenol is a non-selective  $\beta$ -adrenergic receptor agonist. Nifedipine inhibits the L-type calcium channel and is used clinically to treat angina and high blood pressure. These compounds

were selected to demonstrate the functionality of the assay as norepinephrine and isoproterenol were expected to increase the transient frequency and amplitude while nifedipine was expected to decrease or abolish transient amplitude [36, 43, 80].

Consistent with results reported in literature, iPSC-CMs from the healthy control line, HID041004, responded to isoproterenol and norepinephrine with an increase in transient frequency (**Figure 9**) [80-83]. However, no change in amplitude was noted. iPSC-CMs from the DCM patient line, HID041019, increased in amplitude in response to norepinephrine treatment and showed no statistically significant change in transient frequency (**Figure 10**). Despite this, HID041019 results reported in this thesis appear to have a trend of increased transient rate in response to treatment with both norepinephrine and isoproterenol that is obscured by variability within the sample population, as indicated by the large error bars. Further investigation can determine if DCM patient iPSC-CMs are more variable on a cell-to-cell level in their calcium handling properties than those derived from a healthy control, as suggested by preliminary results. This proof-of-concept experiment does not include a large enough sample size to draw conclusions to address this hypothesis and simply indicates changes in calcium handling in response to chronotropic drug treatments can be detected in iPSC-CMs as expected.

iPSC-CMs from control line HID041004 showed an increase in transient frequency in response to 1  $\mu\text{M}$  nifedipine (**Figure 9**). Varying responses were reported in literature with some researchers reporting a decrease in transient frequency in response to 0.02  $\mu\text{M}$  nifedipine while others showing a dose-dependent increase in transient frequency at concentrations ranging from 0.03 to 1  $\mu\text{M}$  [82-85]. Calcium transients were shown to be completely blocked by treatment with 1  $\mu\text{M}$  and 10  $\mu\text{M}$  of nifedipine [80]. It is hypothesized that the increased frequency may be due to shortening of the action potential, allowing the cells to fire more frequently [80, 83, 84].

Differences in maturation state may also contribute to this increase in beat rate in response to nifedipine, as this has been reported in iPSC-CMs but not adult patients [80, 84]. Consistent with previous reports, iPSC-CMs that were evaluated showed a decrease in calcium transient amplitude in response to nifedipine treatment (**Figure 9**). A decrease in the area under the transient was also noted in response to nifedipine treatment, indicating less intracellular calcium compared to the vehicle control (**Figure 9**).

Chronic responses to norepinephrine were measured in an iPSC-CM line derived from a patient with DCM, HID041020. Treatment with clinically relevant beta-blocker carvedilol was also evaluated. Treatment with norepinephrine is of particular interest due to its physiological relevance and the reported changes in iPSC-CMs from DCM patients in response to treatment. Previous reports have used the “norepinephrine stress test” to mimic physiological events leading to the pathogenesis of DCM [43, 51]. One study showed that iPSC-CMs from a DCM patient treated with 10  $\mu$ M norepinephrine for 48h showed a more irregular pattern of calcium transients as well as an increased transient frequency and amplitude [43]. Treatment with carvedilol decreased the transient frequency and amplitude associated with norepinephrine treatment; however, the transient pattern remained irregular [43].

In this work, iPSC-CMs from DCM patient HID041020 showed an increase in transient frequency as well as a decrease in transient duration and time between peaks in response to 7 days of treatment with 10  $\mu$ M norepinephrine (**Figure 11**). This increase was blocked by the presence of 0.25  $\mu$ M carvedilol in addition to norepinephrine, similar to what had been observed in literature [43]. The decrease noted in response to norepinephrine was similarly observed in response to the vehicle and no treatment controls (**Figure S3**). This could result from the change in iPSC-CM maturity over time in culture, as discussed in the limitations section. The single-cell calcium

transients showed variability on a cell-to-cell level before treatment as well as following treatment with vehicle, norepinephrine, and norepinephrine with carvedilol (**Figure S5**). Similar to what had been previously reported, treatment with carvedilol did not alter the irregularity of calcium transient patterns [43].

#### *4.2 Sarcomere organization*

The organization of sarcomeres was visualized using RGECO-TnT. Most researchers use antibodies against  $\alpha$ -actinin or troponin T to visualize sarcomeres; however, since iPSC-CMs were already expressing a fluorescent marker at troponin T in the myofilament, the utility of RGECO-TnT to measure sarcomere organization was investigated. A method was published to stratify cells into groups based on their level of organization [77]. Four levels of organization were empirically generated: severely disorganized, disorganized, fairly organized, and highly organized. Sarcomere organization may be evaluated by eye by a blinded participant. This method is low throughput, may be subject to investigator bias, and is not practical for assessing hundreds of cells per cell line or condition in a single experiment. Programs such as Columbus are useful in high content applications as they can simultaneously measure features of thousands of cells with little user burden. The main drawback of Columbus is that the algorithm struggles to accurately recognize cell borders, especially in cardiomyocytes when sarcomeres are labelled. Since sarcomeres often make a distinct line, software confuses sarcomeres for the cell border. Blurring cells to obscure sarcomeres helps to improve cell identification. Membrane stains such as wheat germ agglutinin and CellMask as well as antibodies against membrane residents such as the sodium-potassium pump and caveolin can be used in attempt to visualize the membrane to allow for better cell distinction. Alternatively, other software packages can be tried [86, 87].

Various groups have reported decreased sarcomere organization in iPSC-CMs derived from patients with DCM compared to healthy controls [44, 51, 52, 88]. The distribution of sarcomere organization was as expected in iPSC-CMs derived from healthy control HID041004, with the largest category being cells with highly organized sarcomeres (**Figure 8**). Unexpectedly, the second control HID041101 showed a distribution similar to the DCM patients. This may result from Columbus recognizing debris as cells; however, this was noted by manual sorting as well. The manual sorting results differed widely from Columbus, likely due to the vastly different sample size with approximately 100 cells being counted manually and up to thousands of cells being counted by Columbus, making the Columbus method more representative of the population. Using Columbus, it was found that iPSC-CMs from DCM patients all had more disorganized sarcomeres than the control HID041004 (**Figure 8**). Between DCM patients, HID041020 had more cells with organized sarcomeres compared to HID041100 and HID041110, which had similar patterns of organization distribution.

A previous study found that features of iPSC-CMs such as sarcomere organization and contractility deteriorated in response to 7 days and 6 hours of 10  $\mu\text{M}$  norepinephrine treatment, respectively [51]. The decrease in sarcomere organization was rescued by 7 days of 10  $\mu\text{M}$  metoprolol co-treatment with norepinephrine [51]. iPSC-CMs derived from DCM patient HID041020 were treated with 10  $\mu\text{M}$  norepinephrine in the presence or absence of 0.25  $\mu\text{M}$  carvedilol for 7 days. At the end of the treatment period, no notable changes were detected in sarcomere organization between the treatment groups (**Figure 13**). It is possible that patient HID041020 is not susceptible to damage caused by chronic norepinephrine treatment; however, further research is required to understand the lack of response to norepinephrine, which is in contrast to what was reported in initial literature. The previous study investigated a patient with a

mutation in troponin T whereas the cause of DCM for HID041020 is unknown to the researcher. It is essential to unblind researchers eventually and determine the etiology of DCM in order to draw associations between phenotype and clinical presentation in order to gain a better understanding of the disease overall. The importance of knowing the cause underlying DCM will be further discussed in future directions.

The next steps in experiments to evaluate sarcomere organization include optimizing membrane stains to better distinguish individual cells and plating at a lower cell density to have better separation of cells in order to aid Columbus in accurate cell identification. Since both the calcium and sarcomere organization assays use RGECO-TnT, it is possible for these experiments to be multiplexed to identify the calcium transients for a single cell and determine the level of organization for that cell. This will give insights to the association between sarcomere organization and calcium handling to gain a better understanding of phenotypes and potential mechanisms underlying DCM.

#### *4.3 Contractility and Electrophysiology*

Contractility and electrophysiology were measured using the CardioExcyte96 (Nanon Technologies). The CardioExcyte96 relies on impedance and extracellular field potential to measure contractility and electrophysiology, respectively. To measure extracellular field potential, cells are plated in a monolayer on the electrodes of the CardioExcyte96 96-well plates. As cells undergo excitation-contraction coupling, the intracellular electrophysiological processes change the extracellular potential in the space between the monolayer and the electrode, which gives an indirect measure of action potentials generated by cardiomyocytes [89]. Impedance relies on the physical changes that cardiomyocytes undergo as they contract. A current flows through cardiomyocytes that are plated on reference and sensing electrodes. As cardiomyocytes contract,

the morphology changes which in turn changes the resistance posed to the current flowing between the electrodes [89]. The resulting output is known as impedance and gives an indirect measure of contractility. A fully formed monolayer is important for both extracellular field potential and impedance to ensure high-resolution and low-noise signals [89]. Furthermore, gaps between cells between cardiomyocytes would disturb the current flowing between the reference and sensing electrodes, thus interfering with accurate impedance readouts.

Proof-of-concept experiments were done to optimize the CardioExcyte96 in our lab. To test the functionality, iPSC-CMs were evaluated in response to positive chronotropes and inotropes norepinephrine and isoproterenol. Previous studies using the CardioExcyte96 have reported an increase in beat rate and amplitude of iPSC-CMs in response to treatment with isoproterenol [90]. Changes in extracellular field potential such as decrease in field potential duration were also reported in response to isoproterenol [90]. Contractility of iPSC-CMs measured by other methods showed an increased beat rate and amplitude in response to norepinephrine [91, 92].

The first experiment done with the CardioExcyte96 made use of the NSP96 standard plate, that does not contain stimulating electrodes for pacing. This experiment confirmed the importance of ensuring a proper monolayer, as indicated by the low amplitude values observed in the wells dedicated norepinephrine-treated cells compared to the wells dedicated to vehicle-treated cells (**Figure 14**). The base impedance was lower in the wells treated with norepinephrine versus those treated with vehicle (data not shown). If the monolayer had been adequately formed, the amplitude values before addition of compound would have been more similar between the treatment groups and the base impedance would have been higher in the norepinephrine group. This experiment also brought attention to technical aspects of the experiment that must be considered. For example, in order to keep the plate sterile, compound addition must be done in a biosafety cabinet. To achieve

this, the plate must either be removed from the CardioExcyte96 and returned following compound addition, or the whole unit must be kept in a biosafety cabinet. Removing the plate disturbs the contact between the electrodes on the plate and the electrodes on the CardioExcyte96, which leads to artifacts such as the one seen in **Figure 14** as vehicle is not expected to increase the beat rate or amplitude of cardiomyocytes. Other factors that can contribute to artifacts include allowing the plate to cool from 37°C when removing from the CardioExcyte96, the addition of compound to the well, and media changes for example during a washout period. Technical experts at Nanion Technologies estimate that if the plate is kept in the CardioExcyte96 at the time of compound addition, the period of time before measurements can be taken reliably is about 2 minutes whereas if the plate is removed, that time increases to about 30 minutes. When measuring the response to fast-acting catecholamines such as norepinephrine it is essential to capture changes in contractility within the first 30 minutes. With the lessons learned from this pilot experiment, careful consideration was given to the experimental design for the subsequent experiment. The seeding density of cell lines was optimized by seeding iPSC-CMs in a 96 well plate at densities from 20,000 to 120,000 cells per well and allowing them to attach for 7 days with media changes every 3 days. One week after plating, cells were stained with membrane marker CellMask and imaged using a high content microscope to visualize the confluency (**Figure S4**). Optimal seeding densities were determined to be 50,000 to 60,000 cells per well for the HID041020 cell line.

For the second experiment using the CardioExcyte96, iPSC-CMs from the DCM patient HID041020 cell line were plated at 50,000 cells per well on a NSP96 plate containing a stimulating electrode to pace the cells. At baseline, iPSC-CMs from DCM patient HID041020 showed an irregular beat shape that indicates an incomplete relaxation before the initiation of the next contraction (**Figure 15**). This may indicate early afterdepolarization, which is defined as abnormal

depolarization of cardiomyocyte membranes during the plateau and rapid repolarizing stages of an action potential [93]. Put simply, a cardiomyocyte action potential follows the following steps:  $\text{Na}^+$  rapidly enters the cell, depolarizing the membrane [94].  $\text{K}^+$  channels then open to allow  $\text{K}^+$  to exit the cell and begin membrane repolarization [94]. The voltage-gated L-type calcium channel (LTCC) then opens to allow  $\text{Ca}^{2+}$  into the cell while  $\text{K}^+$  continues to exit the cell [94]. At this point, the calcium entering the cell initiates the contraction of the cardiomyocyte. The membrane then rapidly repolarizes as the voltage-gated calcium channels close and  $\text{Na}^+$  and  $\text{Ca}^{2+}$  return to the extracellular space while  $\text{K}^+$  returns to the cytoplasm [94]. EADs occur when the inward flux of positive charges is higher than the outward flux during repolarization [93]. A secondary action potential may be triggered if the afterdepolarization reaches the threshold membrane potential [93]. EADs may be caused by channelopathies that affect  $\text{K}^+$  channels involved in repolarization. This could allow the LTCC to reactivate, resulting in an influx of  $\text{Ca}^{2+}$  and membrane depolarization [93]. EADs may also be caused if  $\text{Ca}^{2+}$  is released from the intracellular stores in the sarcoplasmic reticulum which results in the activation of the sodium-calcium exchanger and a net positive inward flux that depolarizes the membrane [93]. Mutations in ion channels involved in action potentials can result in the development of EADs; however, it is unknown whether DCM patient HID041020 has genetic DCM and the mechanism underlying their irregular beats must be further investigated.

iPSC-CMs derived from DCM patient HID041020 were given a 30-minute pre-treatment with 5  $\mu\text{M}$  of  $\beta$ -blocker propranolol before treatment with 10  $\mu\text{M}$  of norepinephrine or 10  $\mu\text{M}$  of isoproterenol. Previous literature has reported an increase in beat rate, amplitude, and field potential duration (FPD) in response to norepinephrine and isoproterenol [90-92]. In iPSC-CMs from patient HID041020, isoproterenol was shown to increase beat rate and amplitude for about

30 minutes before returning to baseline and decrease FPD without recovery to baseline (**Figure 16B**). Propranolol pre-treatment was shown to have some impact on contractility and electrophysiology measurements in response to treatment with isoproterenol or norepinephrine (**Figure 15B** and **Figure 16B**). However, unexpectedly norepinephrine alone only increased amplitude and had no effect on beat rate (**Figure 15B**). Interestingly, as mentioned above iPSC-CMs from HID041020 did not develop disorganized sarcomeres as expected in response to long-term norepinephrine treatment (**Figure 13**) [51]. This unexpected response to norepinephrine must be further investigated to gain a better understanding of patient features. Differences such as these between patients will be key in determining phenotypic clusters of those with similar disease, as discussed in more detail below.

In summary, the CardioExcyte96 is a useful tool to simultaneously measure contractility and electrophysiology in iPSC-CMs and can be used to detect abnormalities in DCM and response to treatment in iPSC-CMs. Initial pilot experiments were aimed at troubleshooting and optimizing to determine how to best use the machine. Results showed the importance of ensuring a fully formed monolayer in acquiring reliable impedance- and EFP-based measurements. It is recommended to optimize plating density for each cell line prior to conducting an experiment in the CardioExcyte96 by staining the membrane and imaging the monolayer. To reduce noise and ensure reliable measurements, it is recommended to keep the NSP96 plates inside the CardioExcyte96 to maintain contact between the plate electrodes and machine electrodes. It is also important to carefully add treatments. For media changes during an experiment, it is recommended to keep 10-20 $\mu$ L of spent media in the wells and refill with fresh media to minimize stress to the cells. If a compound needs to be removed or a washout step performed, this can be repeated several times to functionally dilute out the compound. It is recommended to use NSP96 plates with a

stimulating electrode in order to pace cells and reduce noise associated with spontaneous beating. Future experiments can investigate mechanisms behind the abnormal beating seen in iPSC-CMs derived from DCM patient HID041020 and assess contractility and electrophysiology of additional DCM patient cell lines to compare phenotypes between patients.

#### *4.4 Limitations*

One of the biggest limitations to the iPSC-CM model is their immature state. The use of iPSC-CMs in regenerative medicine for instance, is limited by the spontaneous beating that is not observed in adult CMs. Key features of adult CMs that are not reflected in iPSC-CMs include proper sarcomere alignment and length, the characteristic rod shape, expression of adult isoforms of myofilament proteins (myosin heavy chain, myosin light chain, and troponin I), and developed T-tubule networks [33]. Additionally, features such as contractility, electrophysiology, and calcium handling were shown to be underdeveloped in iPSC-CMs compared to adult CMs [33]. Expression of calcium handling proteins and ion channels involved in action potentials are reduced in iPSC-CMs and a smaller force of contraction is produced in comparison to adult CMs [33].

One group investigated the differences between adult CMs from patients who underwent surgery and iPSC-CMs grown as a monolayer and as engineered heart tissue (EHT) [95]. It was found that basal L-type calcium current density did not differ between iPSC-CMs and adult CMs and that L-type calcium currents were increased in response to  $\beta_1$ - and  $\beta_2$ -adrenergic stimulation by norepinephrine and epinephrine with the same sensitivity between the two cell types [95]. However, the maximum effect size of response to  $\beta$ -AR stimulation was smaller in iPSC-CMs than adult CMs. This may be attributed to the lower pools of cAMP present in iPSC-CMs versus adult CMs [95]. iPSC-CMs prepared as EHT showed improved response size compared to those plated as a monolayer [95]. The ultrastructure of CMs also plays a key role in their function.

Organized CMs have distinct micro-domains that are essential in cellular function [96]. In a healthy adult CM, calcium enters the cell through LTCCs in the T-tubules and calcium stores in the SR are released, leading to calcium binding at the myofilament to initiate contraction [96]. iPSC-CMs have a disorganized ultrastructure compared to adult CMs, with minimal T-tubule formation and disarray of intracellular organelles [96]. As a result, micro-domains are lost and some aspects of physiological communication within the cell are impaired [96]. It was also found that iPSC-CMs express T-type calcium currents, which are not typically expressed in adult CMs [95]. Previous research suggested that the expression of T-type calcium channels decreases over time during fetal development [97]. T-type calcium currents play a role in pace making, potentially contributing to the spontaneous beating of iPSC-CMs [95]. Despite the immature nature of iPSC-CMs, it has been found that important mature molecular components involved in calcium handling including RyR2, SERCA2a, and PLN are expressed and that the functional calcium handling of iPSC-CMs is comparable to adult CMs [85].

Various maturation strategies have been investigated in order to improve the iPSC-CM model. For instance, since adult CMs use fatty acids as energy substrates whereas fetal CMs use glucose, depleting the media of glucose and replacing it with fatty acids can push iPSC-CMs towards a more mature phenotype [98-102]. Other methods rely on prolonged culture time, altering signalling pathways, modulating hormone availability, altering the stiffness of the substrate iPSC-CMs are grown on, and growing iPSC-CMs in co-cultures with cardiac fibroblasts and endothelial cells or as a 3D organoid [103-114]. As shown earlier, iPSC-CMs showed a change in features of calcium transients between baseline and after 7 days of treatment with vehicle or media-only controls (**Figure S3**). This result was unexpected; however, it has been shown that calcium handling can change with prolonged time in culture [115, 116]. One group compared calcium

handling at days 15, 21, and 30 following initiation of the differentiation protocol [116]. Day 15 iPSC-CMs showed slower decay times, smaller transients, and lower sarcoplasmic reticulum calcium stores than day 21 and day 30 iPSC-CMs, which had no significant differences [116]. Another group showed a significant difference in calcium amplitude and decay between 30 and 90 days following differentiation induction; however no difference was observed between 30 and 60 days or 60 and 90 days [115]. They also showed a difference in amplitude in response to isoproterenol treatment in day 90 but not day 30 or 60 iPSC-CMs [115]. An important consideration in this study is that researchers used a protocol to generate ventricular-like iPSC-CMs [115]. Different cardiac cell types generated by the general CM differentiation protocol used in this thesis may contribute to differences noted in calcium handling at the single cell level (**Figure S2**). Going forward, it is recommended to evaluate changes in myofilament-localized calcium handling over time as published studies have only reported on whole-cell calcium handling. Furthermore, it would be interesting to develop a method to label cells using cardiomyocyte subtype-specific markers to interrogate correlations between cell subtypes and calcium transients.

When drawing comparisons between iPSC-CM lines from DCM patients and healthy controls, it is important to consider basic clinical information such as sex and age. Recent research has highlighted the importance of considering differences in heart disease between males and females. Males and females have different epigenetics and endocrinological drivers, which must be taken into consideration during diagnosis and treatment. Men suffer from DCM more often than women; however, women experience a more severe disease [117]. Despite this, women have a more favorable long-term prognosis due to less left ventricular damage and lower rates of mortality and need for transplantation [117]. For instance, in cases of genetic DCM, male patients with TTN

mutations are more likely to experience earlier adverse events than female patients and LMNA mutations cause a more severe long-term prognosis in males with higher prevalence of end stage heart failure, malignant arrhythmias, and higher mortality than in females [118]. X-linked mutations leading to DCM-related conditions such as Duchenne and Becker muscular dystrophies are more common in men, although women may be affected in the event of random X-inactivation [118]. However, women are more commonly affected by peripartum and Takotsubo cardiomyopathies. For obvious reasons, peripartum cardiomyopathy is suffered exclusively by females. While the mechanisms are still not fully understood, it has been suggested that women are more susceptible to Takotsubo cardiomyopathy due to postmenopausal decrease in estrogen [118]. Decreased estrogen can lead to the heart having an increased sensitivity to catecholamines such as norepinephrine, which could contribute to the destructive cycle that leads to the pathogenesis of DCM, as outlined in the introduction [118]. Additionally, one of the most common causes of DCM in women is cardiotoxicity in response to chemotherapeutic anthracyclines indicated for breast cancer [118]. A group of women who were given doxorubicin therapy for breast cancer has been studied in the context of heart disease [57]. This study showed that iPSC-CMs were able to model patient response to doxorubicin in a dish. iPSC-CMs from patients who experienced cardiotoxicity in response to doxorubicin were more sensitive than iPSC-CMs derived from patients who did not have a cardiotoxic response [57]. Researchers were also able to investigate mechanisms underlying DCM in doxorubicin sensitive and tolerant populations [57].

Despite recent consideration and advances in the field, there is still a great need to determine the differences between men and women in regard to cellular phenotypes and disease progression in order to not only offer better personalized treatment options for each sex, but also to develop a screen for biomarkers to track disease progression and therapeutic response. While

much work has been done in the field, there is an ever-growing list of topics to be researched. One avenue that merits exploration is using iPSC-CMs to conduct a large-scale study to evaluate hundreds of DCM patients in order to deeply phenotype the disease and cluster patients based on those with similar phenotypes to generate improved treatment options.

#### *4.5 Future directions*

Currently, DCM is treated in the clinic primarily based on ejection fraction (EF) and NYHA classification, which is based on the degree to which a cardiovascular disease limits physical activity [14]. This approach lacks consideration in regarding the complexity of DCM and the many possible etiologies [14]. Furthermore, the sequence of drugs for the treatment for heart failure is often determined by when drugs underwent their clinical trials rather than biological reasoning [119]. Groups have been working towards improving how DCM and heart failure patients are handled clinically. For instance, in the case of heart failure a new treatment regimen has been suggested that would reduce the amount of time spent onboarding drugs from 6 months to 4 weeks [119]. It has also been suggested that by clustering patients with DCM, we can provide more personalized therapeutic options [14, 15]. Phenotyping DCM patients allows us to create cellular profiles of features underlying disease that can be related back to clinical data. This can be used to cluster patients into groups based on those with similar phenotype and clinical presentation so that we can improve diagnosis and cater treatment options to each of these groups [14, 15]. Using phenotypic clustering, we will be able to make better use of existing drugs as well as generate a venue for drug discovery to target distinct pathological mechanisms for each cluster [15]. Two studies have used machine learning and clustering on populations of DCM patients to identify patterns in clinical data and molecular profiles in order to generate “phenogroups” with unique characteristics that can be used to better guide therapeutic decisions [14, 15]. These studies

made use of genetic, proteomic, and clinical data to improve disease characterization and patient clustering [14, 15]. Since iPSC-CMs recapitulate features underlying disease, they can be used in generating patient-specific cellular profiles to relate back to clinical data for the purpose of phenotypic clustering.

As a first step towards this goal, the research in this thesis focused on developing assays to phenotype underlying disease features in iPSC-CMs derived from patients with DCM. Since contractile deficits are a hallmark of DCM and many DCM-causing mutations affect contractile proteins, assays were developed to evaluate key features related to contractility that have been previously assessed in iPSC-CMs. Our efforts initially focused on addressing the large idiopathic DCM population so that we may gain a better understanding of disease-causing mechanisms to better diagnose and impact treatment options in these patients with so many unknowns. However, since epigenetic markers are lost during reprogramming of somatic cells to iPSCs, iPSC-CMs find better use in modeling DCM caused by genetic disturbances such as mutations or DNA-damaging agents [120-122]. The problem of erasing epigenetic markers can be overcome by direct reprogramming of cells like PBMCs or fibroblasts into cardiomyocytes; however, the generation of iPSC-CMs requires one blood draw for an essentially limitless supply of cells whereas direct reprogramming requires samples taken for every new experiment. The majority of the published literature to date that uses iPSC-CMs to model DCM are in the context of a known mutation. These papers work to functionally characterize the mutation, determine mechanisms underlying pathophysiology, and investigate novel therapeutics. Some studies have also reported that iPSC-CMs can be used to study DCM caused by anthracyclines, which act by damaging DNA [57]. Going forward, patients with familial, genetic, and anthracycline-induced DCM will be the main focus of research for these reasons.

In contrast to the current state of the field, which typically focuses on one or two DCM patient cell lines to compare with familial or isogenic controls, our group will be conducting large-scale studies to characterize hundreds of DCM patient iPSC lines in order to create cellular profiles that can be used to cluster patients into groups with similar phenotypes. The overall idea of the project is to create a “bedside-to-bench-to-bedside” approach to personalized medicine. With our collaborators, we have built a pipeline to recruit DCM patients and healthy controls, reprogram their blood into iPSCs, and derive cardiomyocytes from iPSCs. We are now in the stage of developing assays to deeply phenotype characteristics of disease in iPSC-CM derived from these individuals as well as working to improve the simple 2D model by transitioning to 3D organoid cultures and co-cultures with other cardiac cell types. The goal of this thesis was to establish assays to characterize iPSC-CMs derived from our patient population. Assays were developed to measure calcium handling at the site of contraction in cardiomyocytes, sarcomere organization, functional contractility, and electrophysiology. Troubleshooting was completed to optimize the use of the CardioExcyte96 in our lab to assess contractility and electrophysiology. Future experiments will investigate differences between patients and evaluate their response to stress by neurohormonal stimulation and anthracyclines. The calcium biosensor RGECO-TnT was used to evaluate both myofilament-localized calcium handling and sarcomere organization. Assays to evaluate sarcomere organization require further optimization with membrane stains to more accurately use a machine algorithm to identify cells. The foremost focus of this thesis, evaluating calcium handling in iPSC-CMs using RGECO-TnT, has been shown to detect differences between healthy controls and DCM patients, as well as response to acute and chronic treatment. Future steps for both sarcomere organization and calcium handling will be large-scale comparisons between iPSC-CMs derived from DCM patients and evaluating their response to stress. These assays will be

combined to associate sarcomere organization with calcium handling at the single-cell level. This experiment can be taken a step further by using voltage-sensitive indicators to evaluate electrophysiology alongside calcium handling and sarcomere organization [123]. Genetically-encoded, voltage-sensitive indicators that can be evaluated include ArcLight, ASAP1, ArchD95H, QuasAr2, and VSFP-CR [123]. One group multiplexed RGECO1 with ArcLight to observe abnormalities in action potentials and calcium handling in iPSC-CMs derived from patients with cardiac dysfunction [124]. These assays will nicely complement contractility and electrophysiology determined by the CardioExcyte96.

Assays are currently being developed in our lab to assess cell viability, which will be key in assessing cardiotoxicity of anthracyclines in iPSC-CMs. Common cell viability assays are fluorescent or colorimetric. Fluorescent assays rely on membrane integrity. Dead cell fluorescence assays use membrane impermeable compounds, such as propidium iodide, that fluoresce when bound to DNA. When a cell dies, membrane integrity is lost which allows these compounds to enter the cell and bind DNA. Careful consideration must be kept when using DNA-binding dyes to assess doxorubicin toxicity as doxorubicin also binds DNA and may occupy binding sites, preventing the binding of cell death indicators. Live cell fluorescence assays use a fluorescent compound attached to a membrane permeable moiety, such as calcein-AM. When bound, calcein does not fluoresce and acetoxymethyl (AM) allows the compound to enter the cell, where intracellular esterases cleave AM, resulting in calcein fluorescence. Colorimetric assays such as XTT, MTT, and resazurin rely on the production of a pigmented product from the parent compound by intracellular enzymes. These assays demonstrate the metabolic activity of cells, which serves as a measure of viability. It is important to consider the number of cells in a given well in these assays as a higher number of cells converting the parent compound could be mistaken

for higher metabolic activity of individual cells. The CellCyteX (Cytex) is a microscope that fits inside cell culture incubators and can be used for long-term imaging experiments. This microscope can be used to track viability using the change in area occupied by cells in a well over time in response to treatment. As cells die, they round up and lift off the plate, reducing the overall area. It can also be used to normalize the production of pigmented compound by a population of cells to total area of that population to determine if increased production is due to more cells or higher metabolic activity. Dyes such as CellTox Green (Promega) can be used to assess cell viability over the course of 72 hours. CellTox Green is a dead cell indicator that binds DNA of cells with compromised membrane integrity and can be used in the CellCyteX to monitor cell death over time.

Cell death can be further investigated by measuring production of reactive oxygen species or determining the mechanism of cell death. Collaborators are assessing apoptosis in DCM patient-derived iPSC-CMs in response to cellular stress. Other researchers investigating iPSC-CMs from our patient population are studying cellular signalling pathways to better understand the mechanisms contributing to the pathogenesis of DCM. RNA-seq experiments will also be completed to provide insight to mechanisms behind abnormal phenotypes observed as well as identify pathways that can be targeted by novel therapeutics.

By gaining a wide breadth of phenotypic information, we can make in-depth profiles of iPSC-CMs derived from patients with DCM. This information can be used to evaluate differences on a patient-to-patient basis on a cellular level to gain a better understanding of mechanisms underlying pathophysiology and better direct treatment and drug discovery. Important differences between sexes will also be elucidated. Cellular profiles will be related back to clinical data to

stratify patients into groups, with the end goal being to personalize therapeutic strategies for these groups and improve diagnosis.

## **5. CONCLUSION**

DCM is a cardiac disease that is associated with high morbidity and mortality, often progressing to heart failure and the need for transplantation. It is a heterogeneous disease with many etiologies and mechanisms underlying disease are yet to be fully elucidated and understood. Current therapeutic strategies remain incompletely effective and do not generally modify the course of the disease. There is an evident need to better understand DCM to improve patient outcomes. This thesis contributes to a larger project, called “Heart-in-a-dish”. This project is a collaboration between clinicians and basic researchers to model DCM in a dish in order to better direct therapeutic options to improve patient outcomes. We are establishing a “beside-to-bench-to-bedside” pipeline to achieve this goal. The work of this thesis focuses on development of assays to phenotype iPSC-CMs derived from our patient population.

The goal of this thesis was to develop assays to investigate key features related to contractile deficits associated with DCM. To this end, an assay was developed to measure myofilament-localized calcium handling to assess calcium transients at the site of contractions. This thesis demonstrates that RGECCO-TnT can be used to evaluate differences between both control- and DCM patient- derived iPSC-CMs. Additionally, we are able to measure acute and chronic response to adrenergic ligands. Troubleshooting was done to optimize collection of contractile and electrophysiological data using the CardioExcyte96 and further work is required to fully establish a method to assess sarcomere organization. With our collaborators, we are well on our way to phenotyping iPSC-CMs derived from our patient population and are in the process of further developing assays to measure other interesting features of disease. The prospects of the

“heart-in-a-dish” project are very exciting and it has important implications in the long term that could directly impact the treatment of patients. However, before bringing the pipeline back to the bedside, we must conduct a large-scale characterization of patient-derived iPSC-CMs in part by using assays developed in this thesis.

## 6. REFERENCES

1. Wexler, R.K., et al., *Cardiomyopathy: an overview*. Am Fam Physician, 2009. **79**(9): p. 778-84.
2. Geske, J.B., S.R. Ommen, and B.J. Gersh, *Hypertrophic Cardiomyopathy: Clinical Update*. JACC Heart Fail, 2018. **6**(5): p. 364-375.
3. Cimiotti, D., et al., *Genetic Restrictive Cardiomyopathy: Causes and Consequences-An Integrative Approach*. Int J Mol Sci, 2021. **22**(2).
4. Austin, K.M., et al., *Molecular mechanisms of arrhythmogenic cardiomyopathy*. Nat Rev Cardiol, 2019. **16**(9): p. 519-537.
5. Maron, B.J., et al., *Contemporary definitions and classification of the cardiomyopathies: an American Heart Association Scientific Statement from the Council on Clinical Cardiology, Heart Failure and Transplantation Committee; Quality of Care and Outcomes Research and Functional Genomics and Translational Biology Interdisciplinary Working Groups; and Council on Epidemiology and Prevention*. Circulation, 2006. **113**(14): p. 1807-16.
6. Reichart, D., et al., *Dilated cardiomyopathy: from epidemiologic to genetic phenotypes: A translational review of current literature*. J Intern Med, 2019. **286**(4): p. 362-372.
7. Onrat, S.T., et al., *The Genetic Determination of the Differentiation Between Ischemic Dilated Cardiomyopathy and Idiopathic Dilated Cardiomyopathy*. Genet Test Mol Biomarkers, 2018. **22**(11): p. 644-651.
8. Rosenbaum, A.N., K.E. Agre, and N.L. Pereira, *Genetics of dilated cardiomyopathy: practical implications for heart failure management*. Nat Rev Cardiol, 2020. **17**(5): p. 286-297.
9. Weintraub, R.G., C. Semsarian, and P. Macdonald, *Dilated cardiomyopathy*. Lancet, 2017. **390**(10092): p. 400-414.
10. Kubo, T., et al., *Improvement in prognosis of dilated cardiomyopathy in the elderly over the past 20 years*. J Cardiol, 2008. **52**(2): p. 111-7.
11. Castelli, G., et al., *Improving survival rates of patients with idiopathic dilated cardiomyopathy in Tuscany over 3 decades: impact of evidence-based management*. Circ Heart Fail, 2013. **6**(5): p. 913-21.

12. Gerber, Y., et al., *A contemporary appraisal of the heart failure epidemic in Olmsted County, Minnesota, 2000 to 2010*. JAMA Intern Med, 2015. **175**(6): p. 996-1004.
13. Jefferies, J.L. and J.A. Towbin, *Dilated cardiomyopathy*. Lancet, 2010. **375**(9716): p. 752-62.
14. Verdonschot, J.A.J., et al., *Phenotypic clustering of dilated cardiomyopathy patients highlights important pathophysiological differences*. Eur Heart J, 2021. **42**(2): p. 162-174.
15. Tayal, U., et al., *Precision Phenotyping of Dilated Cardiomyopathy Using Multidimensional Data*. J Am Coll Cardiol, 2022. **79**(22): p. 2219-2232.
16. Hershberger, R.E., A. Morales, and J.D. Siegfried, *Clinical and genetic issues in dilated cardiomyopathy: a review for genetics professionals*. Genet Med, 2010. **12**(11): p. 655-67.
17. Herman, D.S., et al., *Truncations of titin causing dilated cardiomyopathy*. N Engl J Med, 2012. **366**(7): p. 619-28.
18. Lenzi, F. and A. Caniggia, *Nature of myocardial contraction and of action potentials; importance of the cationic gradient*. Acta Med Scand, 1953. **146**(4): p. 300-12.
19. Reddy, Y.S. and C.R. Honig, *Ca<sup>2+</sup>-binding and Ca<sup>2+</sup>-sensitizing functions of cardiac native tropomyosin, troponin, and tropomyosin*. Biochim Biophys Acta, 1972. **275**(3): p. 453-63.
20. LaCombe, P., A. Jose, and S.L. Lappin, *Physiology, Starling Relationships*, in *StatPearls*. 2022: Treasure Island (FL).
21. Meyer, M., et al., *Alterations of sarcoplasmic reticulum proteins in failing human dilated cardiomyopathy*. Circulation, 1995. **92**(4): p. 778-84.
22. Law, M.L., et al., *Dysregulation of Calcium Handling in Duchenne Muscular Dystrophy-Associated Dilated Cardiomyopathy: Mechanisms and Experimental Therapeutic Strategies*. J Clin Med, 2020. **9**(2).
23. Yano, M., Y. Ikeda, and M. Matsuzaki, *Altered intracellular Ca<sup>2+</sup> handling in heart failure*. J Clin Invest, 2005. **115**(3): p. 556-64.
24. Landstrom, A.P., D. Dobrev, and X.H.T. Wehrens, *Calcium Signaling and Cardiac Arrhythmias*. Circ Res, 2017. **120**(12): p. 1969-1993.
25. Wakatsuki, T., J. Schlessinger, and E.L. Elson, *The biochemical response of the heart to hypertension and exercise*. Trends Biochem Sci, 2004. **29**(11): p. 609-17.

26. Gaasch, W.H. and M.R. Zile, *Left ventricular structural remodeling in health and disease: with special emphasis on volume, mass, and geometry*. J Am Coll Cardiol, 2011. **58**(17): p. 1733-40.
27. Nakamura, M. and J. Sadoshima, *Mechanisms of physiological and pathological cardiac hypertrophy*. Nat Rev Cardiol, 2018. **15**(7): p. 387-407.
28. Theocharis, A.D., et al., *Extracellular matrix structure*. Adv Drug Deliv Rev, 2016. **97**: p. 4-27.
29. Kapelko, V.I., *Extracellular matrix alterations in cardiomyopathy: The possible crucial role in the dilative form*. Exp Clin Cardiol, 2001. **6**(1): p. 41-9.
30. Costello, J.M., et al., *Critical care for paediatric patients with heart failure*. Cardiol Young, 2015. **25 Suppl 2**: p. 74-86.
31. Shiels, H.A. and E. White, *The Frank-Starling mechanism in vertebrate cardiac myocytes*. J Exp Biol, 2008. **211**(Pt 13): p. 2005-13.
32. O'Connell, T.D., et al., *Cardiac alpha1-adrenergic receptors: novel aspects of expression, signaling mechanisms, physiologic function, and clinical importance*. Pharmacol Rev, 2014. **66**(1): p. 308-33.
33. Bourque, K., et al., *Biosensor-based profiling to track cellular signalling in patient-derived models of dilated cardiomyopathy*. Cell Signal, 2022. **91**: p. 110239.
34. Xiao, R.P., et al., *Subtype-specific alpha1- and beta-adrenoceptor signaling in the heart*. Trends Pharmacol Sci, 2006. **27**(6): p. 330-7.
35. Movsesian, M.A. and M.R. Bristow, *Alterations in cAMP-mediated signaling and their role in the pathophysiology of dilated cardiomyopathy*. Curr Top Dev Biol, 2005. **68**: p. 25-48.
36. Wu, H., et al., *Epigenetic Regulation of Phosphodiesterases 2A and 3A Underlies Compromised beta-Adrenergic Signaling in an iPSC Model of Dilated Cardiomyopathy*. Cell Stem Cell, 2015. **17**(1): p. 89-100.
37. Zhu, W., et al., *beta-adrenergic receptor subtype signaling in the heart: from bench to the bedside*. Curr Top Membr, 2011. **67**: p. 191-204.
38. Woo, A.Y. and R.P. Xiao, *beta-Adrenergic receptor subtype signaling in heart: from bench to bedside*. Acta Pharmacol Sin, 2012. **33**(3): p. 335-41.

39. Woo, A.Y., et al., *Biased beta2-adrenoceptor signalling in heart failure: pathophysiology and drug discovery*. Br J Pharmacol, 2015. **172**(23): p. 5444-56.
40. Eschenhagen, T., *Beta-adrenergic signaling in heart failure-adapt or die*. Nat Med, 2008. **14**(5): p. 485-7.
41. Katsarou, M.S., et al., *Beta 1, Beta 2 and Beta 3 Adrenergic Receptor Gene Polymorphisms in a Southeastern European Population*. Front Genet, 2018. **9**: p. 560.
42. Wyles, S.P., et al., *Modeling structural and functional deficiencies of RBM20 familial dilated cardiomyopathy using human induced pluripotent stem cells*. Hum Mol Genet, 2016. **25**(2): p. 254-65.
43. Wyles, S.P., et al., *Pharmacological Modulation of Calcium Homeostasis in Familial Dilated Cardiomyopathy: An In Vitro Analysis From an RBM20 Patient-Derived iPSC Model*. Clin Transl Sci, 2016. **9**(3): p. 158-67.
44. Hinson, J.T., et al., *HEART DISEASE. Titin mutations in iPSC cells define sarcomere insufficiency as a cause of dilated cardiomyopathy*. Science, 2015. **349**(6251): p. 982-6.
45. Rudokas, M.W., et al., *Compartmentation of beta2 -adrenoceptor stimulated cAMP responses by phosphodiesterase types 2 and 3 in cardiac ventricular myocytes*. Br J Pharmacol, 2021. **178**(7): p. 1574-1587.
46. Schmitt, J.P., et al., *Dilated cardiomyopathy and heart failure caused by a mutation in phospholamban*. Science, 2003. **299**(5611): p. 1410-3.
47. Takahashi, K., et al., *Induction of pluripotent stem cells from adult human fibroblasts by defined factors*. Cell, 2007. **131**(5): p. 861-72.
48. Ebert, A.D., P. Liang, and J.C. Wu, *Induced pluripotent stem cells as a disease modeling and drug screening platform*. J Cardiovasc Pharmacol, 2012. **60**(4): p. 408-16.
49. Nugraha, B., et al., *Human Cardiac Organoids for Disease Modeling*. Clin Pharmacol Ther, 2019. **105**(1): p. 79-85.
50. Danisovic, L., M. Culenova, and M. Csobonyeiova, *Induced Pluripotent Stem Cells for Duchenne Muscular Dystrophy Modeling and Therapy*. Cells, 2018. **7**(12).
51. Sun, N., et al., *Patient-specific induced pluripotent stem cells as a model for familial dilated cardiomyopathy*. Sci Transl Med, 2012. **4**(130): p. 130ra47.

52. Dai, Y., et al., *Troponin destabilization impairs sarcomere-cytoskeleton interactions in iPSC-derived cardiomyocytes from dilated cardiomyopathy patients*. Sci Rep, 2020. **10**(1): p. 209.
53. Streckfuss-Bomeke, K., et al., *Severe DCM phenotype of patient harboring RBM20 mutation S635A can be modeled by patient-specific induced pluripotent stem cell-derived cardiomyocytes*. J Mol Cell Cardiol, 2017. **113**: p. 9-21.
54. Karakikes, I., et al., *Correction of human phospholamban R14del mutation associated with cardiomyopathy using targeted nucleases and combination therapy*. Nat Commun, 2015. **6**: p. 6955.
55. Stillitano, F., et al., *Genomic correction of familial cardiomyopathy in human engineered cardiac tissues*. Eur Heart J, 2016. **37**(43): p. 3282-3284.
56. Cuello, F., et al., *Impairment of the ER/mitochondria compartment in human cardiomyocytes with PLN p.Arg14del mutation*. EMBO Mol Med, 2021. **13**(6): p. e13074.
57. Burridge, P.W., et al., *Human induced pluripotent stem cell-derived cardiomyocytes recapitulate the predilection of breast cancer patients to doxorubicin-induced cardiotoxicity*. Nat Med, 2016. **22**(5): p. 547-56.
58. Haupt, L.P., et al., *Doxorubicin induces cardiotoxicity in a pluripotent stem cell model of aggressive B cell lymphoma cancer patients*. Basic Res Cardiol, 2022. **117**(1): p. 13.
59. Walters, N.J. and E. Gentleman, *Evolving insights in cell-matrix interactions: elucidating how non-soluble properties of the extracellular niche direct stem cell fate*. Acta Biomater, 2015. **11**: p. 3-16.
60. Kim, J., et al., *AMPK activators: mechanisms of action and physiological activities*. Exp Mol Med, 2016. **48**: p. e224.
61. Rebs, S., et al., *Generation of pluripotent stem cell lines and CRISPR/Cas9 modified isogenic controls from a patient with dilated cardiomyopathy harboring a RBM20 p.R634W mutation*. Stem Cell Res, 2020. **47**: p. 101901.
62. Briganti, F., et al., *iPSC Modeling of RBM20-Deficient DCM Identifies Upregulation of RBM20 as a Therapeutic Strategy*. Cell Rep, 2020. **32**(10): p. 108117.
63. Rebs, S., et al., *RBM20-mutations induce disturbed splicing of calcium relevant genes in patient-specific stem cell models of cardiomyopathies*. European Heart Journal, 2020. **41**: p. 3707-3707.

64. Zanin, S., et al., *Methods to Measure Intracellular Ca(2+) Concentration Using Ca(2+)-Sensitive Dyes*. *Methods Mol Biol*, 2019. **1925**: p. 43-58.
65. Di Virgilio, F., et al., *Structure, function and techniques of investigation of the P2X7 receptor (P2X7R) in mammalian cells*. *Methods Enzymol*, 2019. **629**: p. 115-150.
66. Tong, X., et al., *Genetically encoded calcium indicators and astrocyte calcium microdomains*. *Neuroscientist*, 2013. **19**(3): p. 274-91.
67. Helassa, N., et al., *Design and mechanistic insight into ultrafast calcium indicators for monitoring intracellular calcium dynamics*. *Sci Rep*, 2016. **6**: p. 38276.
68. Nakai, J., M. Ohkura, and K. Imoto, *A high signal-to-noise Ca(2+) probe composed of a single green fluorescent protein*. *Nat Biotechnol*, 2001. **19**(2): p. 137-41.
69. Tallini, Y.N., et al., *Imaging cellular signals in the heart in vivo: Cardiac expression of the high-signal Ca<sup>2+</sup> indicator GCaMP2*. *Proc Natl Acad Sci U S A*, 2006. **103**(12): p. 4753-8.
70. Tian, L., et al., *Imaging neural activity in worms, flies and mice with improved GCaMP calcium indicators*. *Nat Methods*, 2009. **6**(12): p. 875-81.
71. Akerboom, J., et al., *Optimization of a GCaMP calcium indicator for neural activity imaging*. *J Neurosci*, 2012. **32**(40): p. 13819-40.
72. Inoue, M., *Genetically encoded calcium indicators to probe complex brain circuit dynamics in vivo*. *Neurosci Res*, 2021. **169**: p. 2-8.
73. Zhao, Y., et al., *An expanded palette of genetically encoded Ca(2+)(+) indicators*. *Science*, 2011. **333**(6051): p. 1888-91.
74. Sparrow, A.J., et al., *Measurement of Myofilament-Localized Calcium Dynamics in Adult Cardiomyocytes and the Effect of Hypertrophic Cardiomyopathy Mutations*. *Circ Res*, 2019. **124**(8): p. 1228-1239.
75. Okita, K., et al., *A more efficient method to generate integration-free human iPS cells*. *Nat Methods*, 2011. **8**(5): p. 409-12.
76. Lee, S.H., et al., *Generation of a human induced pluripotent stem cell line YCMi004-A from a patient with dilated cardiomyopathy carrying a protein-truncating mutation of the Titin gene and its differentiation towards cardiomyocytes*. *Stem Cell Res*, 2021. **59**: p. 102629.

77. Poon, E.N.Y., et al., *The cell surface marker CD36 selectively identifies matured, mitochondria-rich hPSC-cardiomyocytes*. Cell Research, 2020. **30**(7): p. 626-629.
78. Burridge, P.W., et al., *Modeling Cardiovascular Diseases with Patient-Specific Human Pluripotent Stem Cell-Derived Cardiomyocytes*. Methods Mol Biol, 2016. **1353**: p. 119-30.
79. Bizy, A. and M. Klos, *Optimizing the Use of iPSC-CMs for Cardiac Regeneration in Animal Models*. Animals (Basel), 2020. **10**(9).
80. Sheng, X., et al., *Human pluripotent stem cell-derived cardiomyocytes: response to TTX and lidocain reveals strong cell to cell variability*. PLoS One, 2012. **7**(9): p. e45963.
81. Lin, Y., et al., *Efficient differentiation of cardiomyocytes and generation of calcium-sensor reporter lines from nonhuman primate iPSCs*. Sci Rep, 2018. **8**(1): p. 5907.
82. Altomare, C., et al., *Human-induced pluripotent stem cell-derived cardiomyocytes from cardiac progenitor cells: effects of selective ion channel blockade*. Europace, 2016. **18**(suppl 4): p. iv67-iv76.
83. Guo, L., et al., *Estimating the risk of drug-induced proarrhythmia using human induced pluripotent stem cell-derived cardiomyocytes*. Toxicol Sci, 2011. **123**(1): p. 281-9.
84. Harris, K., et al., *Comparison of electrophysiological data from human-induced pluripotent stem cell-derived cardiomyocytes to functional preclinical safety assays*. Toxicol Sci, 2013. **134**(2): p. 412-26.
85. Itzhaki, I., et al., *Calcium handling in human induced pluripotent stem cell derived cardiomyocytes*. PLoS One, 2011. **6**(4): p. e18037.
86. Zhao, B., et al., *Sarc-Graph: Automated segmentation, tracking, and analysis of sarcomeres in hiPSC-derived cardiomyocytes*. PLoS Comput Biol, 2021. **17**(10): p. e1009443.
87. Sutcliffe, M.D., et al., *High content analysis identifies unique morphological features of reprogrammed cardiomyocytes*. Sci Rep, 2018. **8**(1): p. 1258.
88. McDermott-Roe, C., et al., *Investigation of a dilated cardiomyopathy-associated variant in BAG3 using genome-edited iPSC-derived cardiomyocytes*. JCI Insight, 2019. **4**(22).
89. Doerr, L., et al., *New easy-to-use hybrid system for extracellular potential and impedance recordings*. J Lab Autom, 2015. **20**(2): p. 175-88.

90. Obergrussberger, A., et al., *Safety pharmacology studies using EFP and impedance*. J Pharmacol Toxicol Methods, 2016. **81**: p. 223-32.
91. Liu, J., et al., *Atomic force mechanobiology of pluripotent stem cell-derived cardiomyocytes*. PLoS One, 2012. **7**(5): p. e37559.
92. Maddah, M., et al., *A non-invasive platform for functional characterization of stem-cell-derived cardiomyocytes with applications in cardiotoxicity testing*. Stem Cell Reports, 2015. **4**(4): p. 621-31.
93. Paci, M., et al., *Arrhythmia Mechanisms in Human Induced Pluripotent Stem Cell-Derived Cardiomyocytes*. J Cardiovasc Pharmacol, 2020. **77**(3): p. 300-316.
94. Lester, R.M., S. Paglialunga, and I.A. Johnson, *QT Assessment in Early Drug Development: The Long and the Short of It*. Int J Mol Sci, 2019. **20**(6).
95. Uzun, A.U., et al., *Ca(2+)-Currents in Human Induced Pluripotent Stem Cell-Derived Cardiomyocytes Effects of Two Different Culture Conditions*. Front Pharmacol, 2016. **7**: p. 300.
96. Kane, C., L. Couch, and C.M. Terracciano, *Excitation-contraction coupling of human induced pluripotent stem cell-derived cardiomyocytes*. Front Cell Dev Biol, 2015. **3**: p. 59.
97. Qu, Y. and M. Boutjdir, *Gene expression of SERCA2a and L- and T-type Ca channels during human heart development*. Pediatr Res, 2001. **50**(5): p. 569-74.
98. Correia, C., et al., *Distinct carbon sources affect structural and functional maturation of cardiomyocytes derived from human pluripotent stem cells*. Sci Rep, 2017. **7**(1): p. 8590.
99. Yang, X., et al., *Fatty Acids Enhance the Maturation of Cardiomyocytes Derived from Human Pluripotent Stem Cells*. Stem Cell Reports, 2019. **13**(4): p. 657-668.
100. Lin, B., et al., *Culture in Glucose-Depleted Medium Supplemented with Fatty Acid and 3,3',5-Triiodo-L-Thyronine Facilitates Purification and Maturation of Human Pluripotent Stem Cell-Derived Cardiomyocytes*. Front Endocrinol (Lausanne), 2017. **8**: p. 253.
101. Isu, G., et al., *Fatty acid-based monolayer culture to promote in vitro neonatal rat cardiomyocyte maturation*. Biochim Biophys Acta Mol Cell Res, 2020. **1867**(3): p. 118561.
102. Horikoshi, Y., et al., *Fatty Acid-Treated Induced Pluripotent Stem Cell-Derived Human Cardiomyocytes Exhibit Adult Cardiomyocyte-Like Energy Metabolism Phenotypes*. Cells, 2019. **8**(9).

103. Martewicz, S., et al., *Substrate and mechanotransduction influence SERCA2a localization in human pluripotent stem cell-derived cardiomyocytes affecting functional performance*. Stem Cell Res, 2017. **25**: p. 107-114.
104. Forte, G., et al., *Substrate stiffness modulates gene expression and phenotype in neonatal cardiomyocytes in vitro*. Tissue Eng Part A, 2012. **18**(17-18): p. 1837-48.
105. Feaster, T.K., et al., *Matrigel Mattress: A Method for the Generation of Single Contracting Human-Induced Pluripotent Stem Cell-Derived Cardiomyocytes*. Circ Res, 2015. **117**(12): p. 995-1000.
106. Parikh, S.S., et al., *Thyroid and Glucocorticoid Hormones Promote Functional T-Tubule Development in Human-Induced Pluripotent Stem Cell-Derived Cardiomyocytes*. Circ Res, 2017. **121**(12): p. 1323-1330.
107. Yang, X., et al., *Tri-iodo-L-thyronine promotes the maturation of human cardiomyocytes-derived from induced pluripotent stem cells*. J Mol Cell Cardiol, 2014. **72**: p. 296-304.
108. Garbern, J.C., et al., *Inhibition of mTOR Signaling Enhances Maturation of Cardiomyocytes Derived From Human-Induced Pluripotent Stem Cells via p53-Induced Quiescence*. Circulation, 2020. **141**(4): p. 285-300.
109. Hu, D., et al., *Metabolic Maturation of Human Pluripotent Stem Cell-Derived Cardiomyocytes by Inhibition of HIF1alpha and LDHA*. Circ Res, 2018. **123**(9): p. 1066-1079.
110. Winbo, A., et al., *Functional coculture of sympathetic neurons and cardiomyocytes derived from human-induced pluripotent stem cells*. Am J Physiol Heart Circ Physiol, 2020. **319**(5): p. H927-H937.
111. Yoshida, S., et al., *Maturation of Human Induced Pluripotent Stem Cell-Derived Cardiomyocytes by Soluble Factors from Human Mesenchymal Stem Cells*. Mol Ther, 2018. **26**(11): p. 2681-2695.
112. Giacomelli, E., et al., *Human-iPSC-Derived Cardiac Stromal Cells Enhance Maturation in 3D Cardiac Microtissues and Reveal Non-cardiomyocyte Contributions to Heart Disease*. Cell Stem Cell, 2020. **26**(6): p. 862-879 e11.
113. Dunn, K.K., et al., *Coculture of Endothelial Cells with Human Pluripotent Stem Cell-Derived Cardiac Progenitors Reveals a Differentiation Stage-Specific Enhancement of Cardiomyocyte Maturation*. Biotechnol J, 2019. **14**(8): p. e1800725.

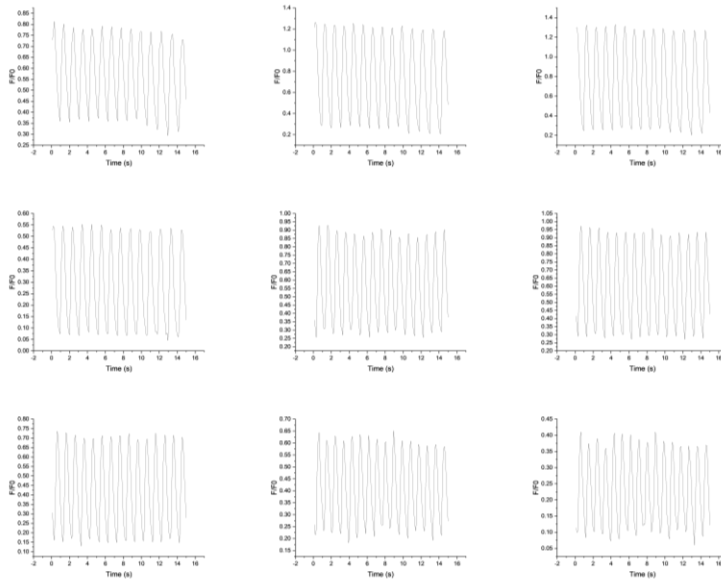
114. Pasquier, J., et al., *Coculturing with endothelial cells promotes in vitro maturation and electrical coupling of human embryonic stem cell-derived cardiomyocytes*. *J Heart Lung Transplant*, 2017. **36**(6): p. 684-693.
115. Oh, J.G., et al., *Generation of Ventricular-Like hiPSC-Derived Cardiomyocytes and High-Quality Cell Preparations for Calcium Handling Characterization*. *J Vis Exp*, 2020(155).
116. Hwang, H.S., et al., *Comparable calcium handling of human iPSC-derived cardiomyocytes generated by multiple laboratories*. *J Mol Cell Cardiol*, 2015. **85**: p. 79-88.
117. Kucher AN, S.A., Nazarenko MS, *Genetic Landscape of Dilated Cardiomyopathy*. *Russian Journal of Genetics*, 2022. **58**(4): p. 369-383.
118. De Bellis, A., et al., *Gender-related differences in heart failure: beyond the "one-size-fits-all" paradigm*. *Heart Fail Rev*, 2020. **25**(2): p. 245-255.
119. McMurray, J.J.V. and M. Packer, *How Should We Sequence the Treatments for Heart Failure and a Reduced Ejection Fraction?: A Redefinition of Evidence-Based Medicine*. *Circulation*, 2021. **143**(9): p. 875-877.
120. Zhou, Y., et al., *Comparative Gene Expression Analyses Reveal Distinct Molecular Signatures between Differentially Reprogrammed Cardiomyocytes*. *Cell Rep*, 2017. **20**(13): p. 3014-3024.
121. Brix, J., Y. Zhou, and Y. Luo, *The Epigenetic Reprogramming Roadmap in Generation of iPSCs from Somatic Cells*. *J Genet Genomics*, 2015. **42**(12): p. 661-70.
122. Thomas, D., S. Shenoy, and N. Sayed, *Building Multi-Dimensional Induced Pluripotent Stem Cells-Based Model Platforms to Assess Cardiotoxicity in Cancer Therapies*. *Front Pharmacol*, 2021. **12**: p. 607364.
123. Dhahri W., W.F., Laflamme, M.A., *Creating and Validating New Tools to Evaluate the Electrical Integration and Function of hPSC-Derived Cardiac Grafts In Vivo*, in *Advanced Technologies in Cardiovascular Bioengineering.*, J. Zhang, Serpooshan, V. , Editor. 2022, Springer, Cham. p. 313-332.
124. Song, L., et al., *Dual optical recordings for action potentials and calcium handling in induced pluripotent stem cell models of cardiac arrhythmias using genetically encoded fluorescent indicators*. *Stem Cells Transl Med*, 2015. **4**(5): p. 468-75.

## SUPPLEMENTAL FIGURES

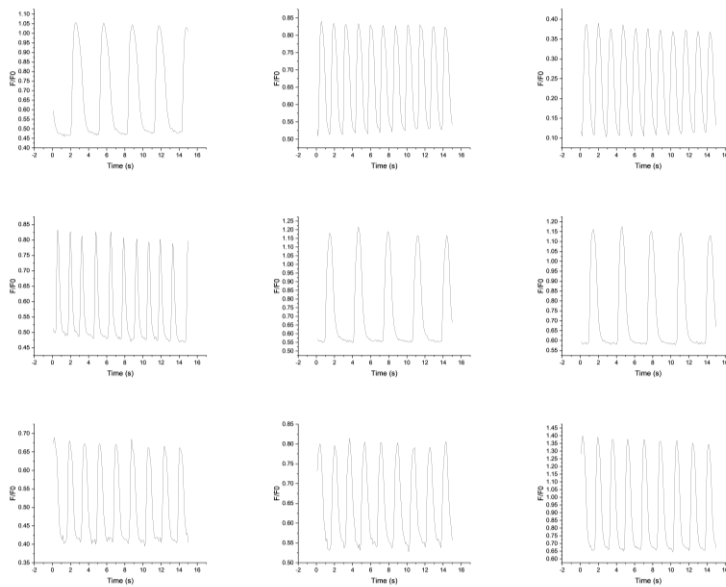
<https://www.youtube.com/shorts/Fx8vIkCp4hY>

**Figure S1.** Intensiometric calcium biosensor RGECO-TnT expressed in iPSC-CMs.

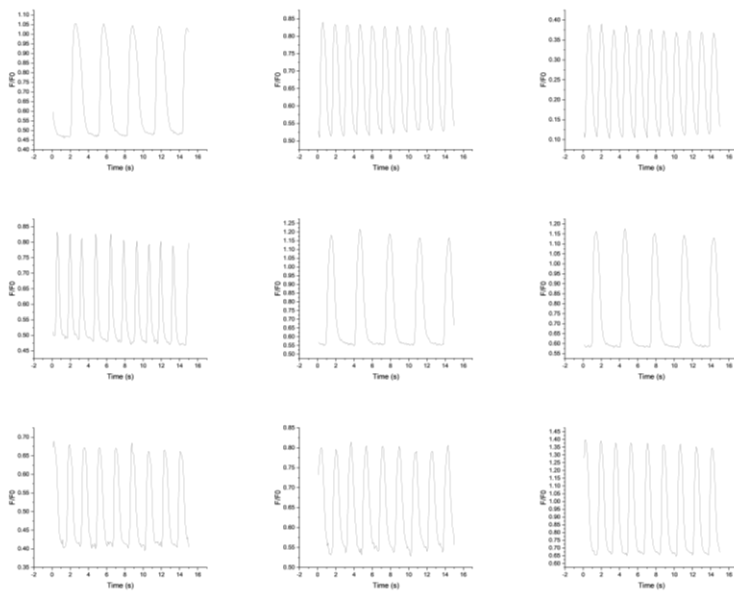
HID041004



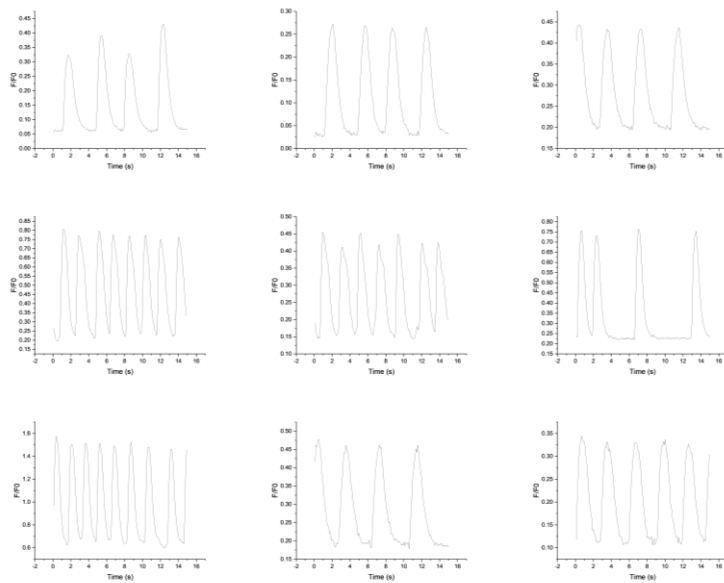
HID041101



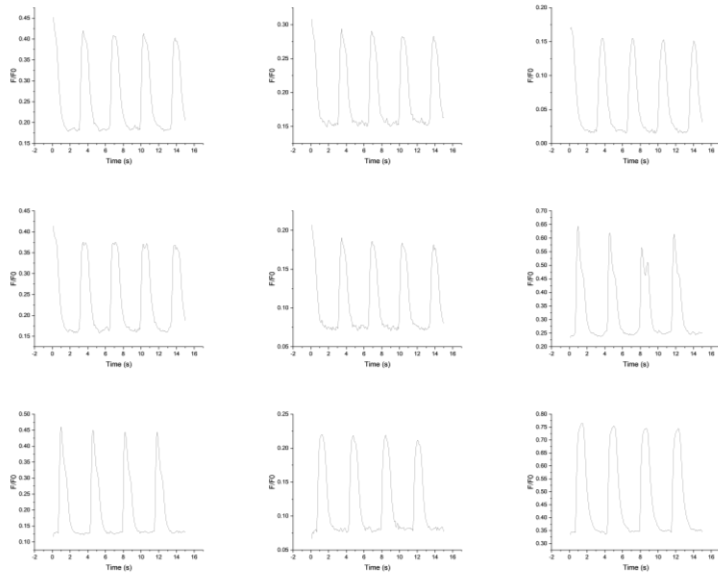
## HID041020



## HID041019



HID041100



HID041110

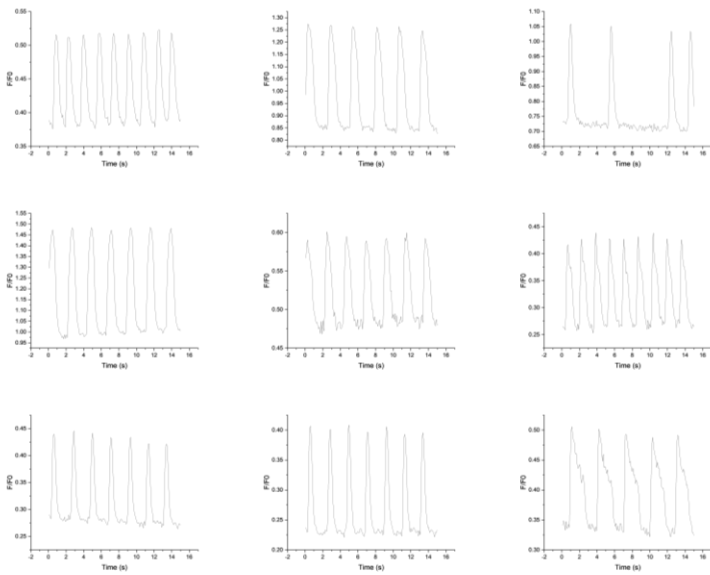


**Figure S2.** Single cell calcium transients for iPSC-CMs derived from healthy controls and DCM patients. Figure corresponds to Figure 7 in the main text.

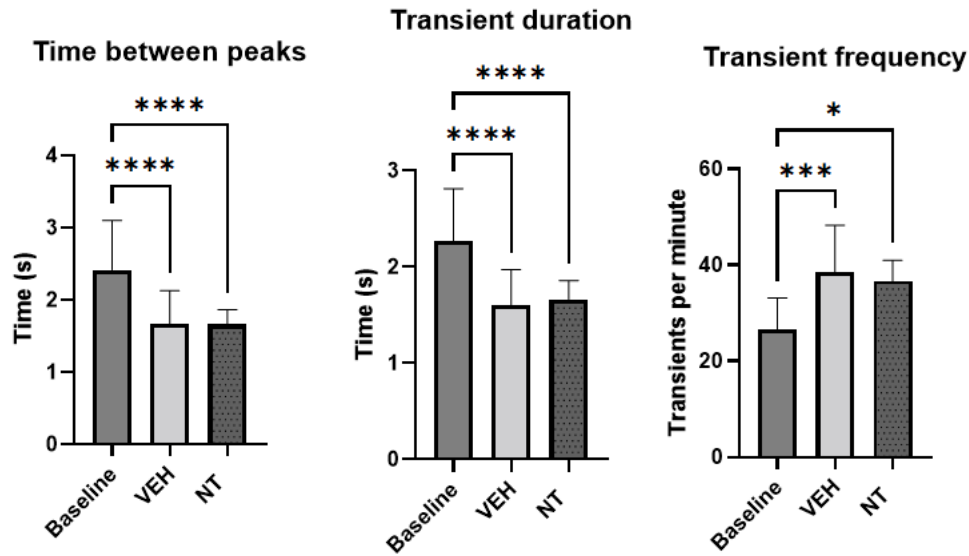


**Figure S3.** Features of calcium transients in iPSC-CMs from DCM patient HID041020 in response to 7 days of treatment. Transients were recorded before treatment and every 24 hours after treatment for 7 days. Media was refreshed daily with DMSO (VEH) or media (NT) added at the same volume as treatments found in figure 12 of the main text. n = 4, 15-25 cells per condition \* =  $p < 0.05$ , \*\*\* =  $p < 0.001$ , \*\*\*\* =  $p < 0.0001$ .

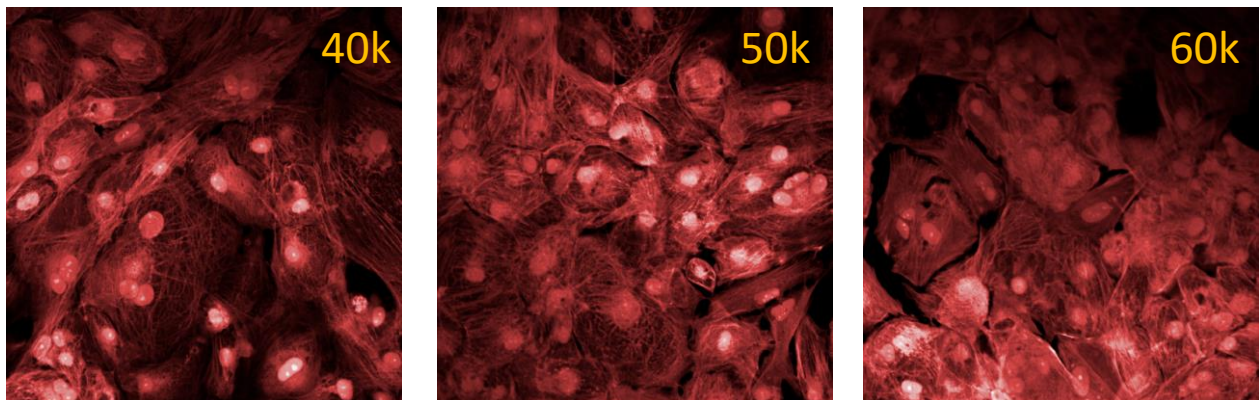
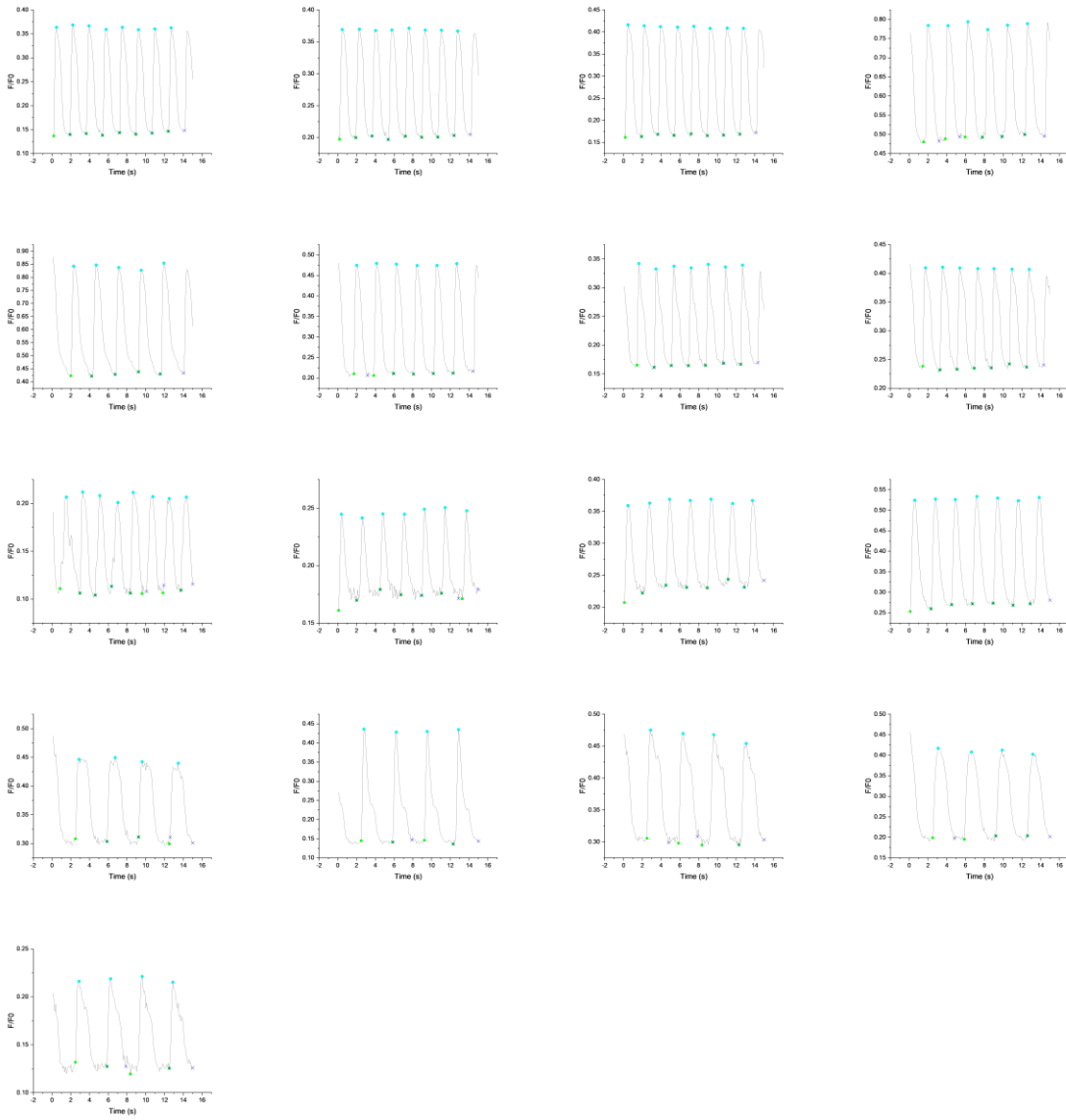
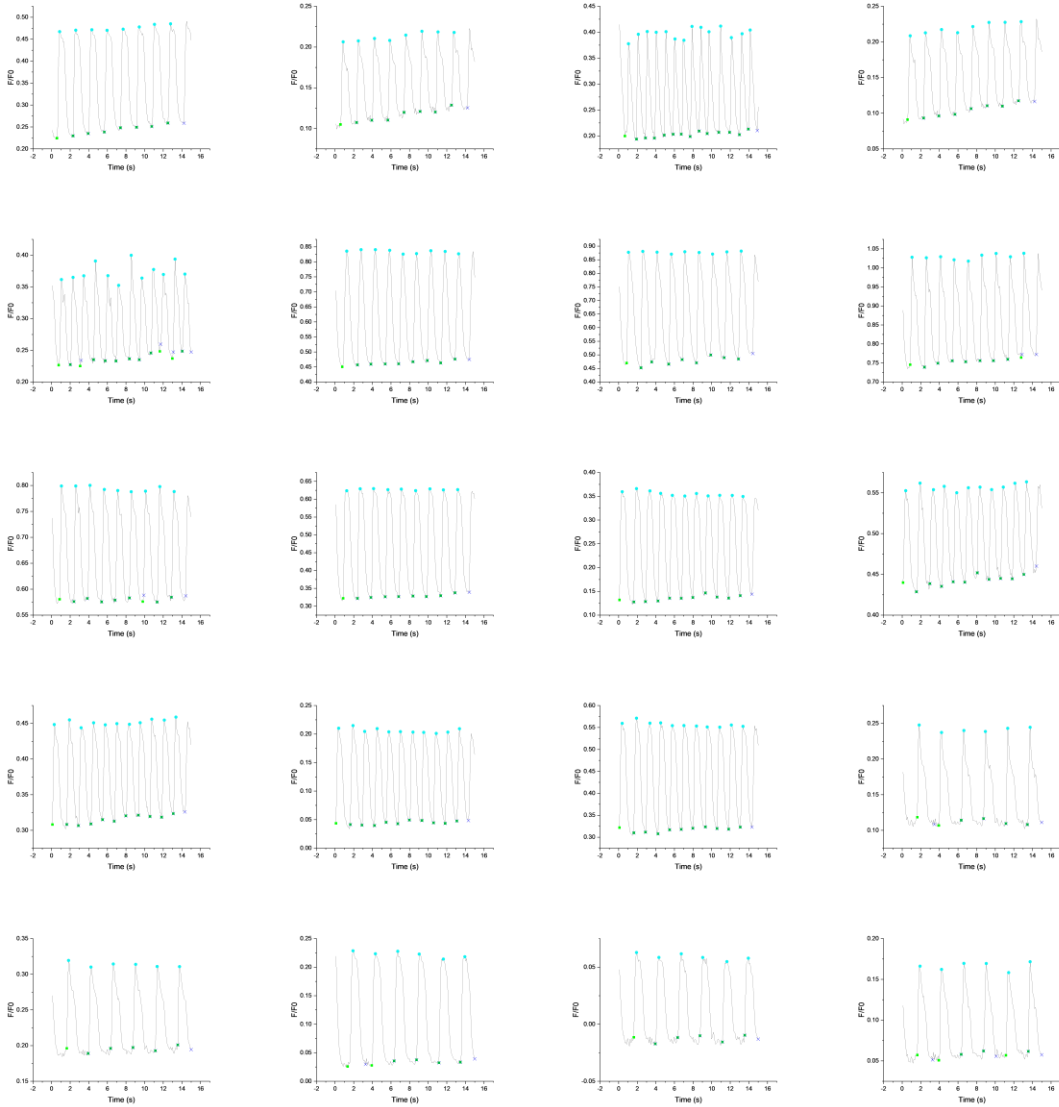


**Figure S4.** Optimizing the seeding density of DCM patient line HID041020 iPSC-CMs. iPSC-CMs were plated at densities ranging from 20,000 to 100,000 cells per well and stained with CellMask to determine which seeding density achieves a monolayer 7 days after plating.

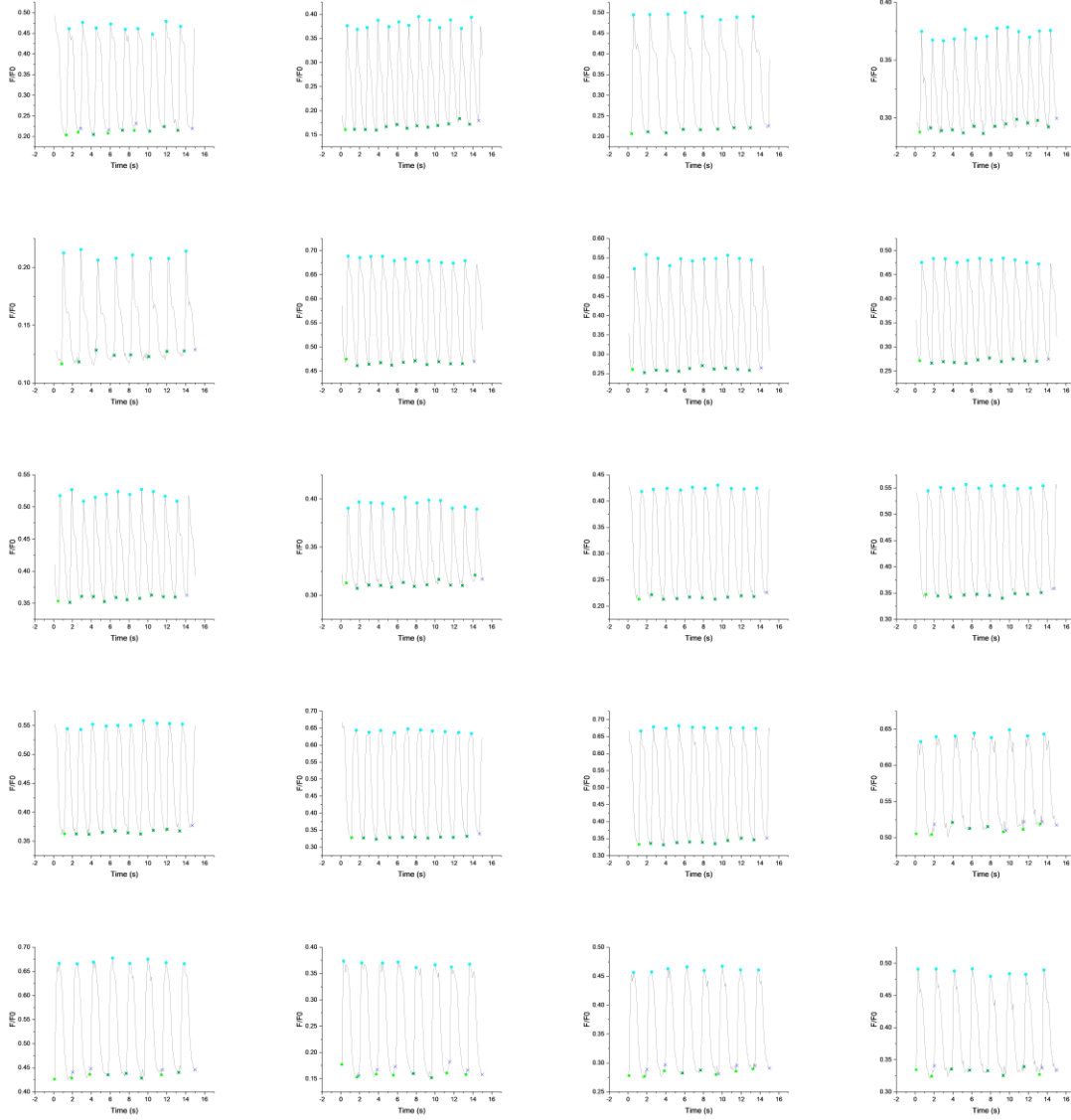
# Baseline (D0, before treatment)



# Vehicle



# Norepinephrine



## Norepinephrine with carvedilol

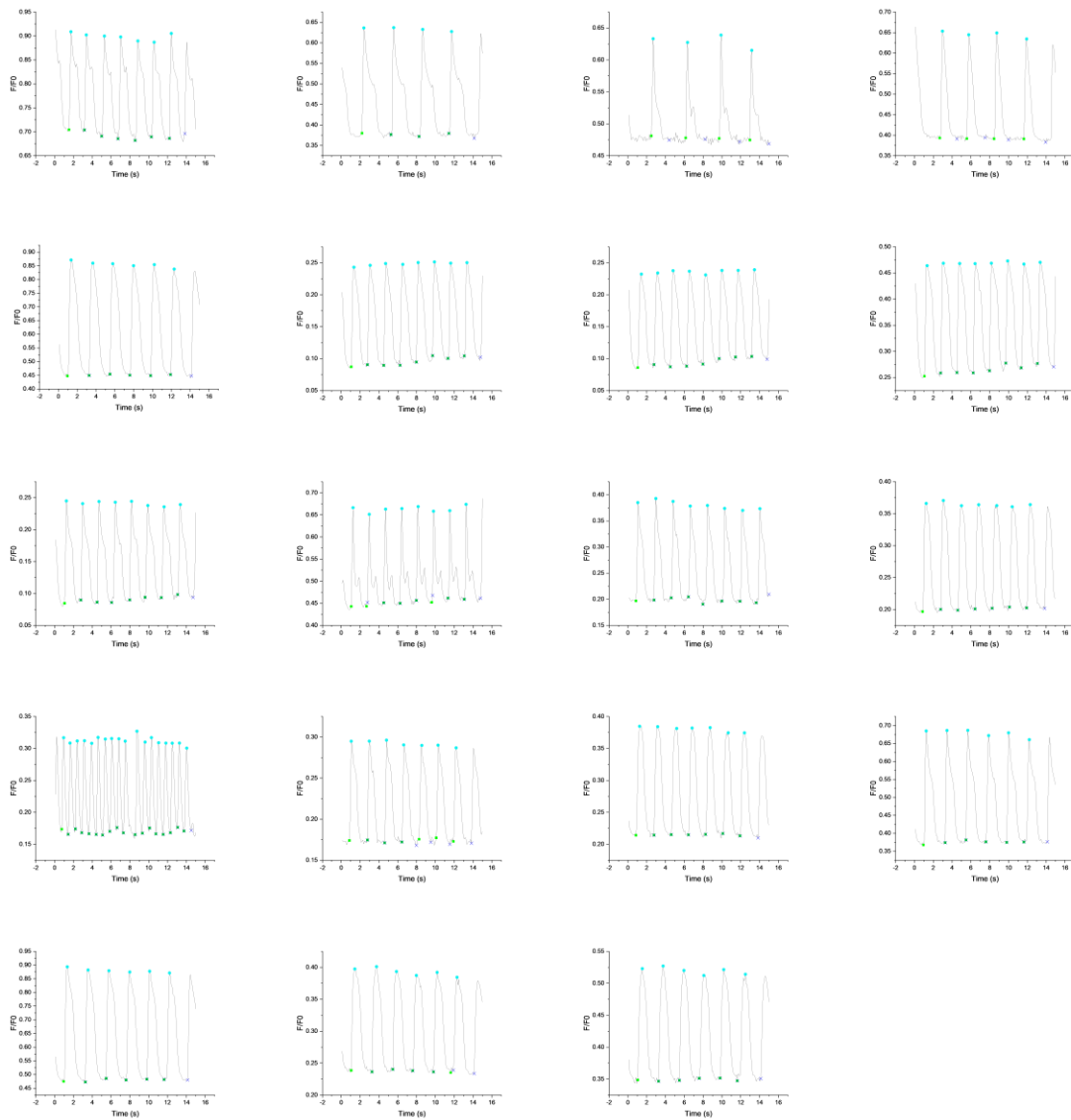


**Figure S5.** Single cell calcium transients for iPSC-CMs derived from DCM patient HID041020 in response to 7 days of treatment. Calcium handling was recording before treatment and following 7 days of treatment with vehicle, norepinephrine, and norepinephrine with carvedilol. Figure corresponds to Figure 11 in the main text.

## Annual renewal submission form - Harmonized

Protocol title: **Heart-In-A-Dish Project**

Project number(s): **2020-6362**

Nagano identifier: **HID-B**

Principal investigator: **Nadia Giannetti**

Project's REB approbation date: **2020-05-08**

Form: **F9H-92558**

First submit date: **2022-03-30**

Last submit date: **2022-03-30**

Form status: **Form approved**

### Administration - REB

1. **MUHC REB Panel & Co-chair(s):**

Cells, tissues, genetics & qualitative research (CTGQ)

**Co-chair: Marie Hirtle**

[reb.ctgq@muhc.mcgill.ca](mailto:reb.ctgq@muhc.mcgill.ca)

2. **REB Decision:**

Approved - REB delegated review

3. **Renewal Period Granted:**

From 2022-05-09 to 2023-05-08

4. **Date of the REB final decision & signature**

2022-05-03

**Signature**



James Ellasus  
MUHC REB Coordinator  
for MUHC Co-chair mentioned above  
2022-05-03 11:35

### General information

1. **Indicate the name of the Principal Investigator in our institution (MUHC)**

Giannetti, Nadia

**From which department is the principal investigator?**

Medicine

**Division**

Cardiology

## Required information for renewal

1. **Date when the research project is expected to end at your institution:**

Date unknown

**Please indicate (approximately) in what year you expect the project to end.**

2024

2. **Indicate the current status of the research project at your institution:**

Project is in progress and recruitment is ongoing

3. **Briefly describe in a few lines, the current status of the project:**

Recruitment of samples moving along well, have obtained 2/3 of our objective.

4. **Please indicate the type of "participants" implicated in your research project**

Human samples

**Did you obtain all the data / samples you needed for the realization of your project as described in the protocol?**

No

**Please specify**

Still obtaining samples from biorepository for our patient population.

5. **In terms of what you are responsible to report, over the past year, relative to the situation at the time of the last REB renewal (or initial approval):**

**Have there been any unreported changes to the REB affecting the study documents?**

No

**Were there unanticipated problems, serious adverse reactions, major deviations or other events or information altering the ethical acceptability or balance between risks and benefits of the project that were not reported to the REB?**

No

**Were there any temporary interruptions to the project?**

No

**Have the results of the project been submitted for publication, presented or published?**

No

**Should the REB be notified of a conflict of interest situation (of any kind) affecting one or more members of the research team, that was not reported at the time of the last approval of the project?**

No

**Has there been an allegation related to a breach in ethical compliance (eg: complaint from a participant, non-compliance with rules relating to ethics or integrity) concerning one or more researchers?**

No

**Signature**

Answer of: Gendron, Nathalie

1. **I certify that the information provided on this form is correct.**

Nathalie Gendron  
2022-03-30 14:59